Two-particle Bose-Einstein correlations in pp collisions at $\sqrt{s}$=13 TeV measured with ATLAS detector at LHC

Yuri Kulchitsky

For BEC team of ATLAS Collaboration

Y. K., E. Plotnikova, N. Russakovich, P. Tsiareshka,
R. Astalos, D.Bruncko, S. Hrynyc, I. Sykora, S.Tokar, T.Zenis

13.02.2019, Seminar LNP, JINR, Dubna

STUDY OF MINIMUM-BIAS EVENTS

Understanding of soft-QCD interactions has direct impact on – precision measurements; searches for new physics

Studies include: Charged-particle distributions in pp interactions at 0.9 – 13 TeV

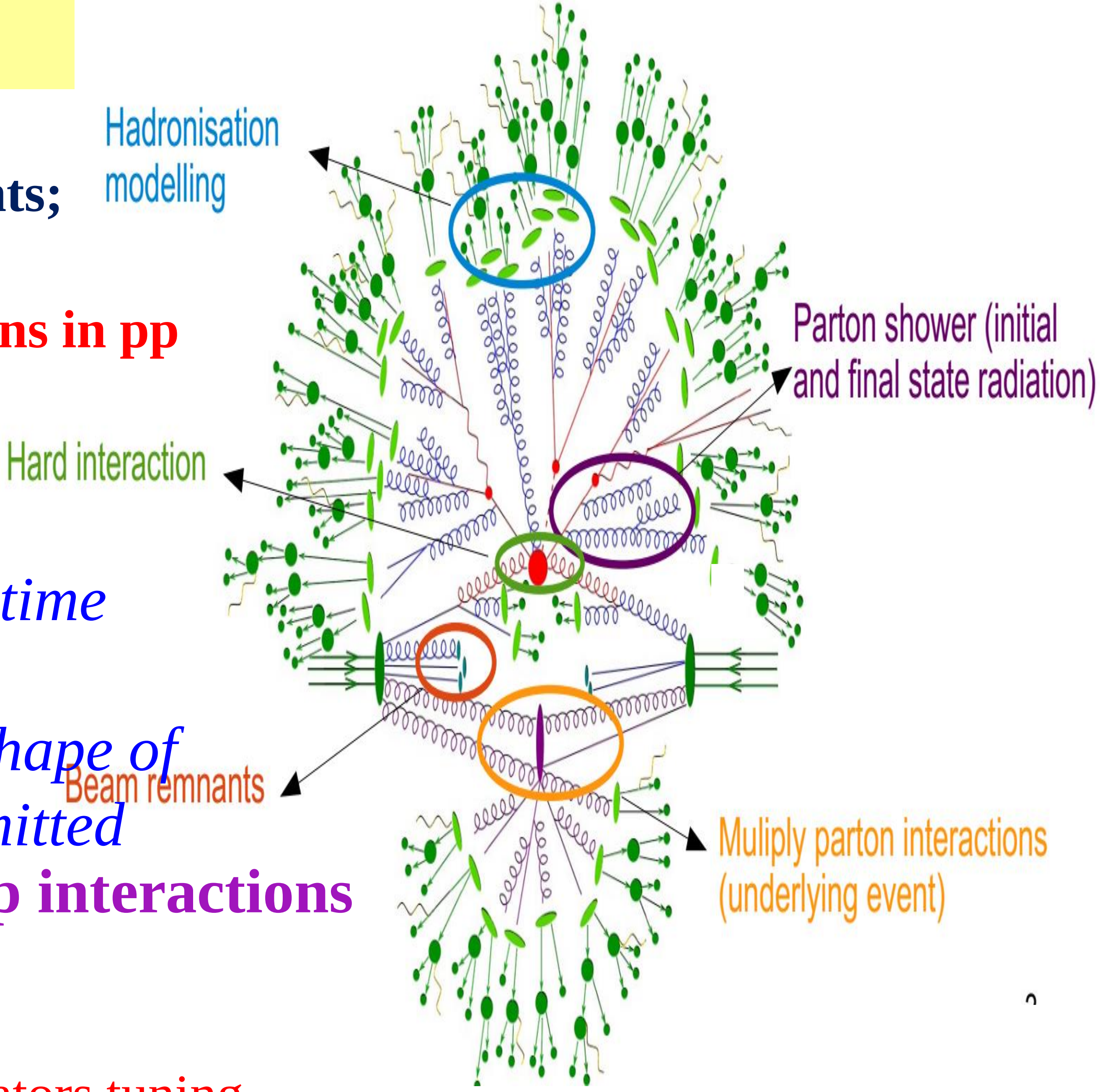

- Satyendra Nath **Bose** – Albert **Einstein correlations** **(BEC)**
  - represent a unique probe of the *space-time geometry* of the *hadronization region*
  - allow the *determination the size and shape of the source* from which particles are *emitted*
- **Underlying events distributions in pp interactions**

Provides insight into strong interactions in non-perturbative QCD regime:

- Soft QCD results used in Monte-Carlo generators tuning,
- Low energy QCD description essential for simulating multiple pp interactions

BOSE-EINSTEIN CORRELATIONS AND HANBURY BROWN –TWISS INTERFEROMETRY

Bose-Einstein correlations (BEC) are often considered to be the analogue of the Robert **Hanbury Brown** and Richard **Twiss** (**HBT**) effect in astronomy, describing the interference of incoherently-emitted identical bosons

Intensity interferometry of photons in radio-astronomy:

- **measures angular diameter of two stars, so the physical size of the source**

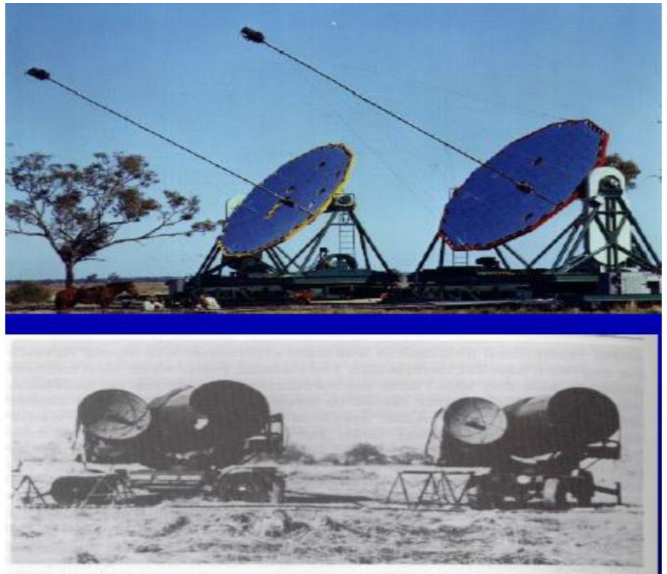

Figure 10.1 The first stellar intensity interferometer; the pilot model of the stellar intensity interferometer at Jodrell Bank in 1955. Two Army searchlights were used to make the first measurement of the angular diameter of a main sequence star (Sirius).

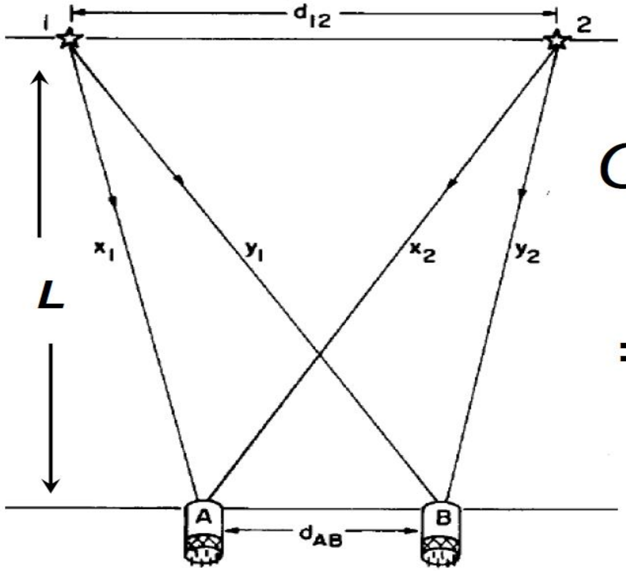

$$C(d) = \frac{\langle I_1 I_2 \rangle}{\langle I_1 \rangle \langle I_2 \rangle}$$

$$= 1 + A\cos(d_{AB})$$

$$d_{AB} = \lambda/\theta$$

$I_{1(2)}$ - intensities, $<x>$ - averaging over random phases

λ is the wavelength of the light, $\theta = d_{12}/L$

Varying d_{AB} one learns the angle, and using the individual wave vectors, the physical size of the source

*Roy Jay **Glauber*** - awarded in 2005 Nobel Prize in Physics "for his contribution to the quantum theory of optical coherence"

Bose-Einstein Correlations

Correlations in phase space **between two identical bosons** from symmetry of wave functions.

► Enhances likelihood of *two particles close* in phase space

► Allows one to 'probe' the source of the bosons *in size* and *shape*

► Dependence on particle multiplicity and transverse momentum probes *the production mechanism*

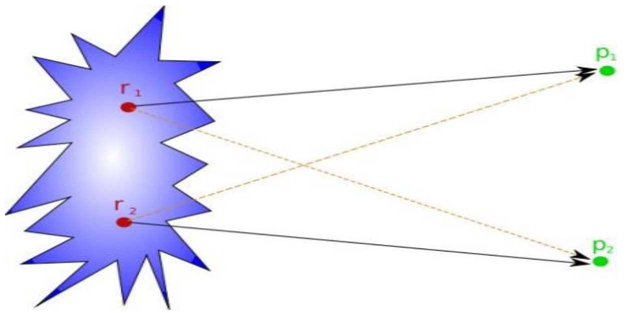

Correlation function $C_2(Q)$ a ratio of probabilities:

$$C_2(Q) = \frac{\rho(p_1, p_2)}{\rho_0(p_1, p_2)} = C_0\left(1 + \Omega(\lambda, RQ)\right)\cdot\left(1 + Q\varepsilon\right), \quad Q^2 = -(p_1 - p_2)^2$$

$$\Omega^G(\lambda, RQ) = \lambda e^{-R^2Q^2}$$

$$\Omega^E(\lambda, RQ) = \lambda e^{-RQ}$$

C_0 is a *normalisation*, **ε** accounts for *long range effects*, **R** is the **effective radius parameter of the source**, **λ** is the **strength of the effect parameter**, 0/1 for coherent/chaotic source. Two possible parameterisation: **Gaussian and Exponential**.

$$C_2(Q) = \frac{N^{++,--}(Q)}{N^{ref}(Q)}$$

N_{ref} without BEC effect from: unlike-charge particles (UCP), opposite hemispheres, event mixing. **Basic Reference**: distribution of UCP pairs of non-identical particle taken from the same event.

$$R_2(Q) = \frac{C_2^{Data}(Q)}{C_2^{MC}(Q)} = \frac{\rho(++,--)/\rho(+-)}{\rho^{MC}(++,--)/\rho^{MC}(+-)}$$

The studies are carried out using the **double ratio correlation function**. The **$R_2(Q)$** eliminates problems with energy-momentum conservation, topology, resonances, hadronic jets, mini-jets etc.

MC without BEC.

ATLAS DETECTOR

The focus of ATLAS is high-p_T physics, and also provides a window onto important soft QCD processes.
These have intrinsic interest but also the understanding of underpins searches for new physics.

Task ►Bose Einstein Correlations

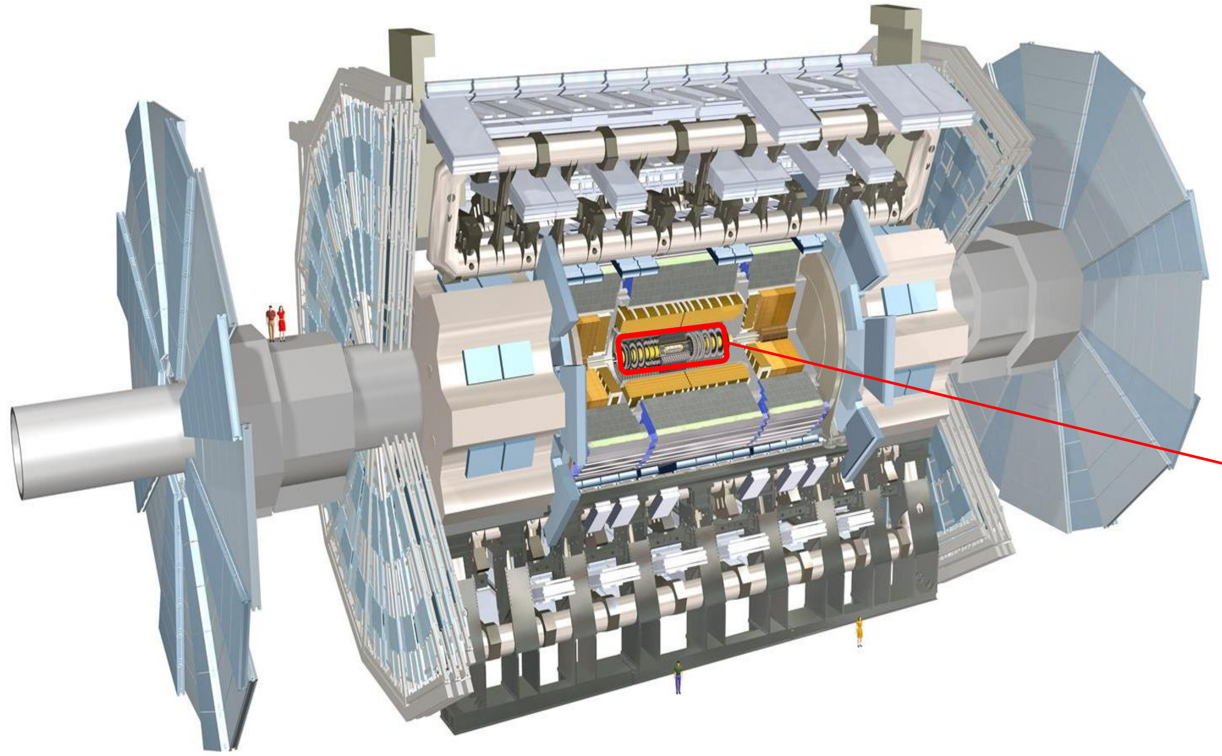

Two times better tracks impact parameters resolution at 13 TeV

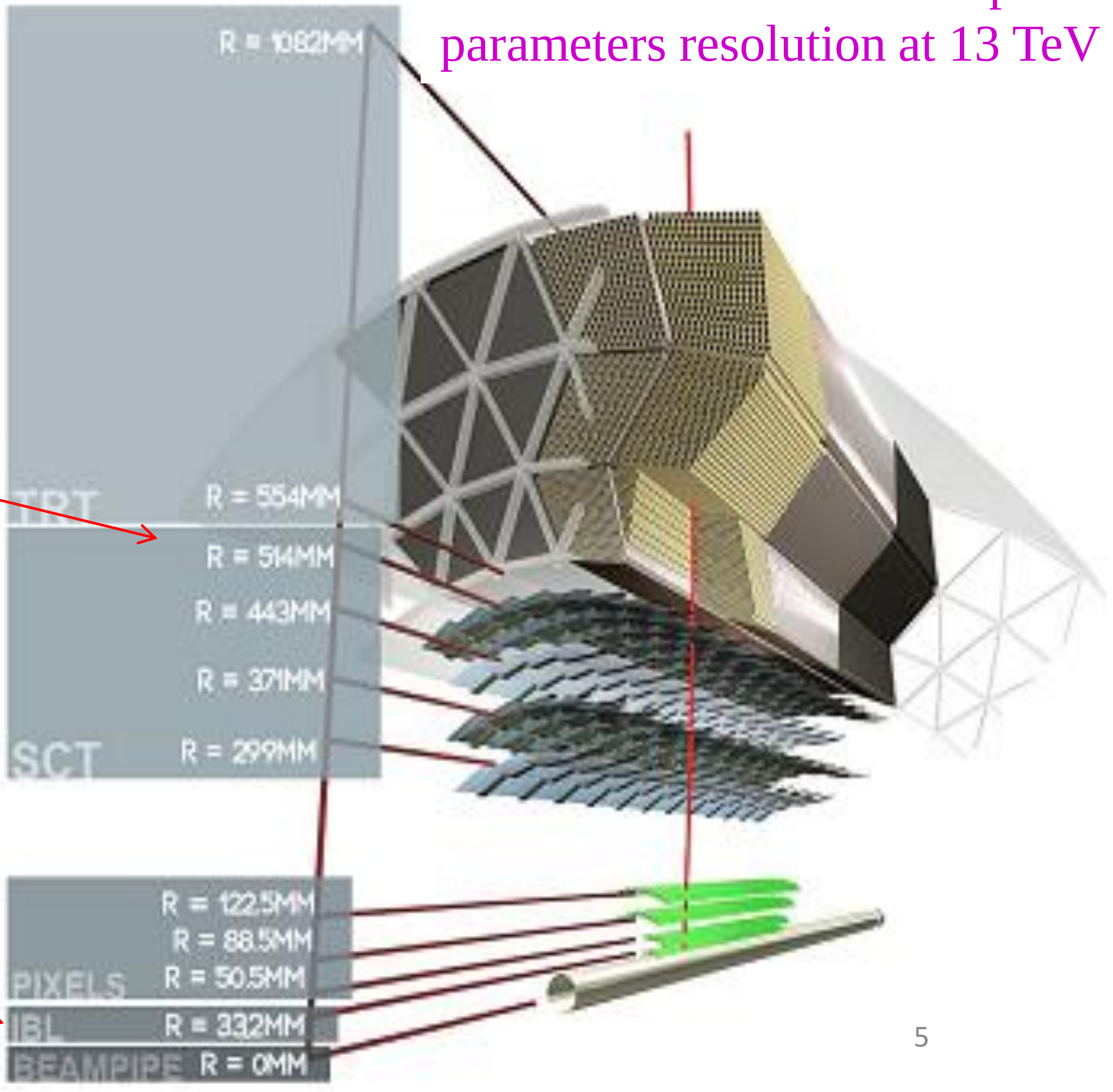

ATLAS Inner Detector (ID) **main tracking device**:

Consists of **Pixel, Silicon strip (SCT) and drift tube (TRT) detectors.** Single hit resolution between 10 μm (Pixel) and 1 μm (TRT). **New: *Insertable B-Layer* (IBL)** in the Pixel

MINIMUM BIAS TRIGGER SCINTILLATOR

24 independent wedge-shaped plastic scintillators (12 per side) read out by PMTs, $2.08<|\eta|<3.86$*

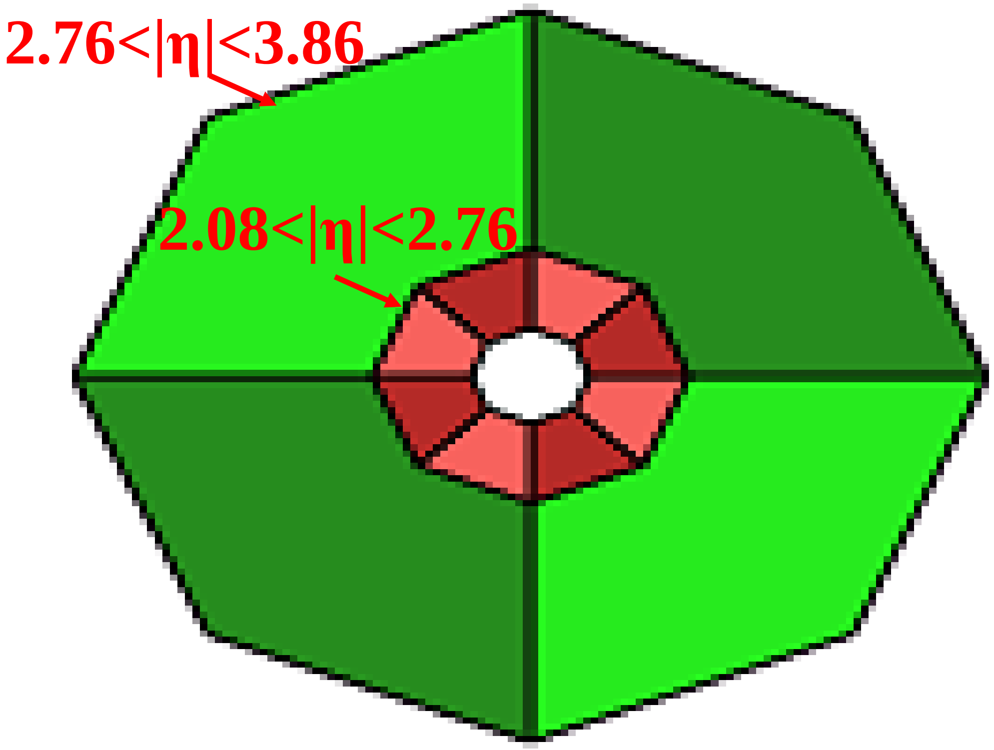

* Pseudorapidity is defined as $\eta = -\frac{1}{2} \ln(\tan(\theta/2))$, θ is the polar angle with respect to the beam.

- Designed for triggering on min bias events, >99% efficiency
- MBTS timing used to veto halo and beam gas events
- Also being used as gap trigger for various diffractive subjects

Minimum-Bias and High Multiplicity Track Triggers

- For these analysis the events collected with **Minimum-bias (MB)** trigger named as ***HLT_noalg_mb_L1MBTS _1*** were used.
  - This trigger required at least one hit in one of the 12+12 sectors (A and C sides) of the MBTS detector.

✓ ***Integral Luminosity ~151 μb^{-1}; Statistic: 9.6×10^{6} events with 2.8×10^{8} tracks***

- For these analysis the events collected with **High multiplicity track (HMT)** trigger named as ***HLT_mb_sp900_trk60_hmt_L1MBTS_1_1*** were used.
  - High-multiplicity track (HMT) events were collected at 13 TeV using a dedicated high-multiplicity track trigger:
    - requires more than **900 SCT** space-points,
    - more than **60 reconstructed** good quality charged **tracks** with p_T>0.4 GeV associated with the primary vertex.

✓ ***Integral Luminosity ~8.4 nb^{-1}; Statistic: 9.1×10^{6} events with 9.8×10^{8} tracks***

Example of Very-High-Multiplicity event

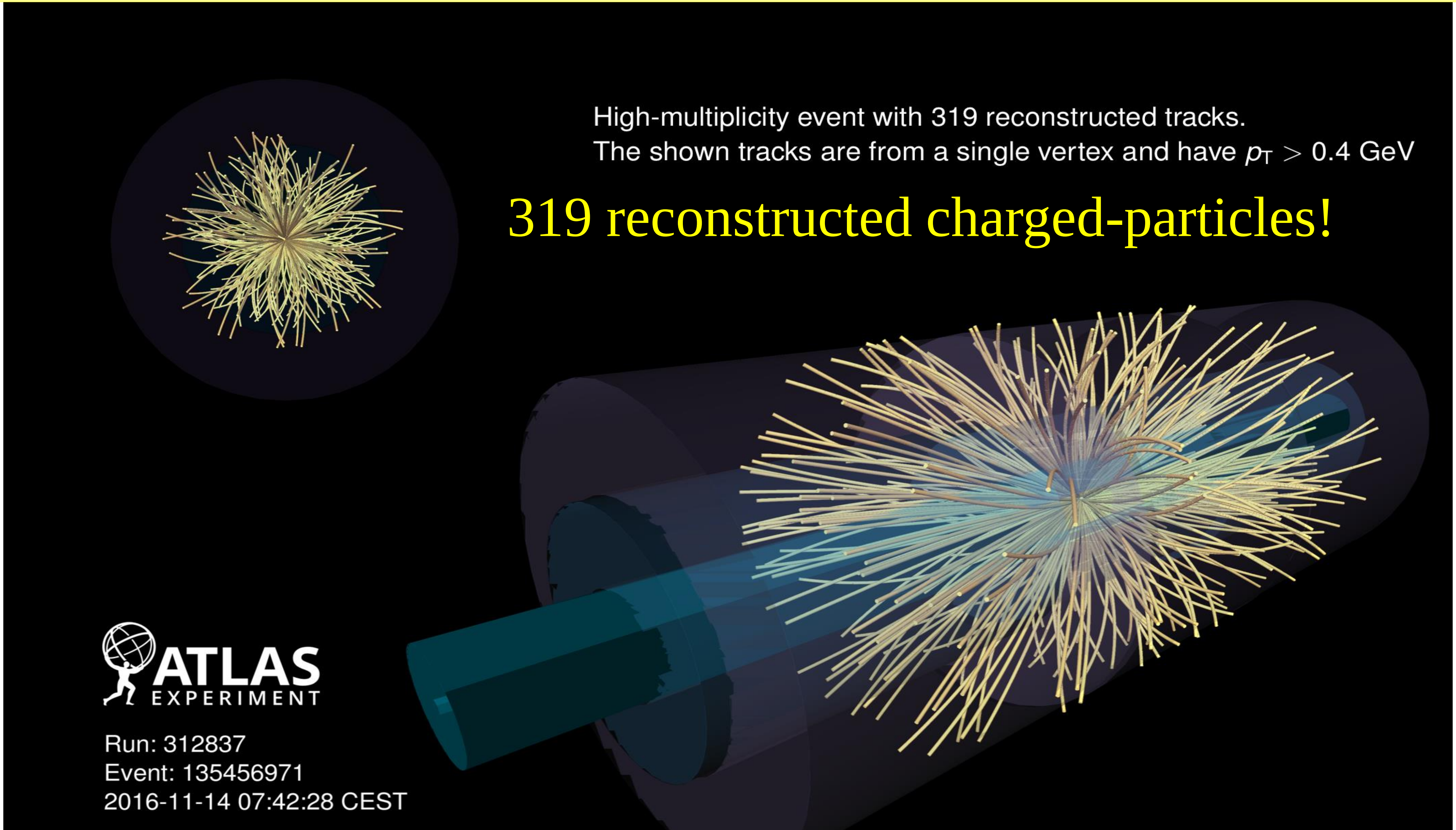

MINIMUM-BIAS EVENT SELECTION CRITERIA

Events pass the data quality criteria. “Good events”:

- **all ID sub-systems nominal conditions,**
- **stable beam,**
- **defined beam spot**

➢ **Trigger:**
- Accept on signal-arm Minimum Bias Trigger Scintillator for minimum-bias or high multiplicity track triggers

➢ **Vertex:**
- Primary vertex (2 tracks with p_T>100 MeV),
- Veto to any additional vertices with ≥4 tracks,

➢ **Tracks:** At least 2 tracks with p_T>100 MeV, $|\eta|<2.5$;
- At least 1 first Pixel layer hit;
- At least 2, 4, or 6 SCT hits for p_T>100, 300, 400 MeV respectively;
- IBL hit required if expected (if not expected, next to innermost hit required if expected);
- Cuts on the transverse impact parameter: $|d_0^{BL}|<1.5$ mm (w.r.t beam line);
- Cuts on the longitudinal impact parameter: $|\Delta z_0 \sin\Theta|<1.5$ mm, where Δz_0 is difference between z_0^{tracks} & z^{vertex};
- Track fit χ^2 probability >0.01 for tracks with p_T>10 GeV.

Correct distributions for detector effects:

- where possible the data used to reduce the MC dependencies
- Monte Carlo derived corrections for tracking

EVENT CORRECTIONS

We correct the events on:

$$w(n) = \frac{1}{\varepsilon_{trig}(n) \cdot \varepsilon_{vert}(n)}$$

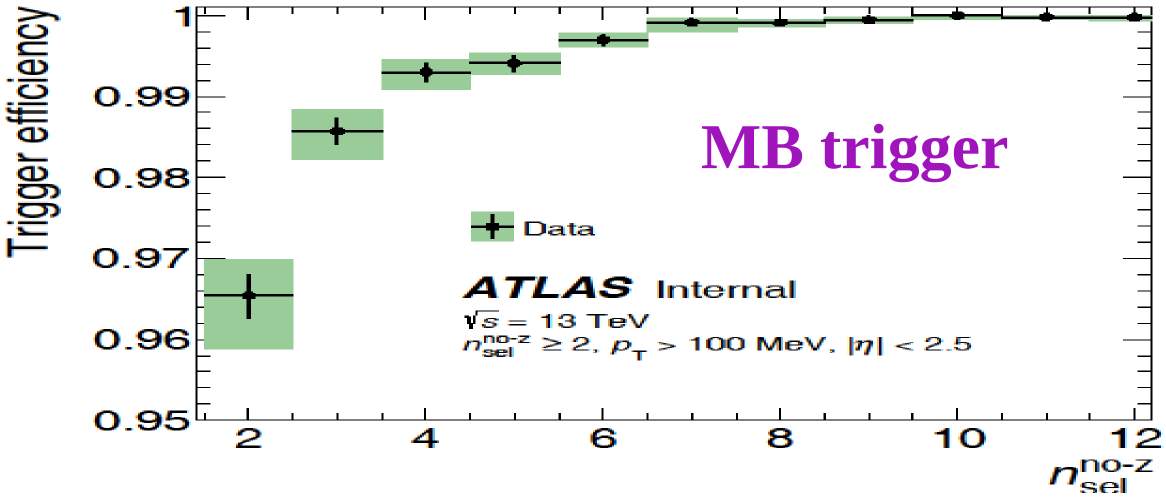

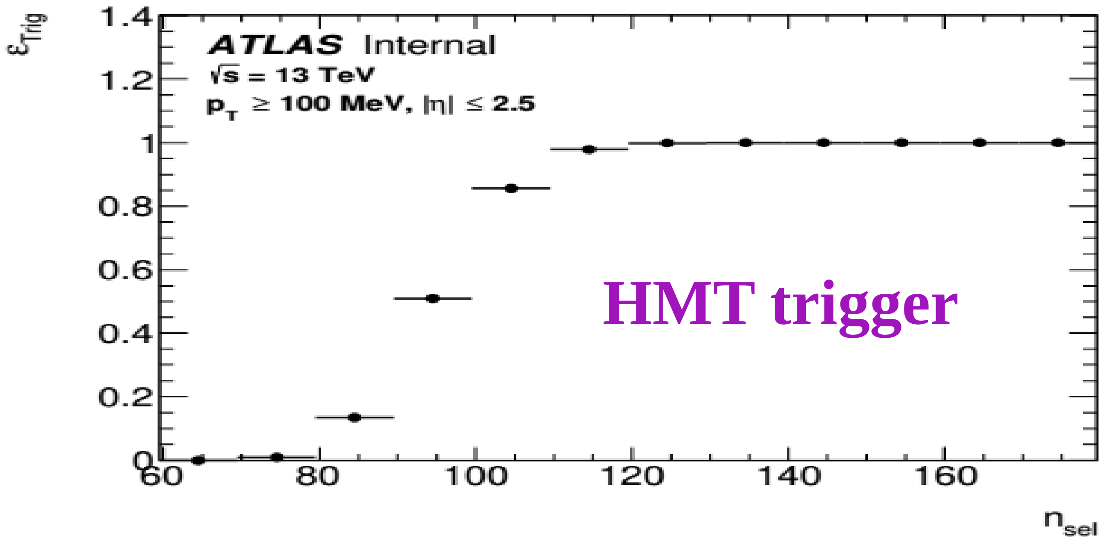

The MB or HMT triggers efficiency, $\varepsilon_{trig}(n)$

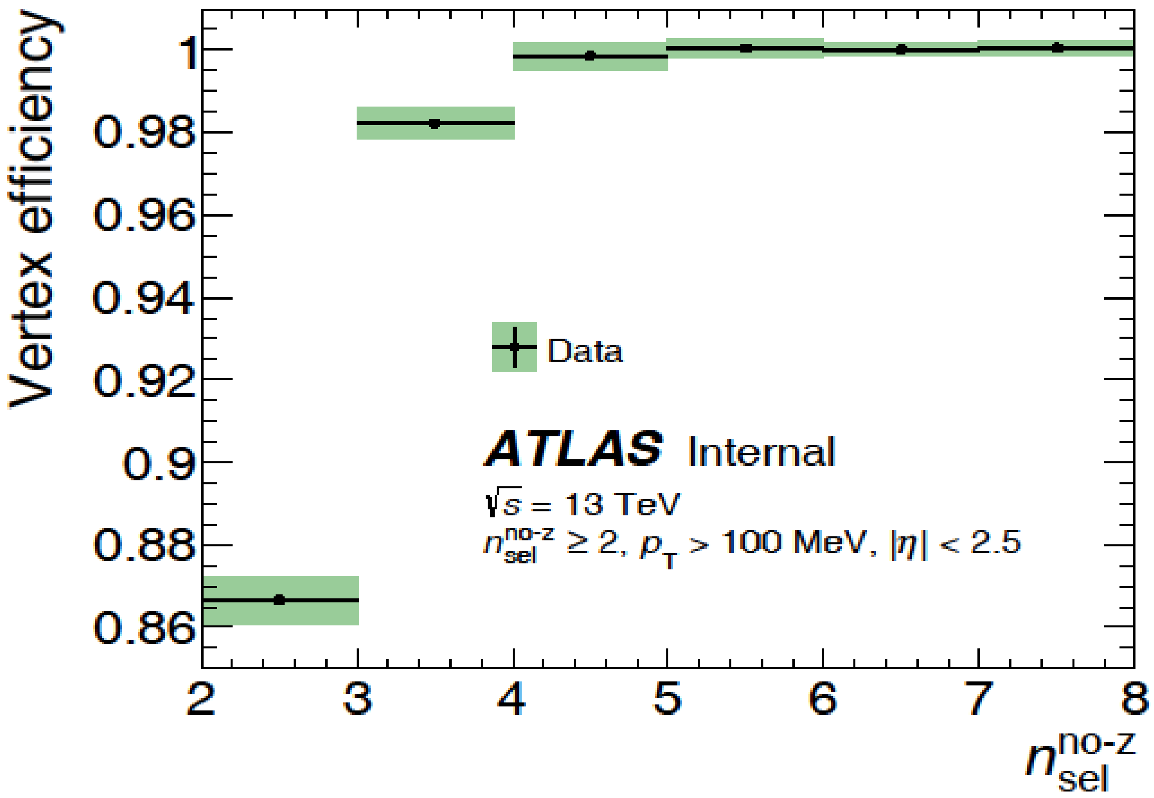

The vertex reconstruction efficiency, ε_{vert} (n)

R

TRACK RECONSTRUCTION CORRECTIONS

Performed corrections on:

1. The reconstruction track efficiency – ε (pt,η),
2. The fraction of non-primary (secondaries and fake) tracks – f_{nonp}(pt,η),
3. The fraction of tracks for which the corresponding primary particles are outside the kinematic range – f_{okr}(pt,η),
4. The strange barion tracks – f_{sb}(pt,η),

We use the formula, **as in MB studies**:

$$w_i\,(pT,\eta) = \frac{(1 - fnonp(p_T,\eta) - fokr(p_T,\eta) - fsb(p_T,\eta))}{\varepsilon(p_T,\eta)}$$

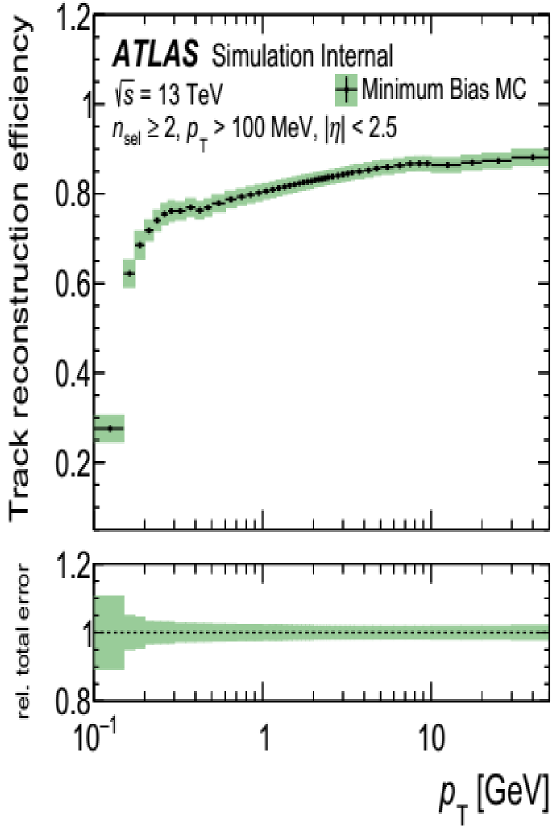

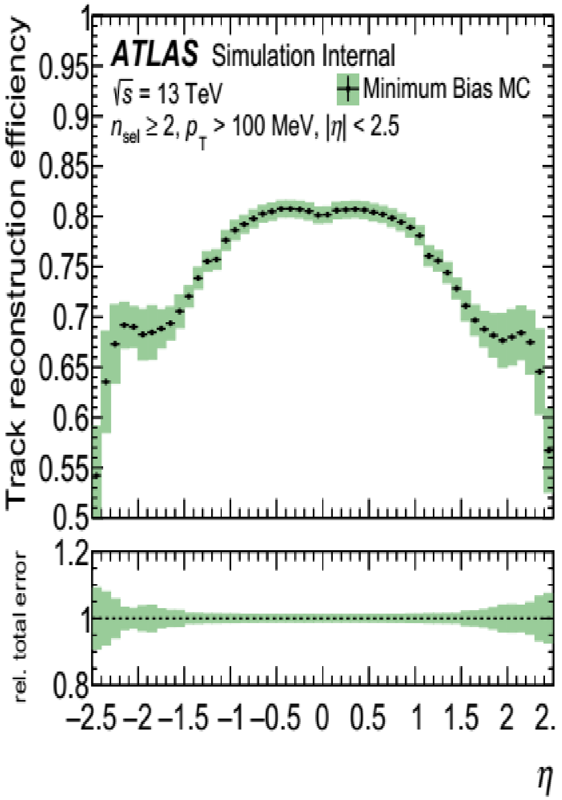

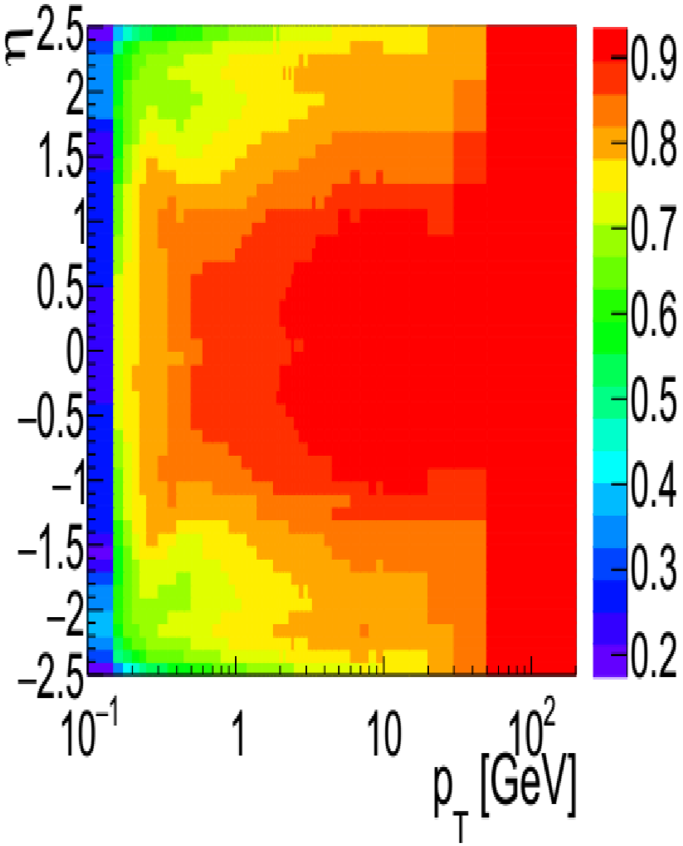

The primary track reconstruction efficiency integrated over p_T (left), integrated over η (middle) and as function of p_T and η (right). The green shaded error band includes the total systematic and statistical uncertainty

Multiplicity unfolding from MB analysis

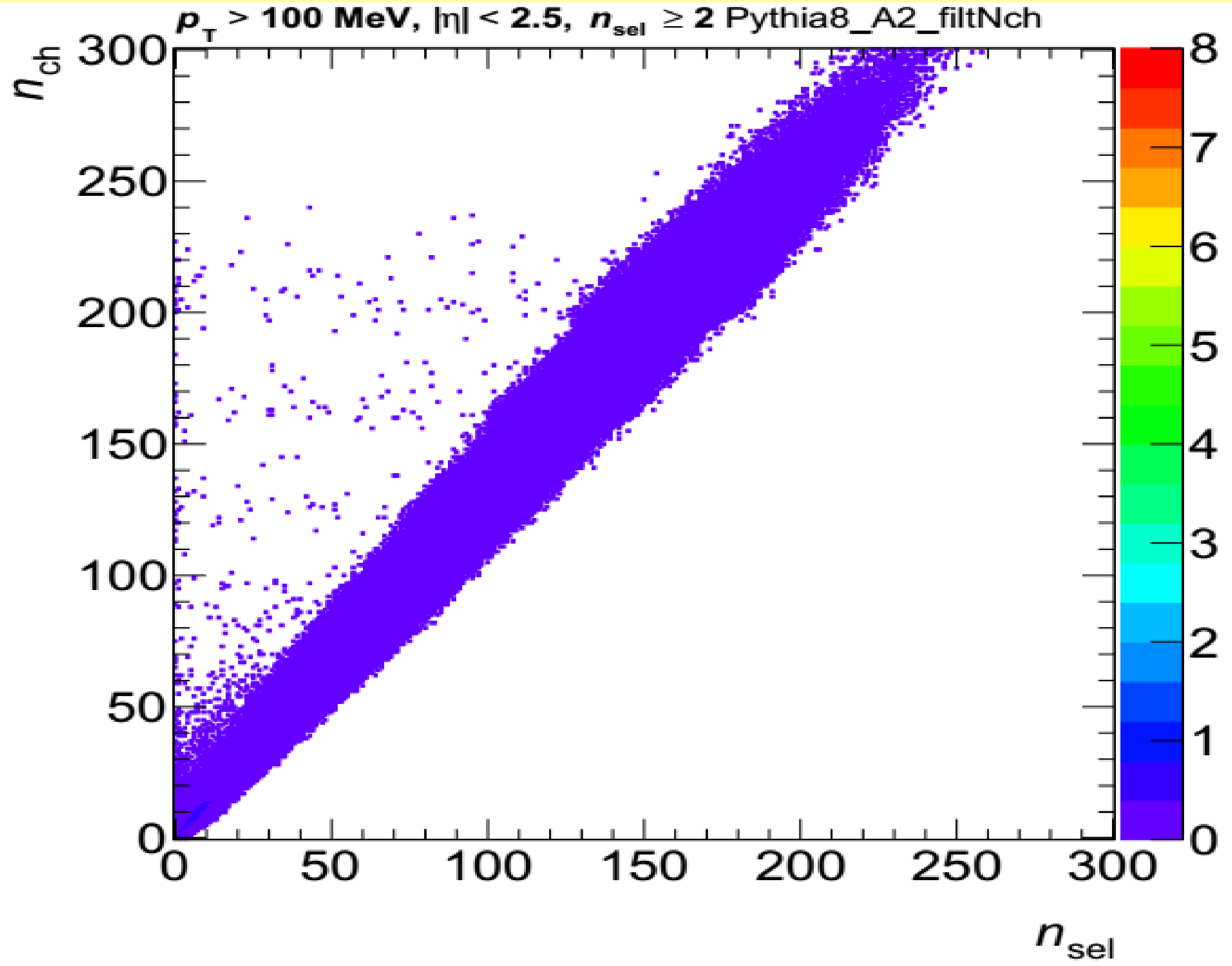

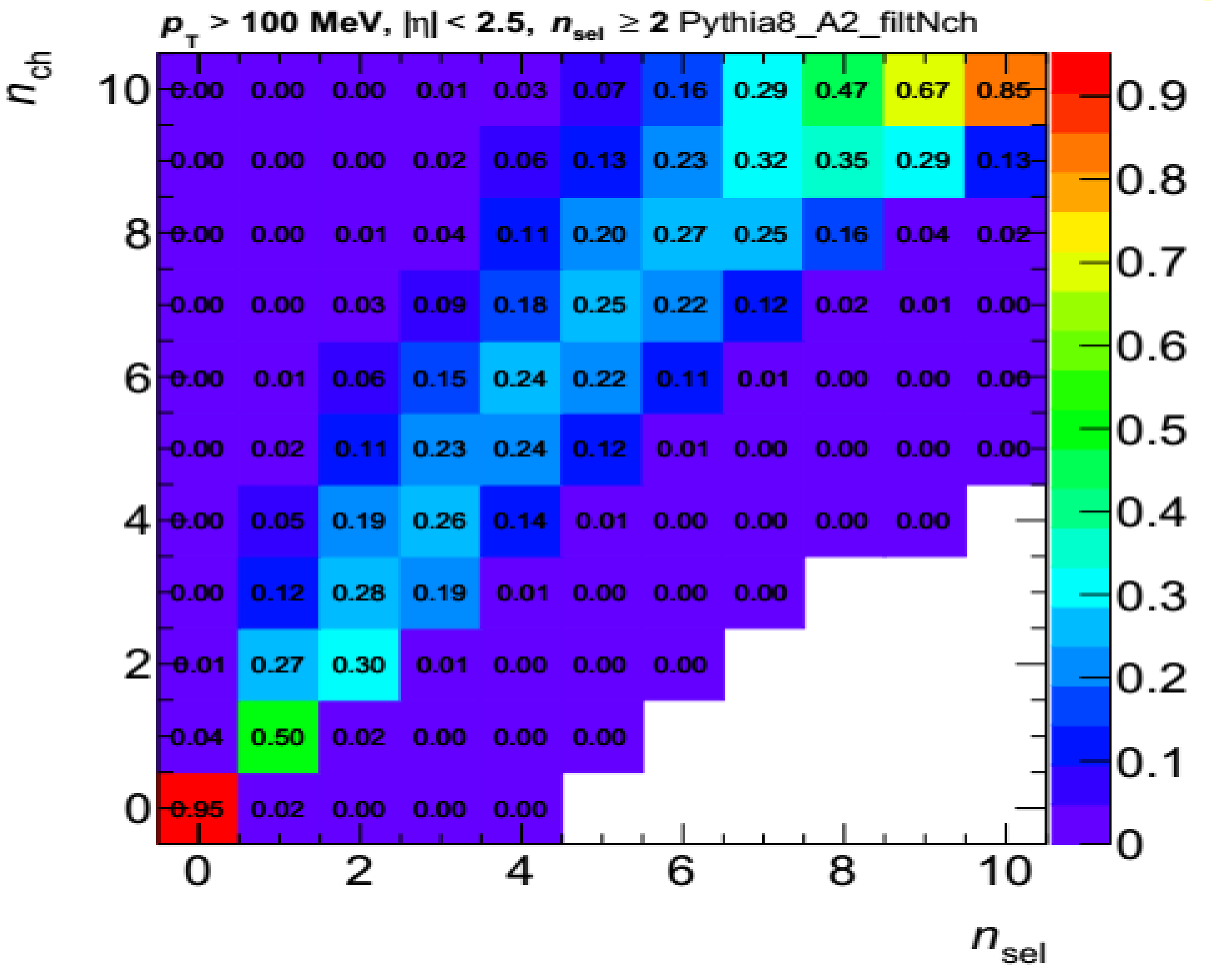

Migration matrix derived from Pythia 8 A2. Left: The full unfolding matrix. Right: The rows are normalized to one. The matrix is shown for the first iteration. There are several events with low n_{sel} but high n_{ch}. These events are caused by the tracking inefficiency where no track were found.

COULOMB CORRECTION

The measured N(Q) distribution for like or unlike signed particle (track) pairs in presence of the Coulomb interaction is given by:

$$N_{meas}(Q) = G(Q)N(Q)$$

where $N_{meas}(Q)$ is the measured distribution, *N(Q) is the distribution free of Coulomb correlations.*

Gamow penetration G(Q) factor $G(Q) = \frac{2\pi\eta}{e^{2\pi\eta} - 1}$

Sommerfeld parameter η $\eta = \frac{\pm\alpha_m}{|Q|}$

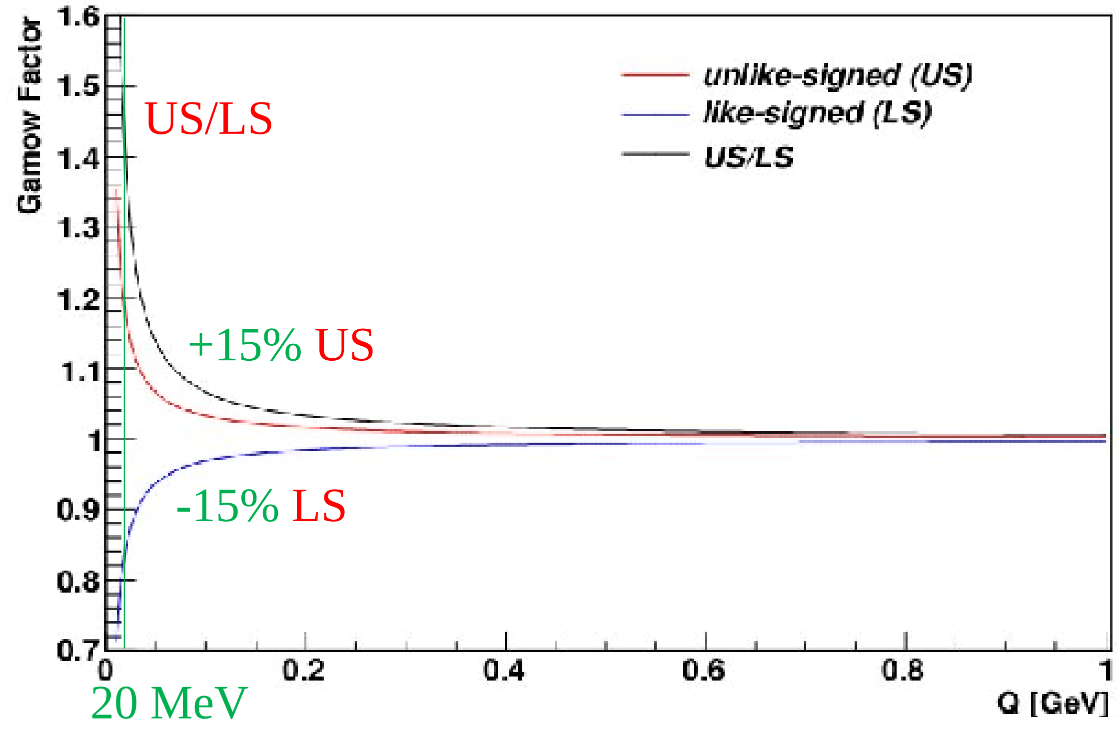

Gamow correction factor for like-signed (LS) particle pairs (blue curve), unlike-signed (US) particle pairs (red curve), for ratio of US to LS (black curve)

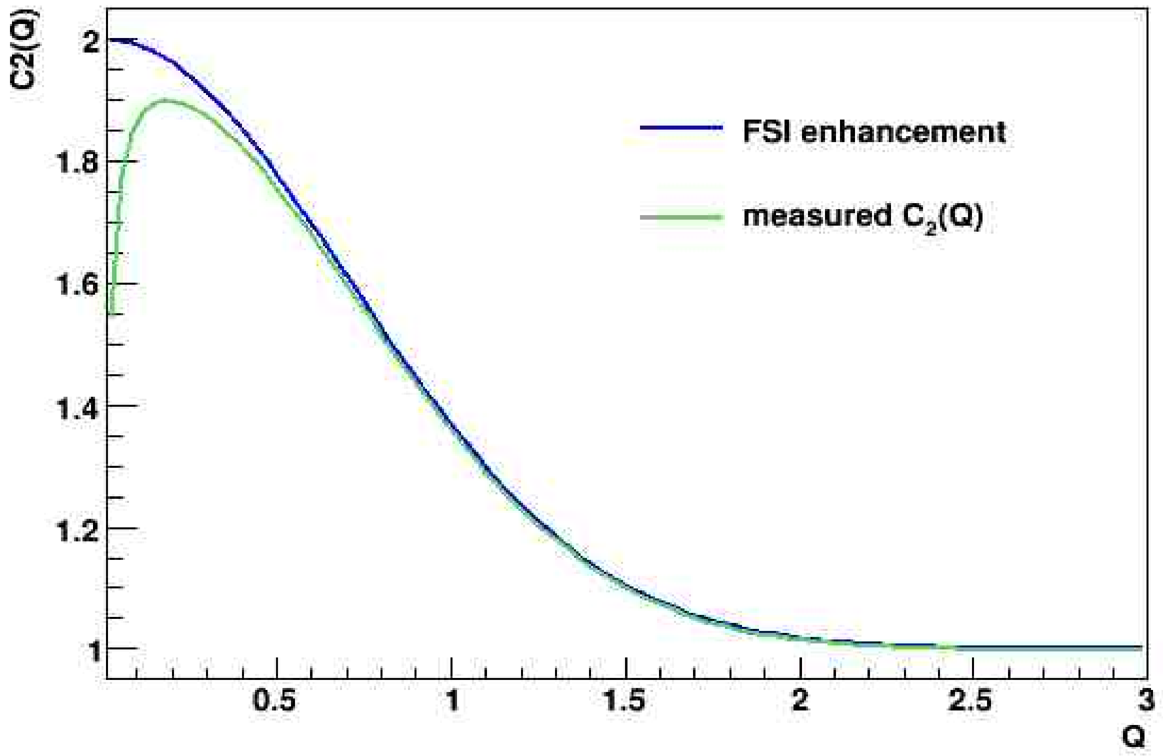

Ratio of the same two particle $C_2(Q)$ correlation functions with and without Coulomb correction. FSI is final state interactions

RESONANCES STUDY

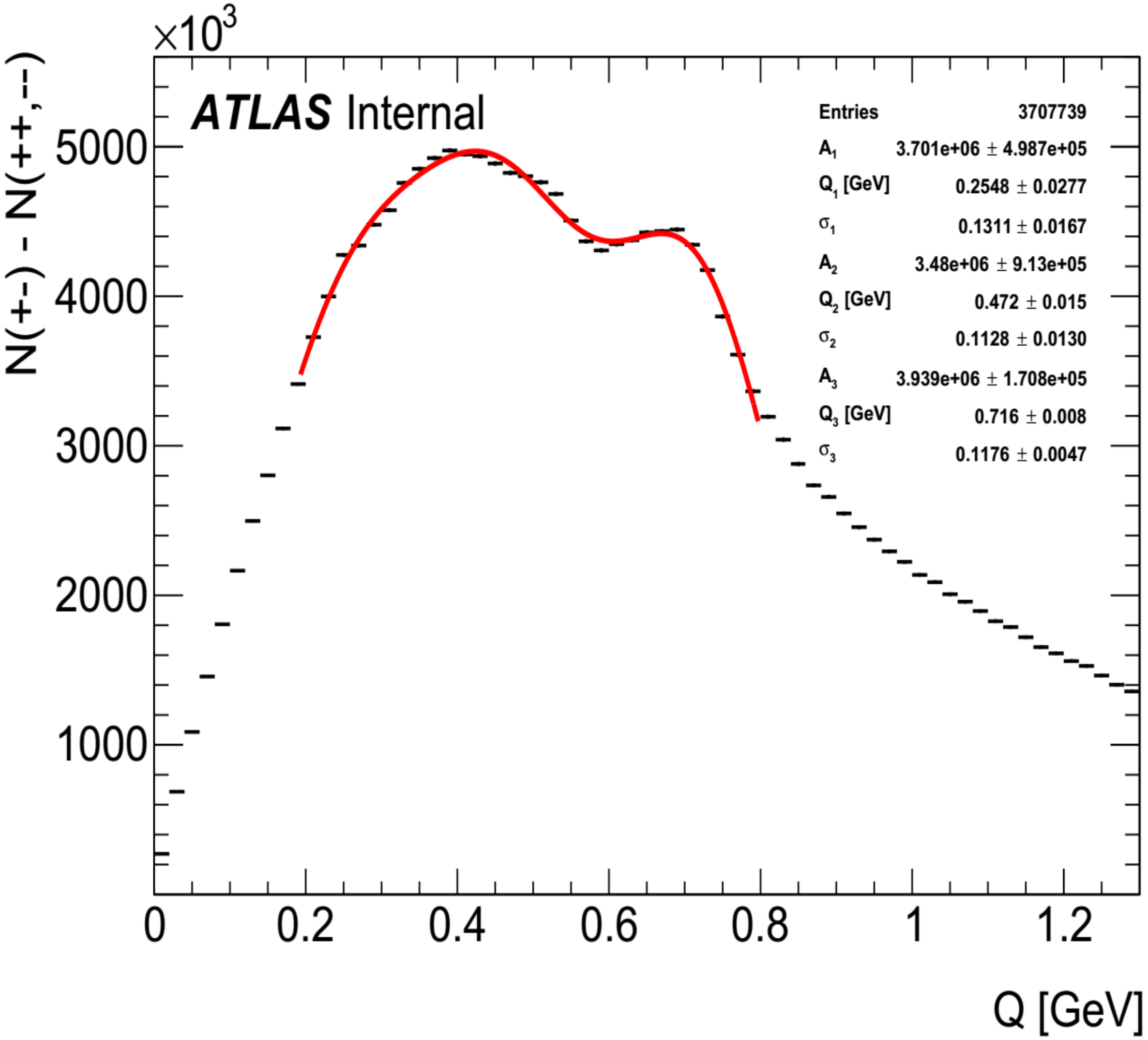

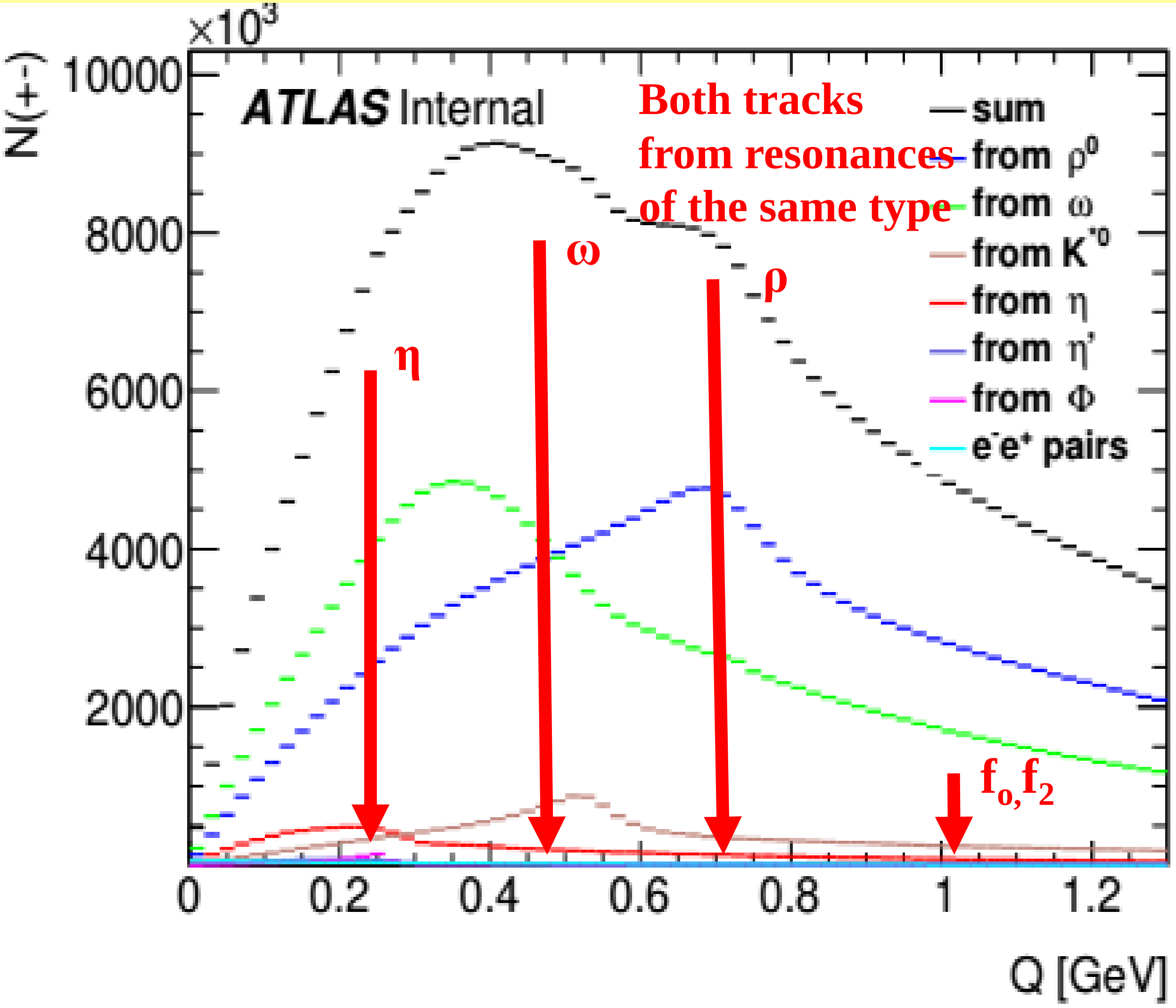

Left: Difference of unlike-charge particles (UCP) and like-charge particles (LCP) distributions fitted by 3 Gaussian.

Right: UCP N(Q) spectra for the track pairs with both tracks from resonances of the same type.

The Q spectrum generated by Pythia8 A2.

Zoom of inclusive R_2 distribution

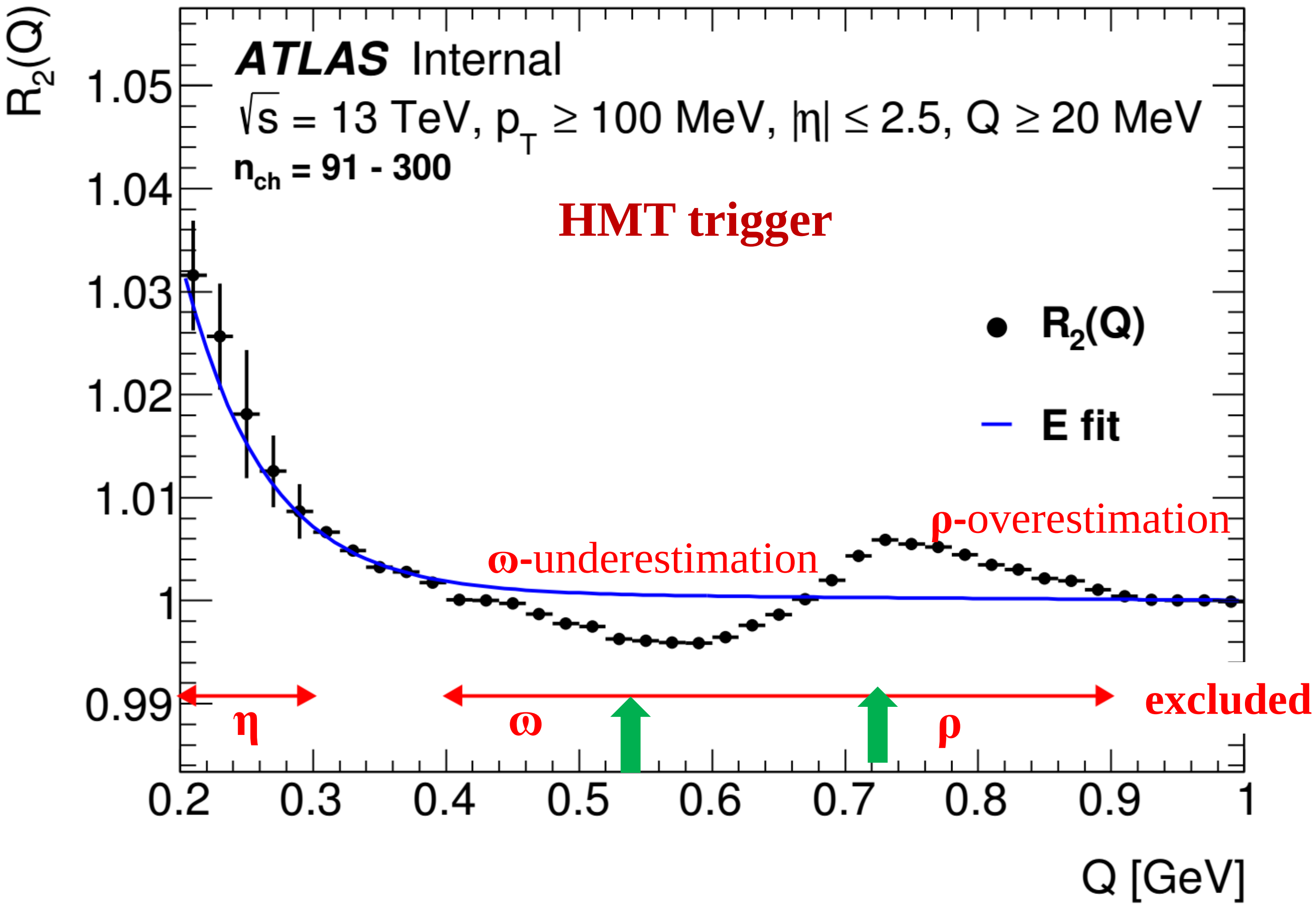

Inclusive HMT two particles R_2 correlation function

$R_2 = C_2^{data}/C_2^{MC} = N_{data}^{\pm\pm}/N_{MC}^{\pm\pm}\ \ N_{MC}^{+-}/N_{data}^{+-}$

Three bump regions because MC underestimated or overestimates:

1) $\eta \to \pi^+\pi^-\pi^o$ and $\eta' \to \pi^+\pi^-\gamma$;
2) $\omega \to \pi^+\pi^-\pi^o$ and $\rho \to \pi^+\pi^-$,
3) $f_2 \to \pi^+\pi^-$;

The excluded regions at 13 TeV

1) 0.2–0.3 GeV – not important after non-closure correction;
2) 0.4–0.9 GeV – important;
3) 1.0–1.16 GeV (only for $2 \le n_{ch} \le 40$ and $100 \le k_T \le 200$ MeV) – not important for BEC.

The excluded region at 7 TeV was 0.5–0.9 GeV.

Examples of $R_2(Q)$ distributions for p_T>100 MeV

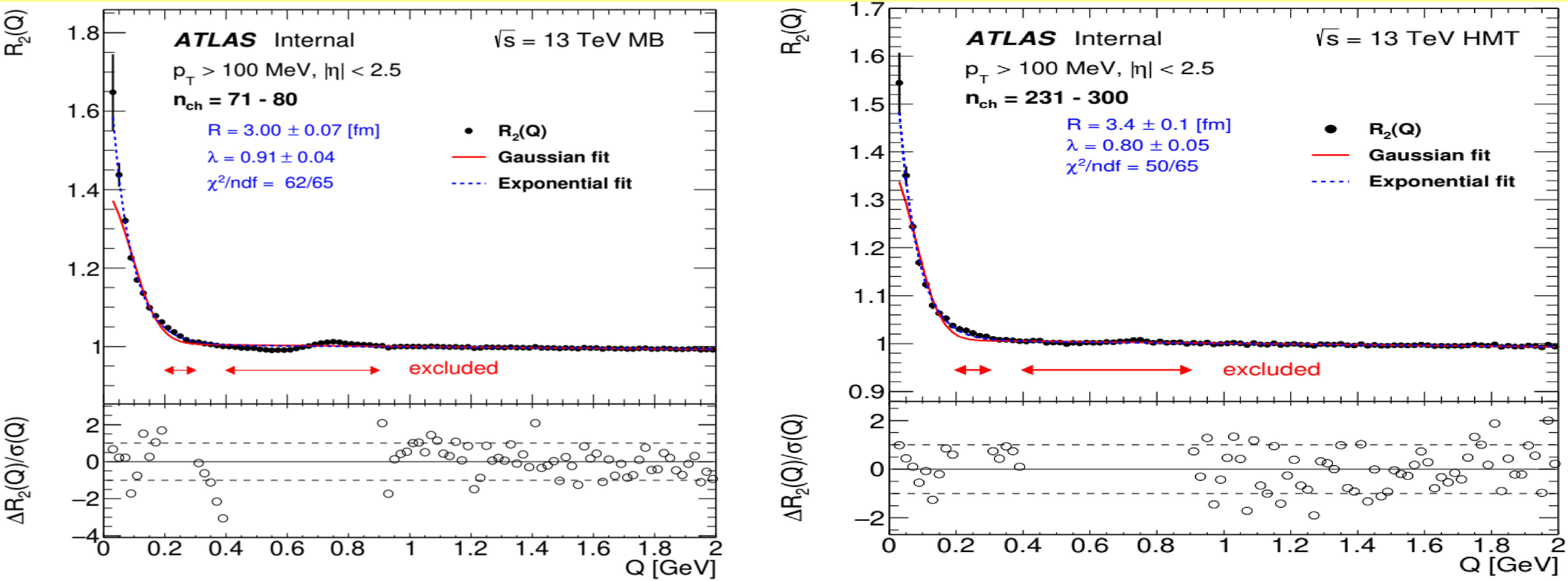

The two-particle double-ratio correlation function, $R_2(Q)$, for *pp* collisions for track p_T>100 MeV at 13 TeV in the multiplicity intervals (left) 71≤n_{ch}<80 for MB events, and (right) 231≤n_{ch}<300 for HMT events. The blue dashed lines show the results of the exponential fit. The region excluded from the fits is shown. The statistical uncertainty and the systematic un-closure uncertainty taken in quadrature are indicated. The difference between the experimental $R2(Q)$ function and the result of the exponential fit normalised to the experimental uncertainty, $\Delta R2(Q)/\sigma(Q)$, is presented.

Comparison of $C_2(Q)$ and $R_2(Q)$ with OHP reference sample

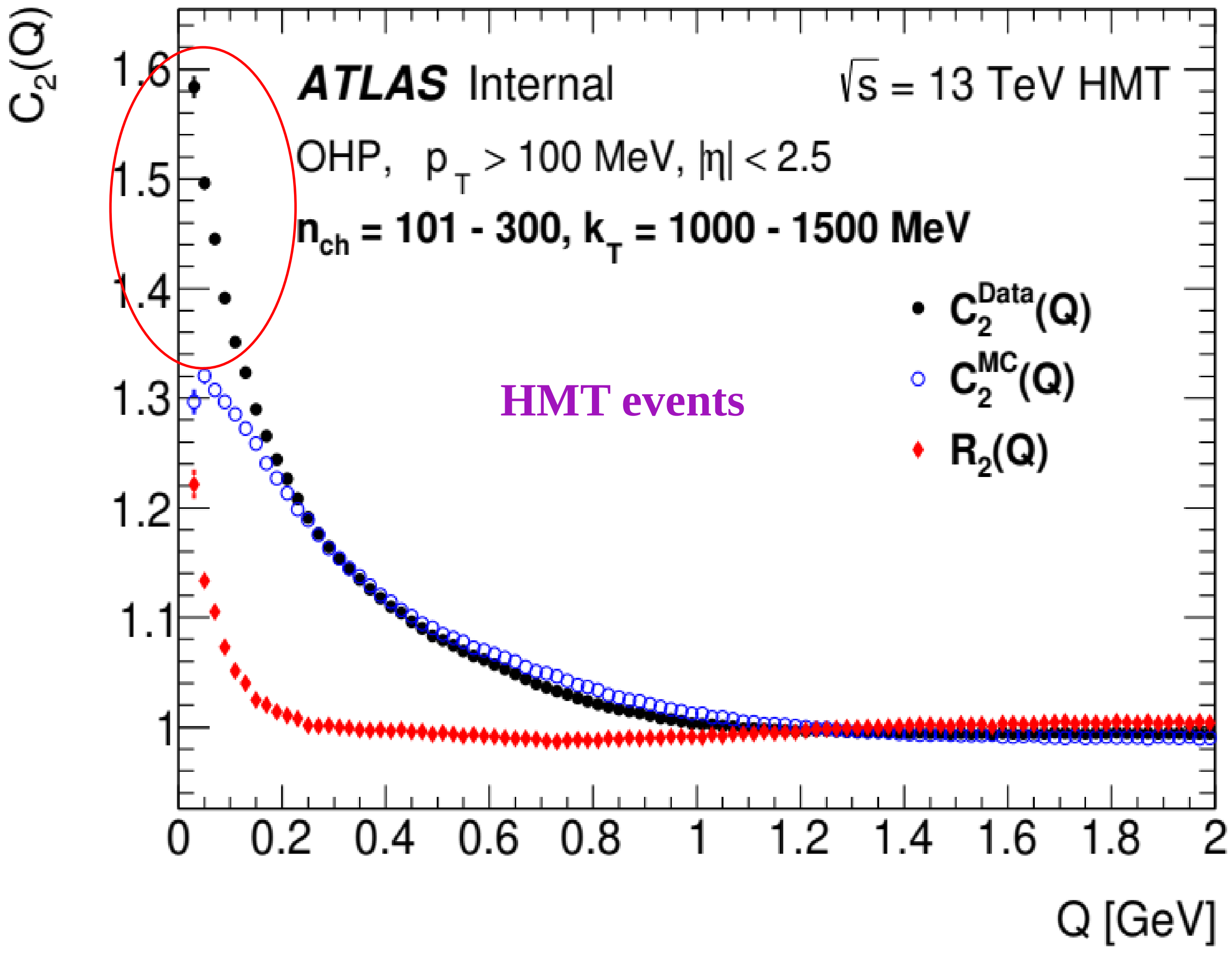

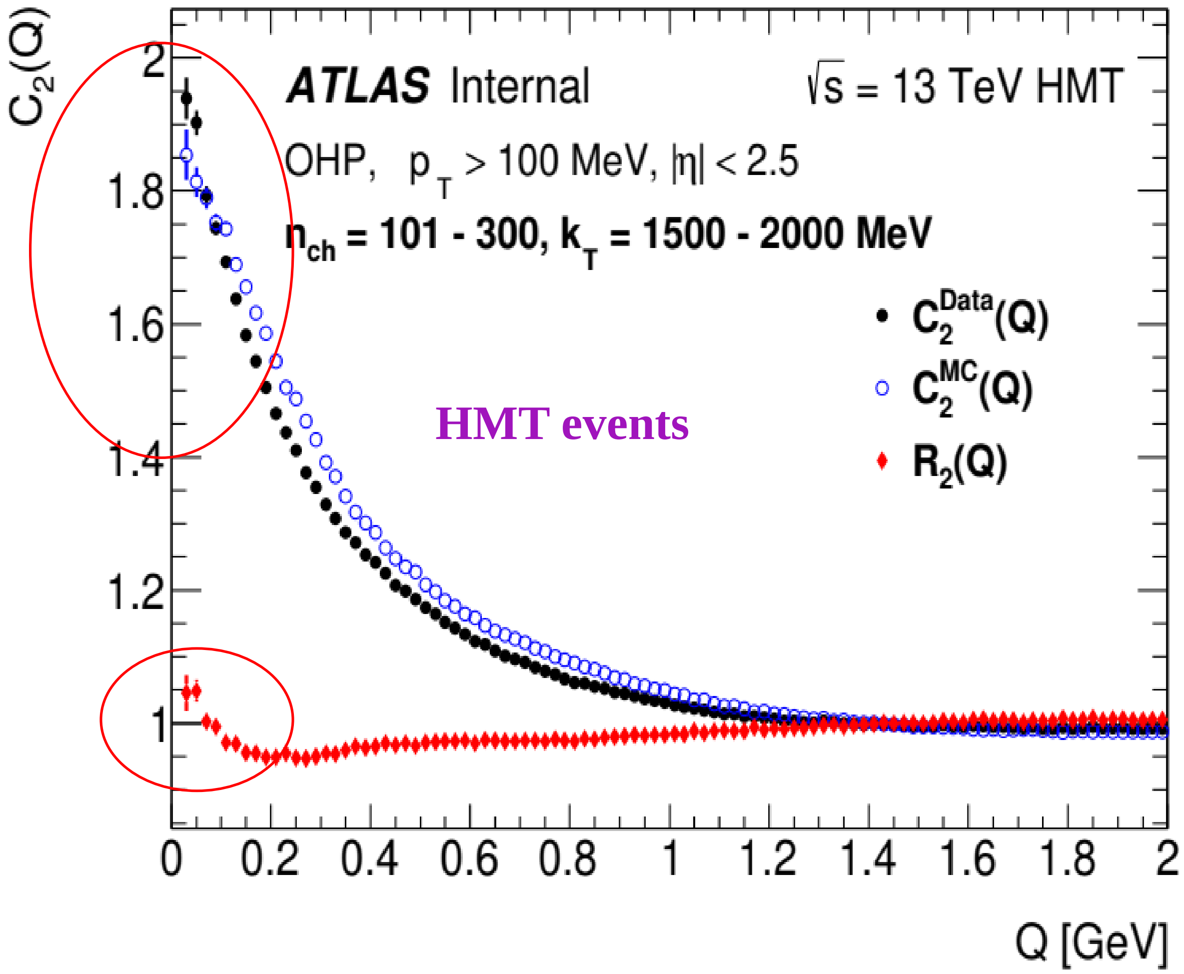

Comparison of single-ratio two-particle correlation functions, $C_2^{data}(Q)$ and $C_2^{MC}(Q)$, with two-particle double-ratio correlation function, $R_2(Q)$, with the opposite hemisphere (OHP) like-charge particles pairs reference sample for HMT events for kT-intervals: (left) $1000 \leq k_T \leq 1500$ MeV and (right) $1500 \leq k_T \leq 2000$ MeV.

SYSTEMATIC UNCERTAINTIES FOR BEC AT 13 TeV

The systematic uncertainties of the spread for n_{ch} distribution and inclusive fit BEC parameters, *R* and *λ*. The systematic uncertainties are combined by adding them in quadrature and the resulting values are given in the bottom row. The same sources of uncertainty are considered for the measurements in multiplicity, n_{ch}; the average pair transverse momentum, k_T; the two-differential measurements in (n_{ch}; k_T)- intervals, and their impact on the fit parameters is found to be similar in size.

1. **Track reconstruction efficiency:** ω±δω
2. **Monte Carlo: EPOS, Pythia8 Monash**
3. **Coulomb correction:** ±15%
4. **Fitted range of Q:** 2 GeV±3σ_Q(0.1 GeV)
5. **Starting value, Q_{min}:** 10, 20, 30 MeV
6. **Bin size:** 10, 20, 30 MeV
7. **Excluded intervals:** ±20 MeV

Sources	13 TeV				13 TeV (HMT)			
	λ (%)	R (%)	λ (%)	R (%)	λ (%)	R (%)	λ (%)	R (%)
	n_{ch} − spread		Inclusive		n_{ch} − spread		Inclusive	
Track reconstr. efficiency	0.0–0.4	0.1–0.4	0.3	0.1	0.1–0.2	0.01–0.1	0.2	0.01
Track splitting and merging	negligible				negligible			
Monte Carlo samples	0.0–6.9	0.5–7.0	1.1	1.4	1.0–16.	1.0–14.	1.4	0.7
Coulomb correction	1.3–2.0	0.01–0.6	1.8	0.1	1.7–1.9	0.2–0.4	1.8	0.3
Fitted range of Q	0.0–0.5	0.02–0.9	0.2	0.3	0.0–0.2	0.0–0.2	0.02	0.03
Starting value of Q	0.0–1.9	0.01–1.1	0.3	0.2	0.5–1.4	0.3–0.7	0.7	0.4
Bin size	0.0–2.4	0.1–1.5	0.8	0.4	1.0–1.7	0.4–0.9	1.3	0.6
Exclusion intervals	0.0–1.1	0.3–0.8	0.1	0.3	0.4–0.6	0.3–0.6	0.5	0.5
Total	1.3–7.9	0.9–7.2	2.4	1.5	3.0–17.	1.0–15.	2.8	1.2

MULTIPLICITY DEPENDENCE OF BEC PARAMETERS AT 0.9 –13 TEV

EPJC 75 (2015) 10, 466; ATL-COM-PHYS-2016-1621

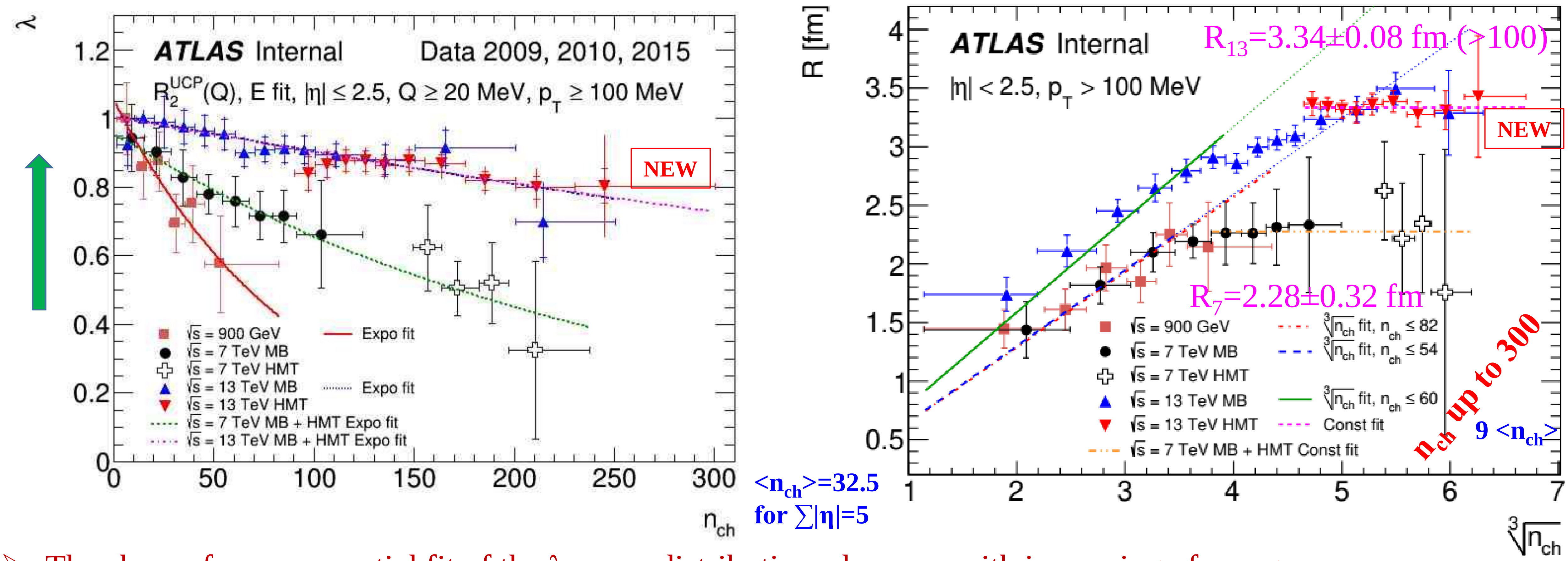

- The slope of an exponential fit of the λ vs n_{ch} distributions decrease with increasing of energy.
- The parameters α of the $\alpha \cdot n_{ch}^{1/3}$ fit of R vs n_{ch} for $n_{ch} \leq 55$ at 0.9 TeV is **α=0.64±0.07 fm,** 7 TeV is **α=0.63±0.05 fm** and for $n_{ch} \leq 70$ at 13 TeV is **α=0.77±0.03 fm.**
  For multiplicity region $n_{ch} \leq 70$, the R values are systematically higher at 13 TeV than at 7 TeV.
- The R is a constant for $n_{ch}>55$ at 7 TeV **R=2.28±0.32 fm** and for $n_{ch}>100$ at 13 TeV **R=3.35±0.08 fm.** The R is systematically higher at 13 TeV than at 7 TeV but in the error bars is in agreement.

AVERAGE MULTIPLICITY DEPENDENCE OF BEC PARAMETERS AT 0.9 –13 TEV

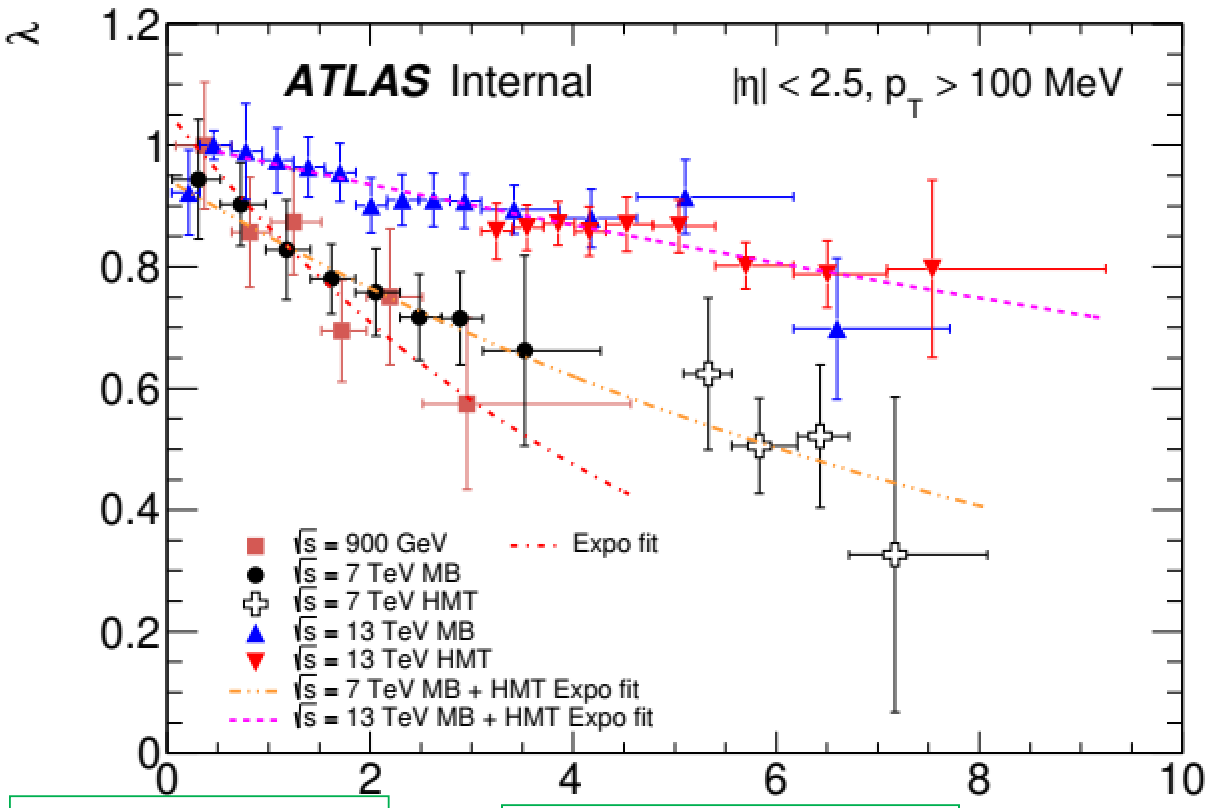

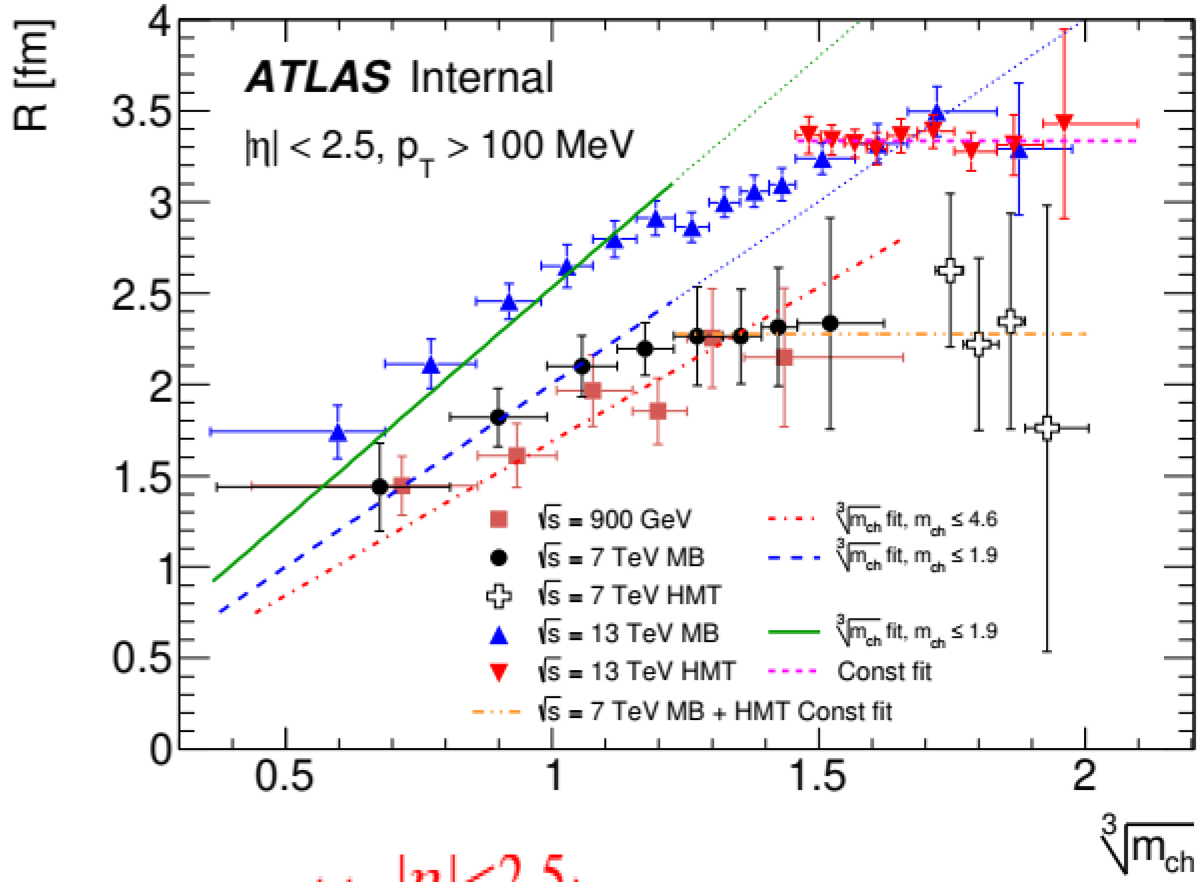

$$\langle n^0_{\rm ch}\rangle = \frac{1}{N_{\rm ev}}\frac{dn_{\rm ch}}{d\eta}\bigg|_{\eta=0}$$

$$\langle n_{\rm ch}\rangle = \langle n^0_{\rm ch}\rangle \int_{-2.5}^{2.5} d\eta = 5\,\langle n^0_{\rm ch}\rangle$$

$$m_{\rm ch} = n_{\rm ch}/\langle n_{\rm ch}^{|\eta|<2.5}\rangle$$

Dependence of the correlation strength, $\lambda(m_{\rm ch})$, and source radius, $R(m_{\rm ch})$, on average rescaled multiplicity, $m_{\rm ch}$, obtained from the exponential fit to the two-particle double-ratio correlation functions, $R_2(Q)$, for $p_{\rm T}$ > 100 MeV at 0.9, 7 and 13 TeV for the minimum-bias (MB) and high multiplicity track (HMT) data.

The uncertainties shown represent the quadratic sum of the statistical and systematic contributions.

ENERGY DEPENDENCE FOR <N_{CH}> AT 0.9 –13 TEV

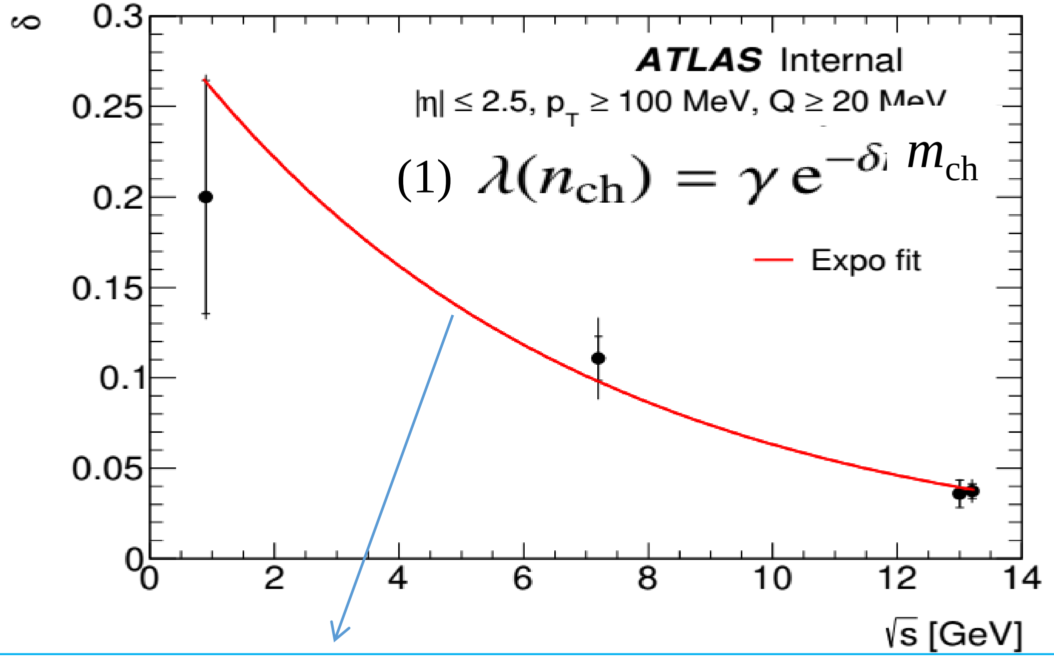

(1) $\lambda(n_{ch}) = \gamma\, e^{-\delta\, m_{ch}}$

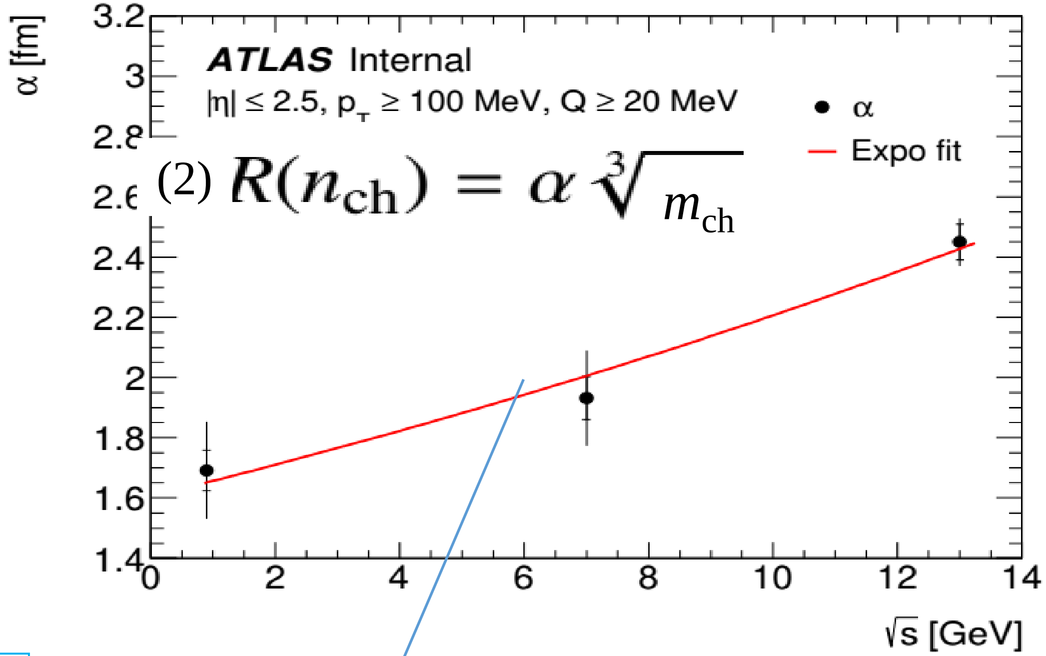

(2) $R(n_{ch}) = \alpha \sqrt[3]{m_{ch}}$

$$(0.30 \pm 0.06 \pm 0.05)\, e^{-(0.157\pm0.019\pm0.003)\,[\mathrm{GeV}^{-1}]\,\sqrt{s}} \quad (\chi^2/ndf = 2/2)$$

Energy dependence of the parameter δ in Eq. (1) for correlation strength λ from the average charged particle multiplicity. Energy dependence of the parameter α in Eq. (2) for source radius R from the average charged particle multiplicity. The two points at 13 TeV are MB and HMT results, respectively. The error bars represent the statistical and systematic uncertainties.

$$(1.60 \pm 0.08 \pm 0.16)\,[\mathrm{fm}]\; e^{(0.032\pm0.005\pm0.006)\,[\mathrm{GeV}^{-1}]\,\sqrt{s}} \quad (\chi^2/ndf = 1.6/1)$$

AVERAGE MULTIPLICITY DEPENDENCE OF BEC PARAMETERS FOR p_T-CUTS

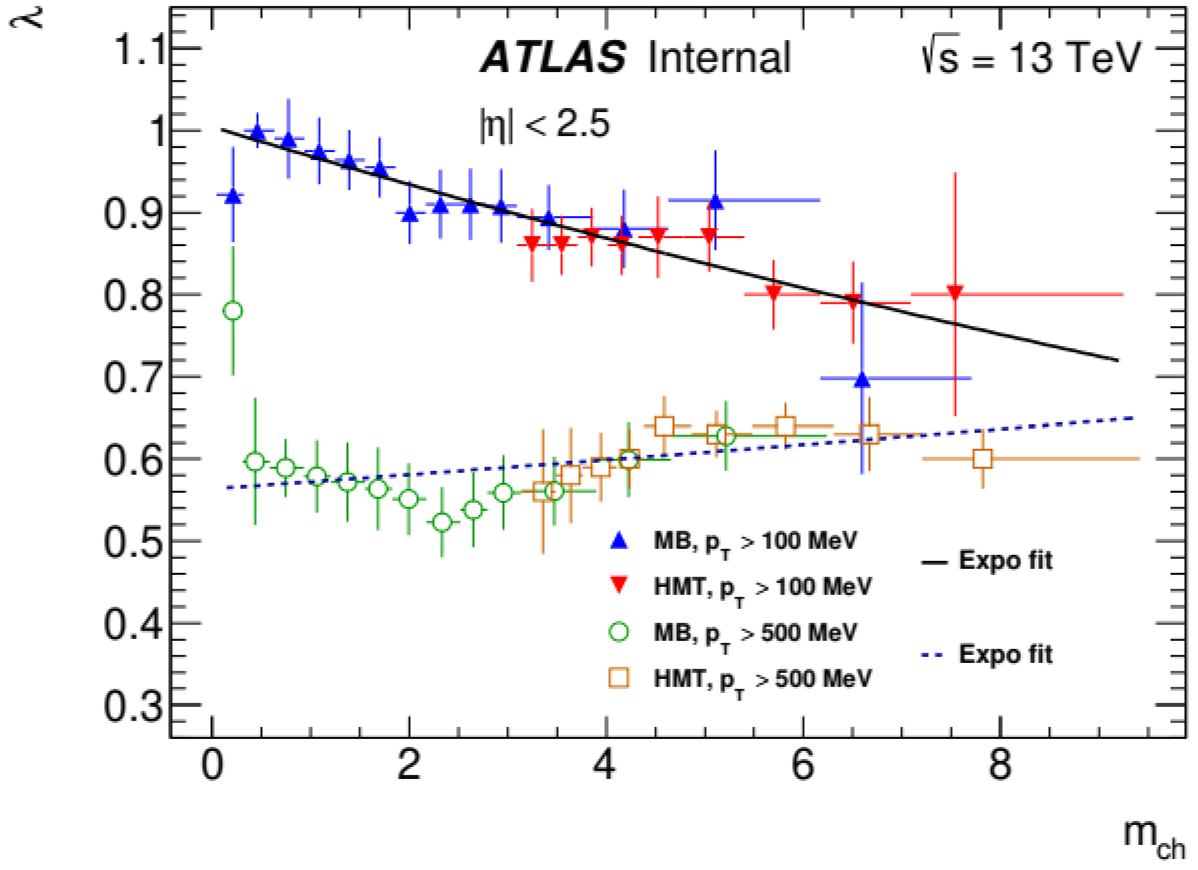

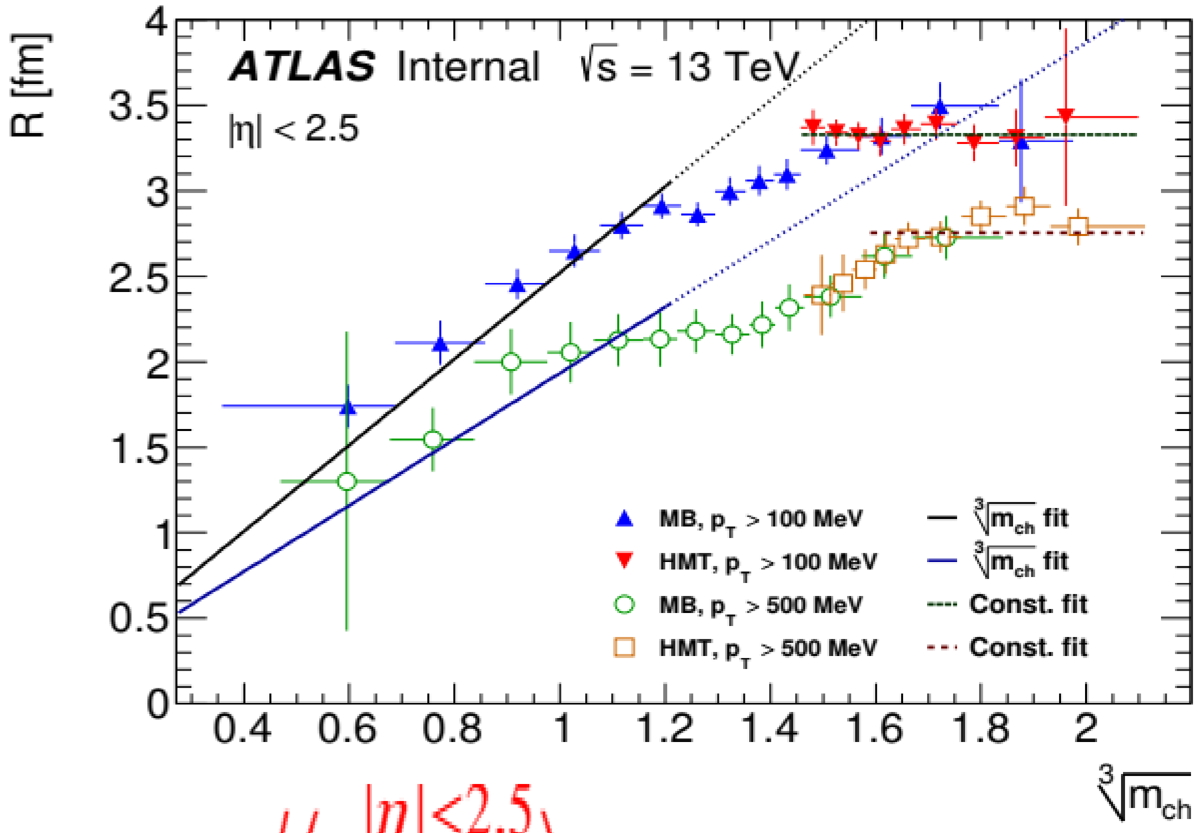

$$m_{\rm ch} = n_{\rm ch} / \langle n_{\rm ch}^{|\eta|<2.5} \rangle$$

The dependence of the parameter correlation strength , $\lambda(m_{\rm ch})$, on rescaled multiplicity, $m_{\rm ch}$, obtained from the exponential fit of the $R_2(Q)$ correlation functions for tracks with $p_T > 100$ MeV and $p_T > 500$ MeV at 13 TeV for the MB and HMT data. The dependence of the parameter source radius, $R(m_{\rm ch})$, on $\sqrt[3]{m_{\rm ch}}$.

The uncertainties represent the quadratic sum of the statistical and systematic contributions.

EPJC 75 (2015) 10, 466;
ATL-COM-PHYS-2016-1621

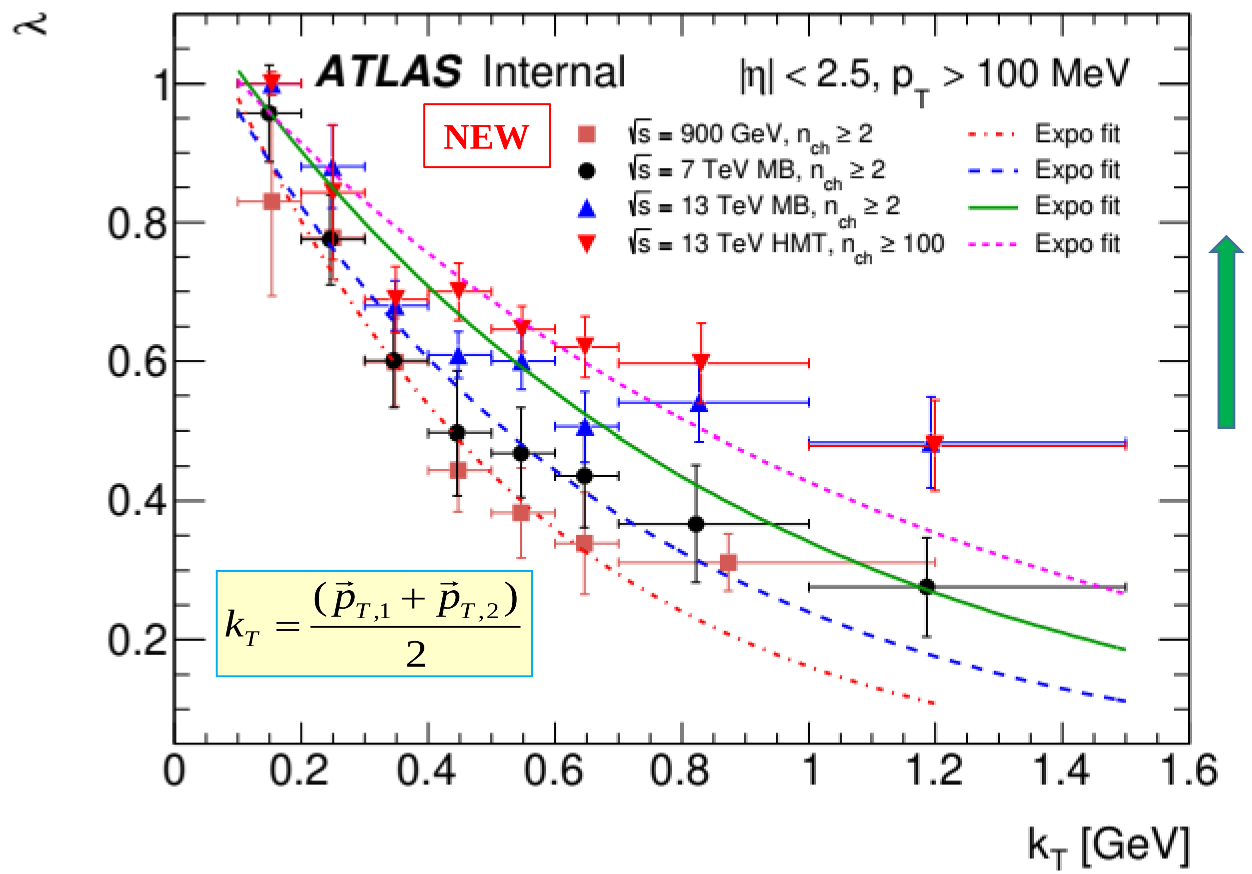

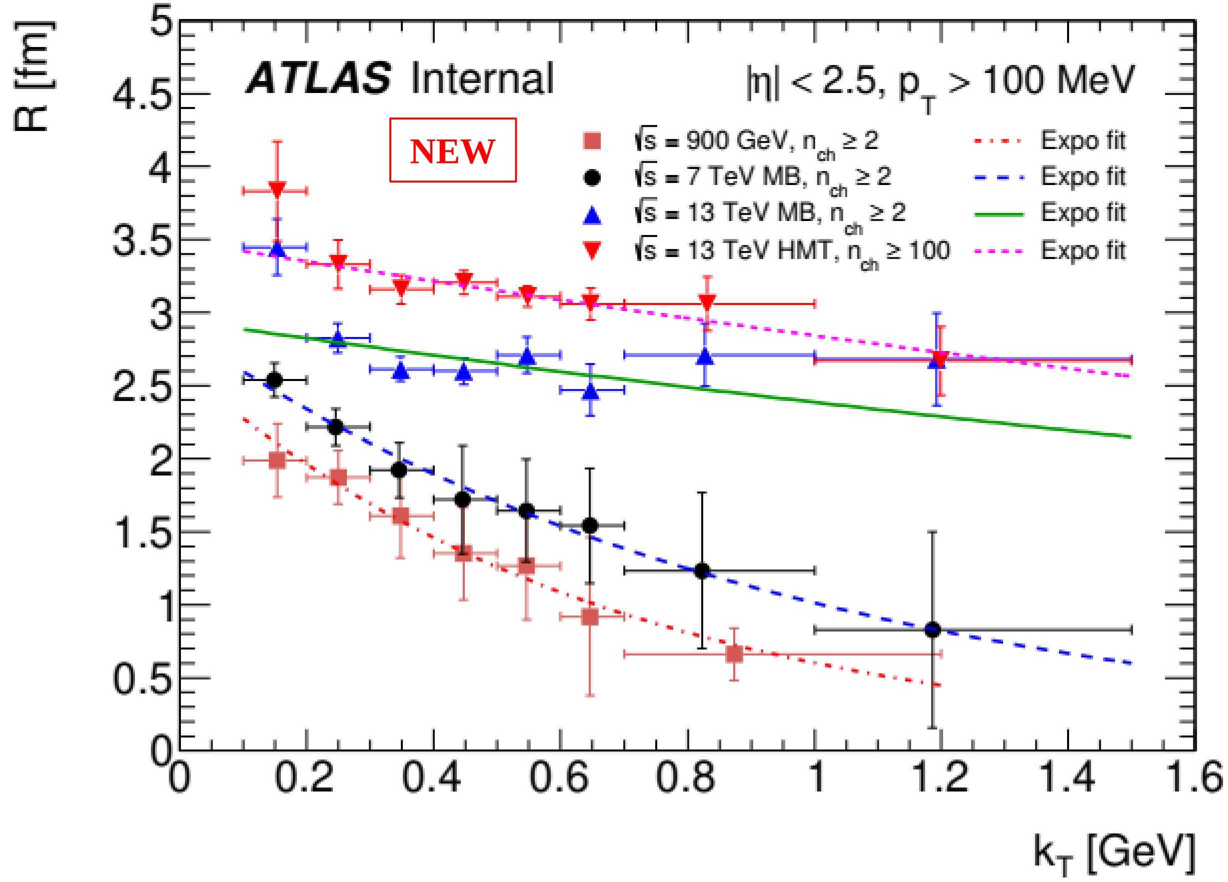

- The amplitude of fit of λ^{MB} vs k_T distributions is decrease from 1.2 to 0.23 with energy increasing.
- The slope of exponential fit of the R values vs k_T distributions decrease from 1.5 to 0.2 with increasing of energy.

ENERGY DEPENDENCE FOR k_T AT 0.9 –13 TEV

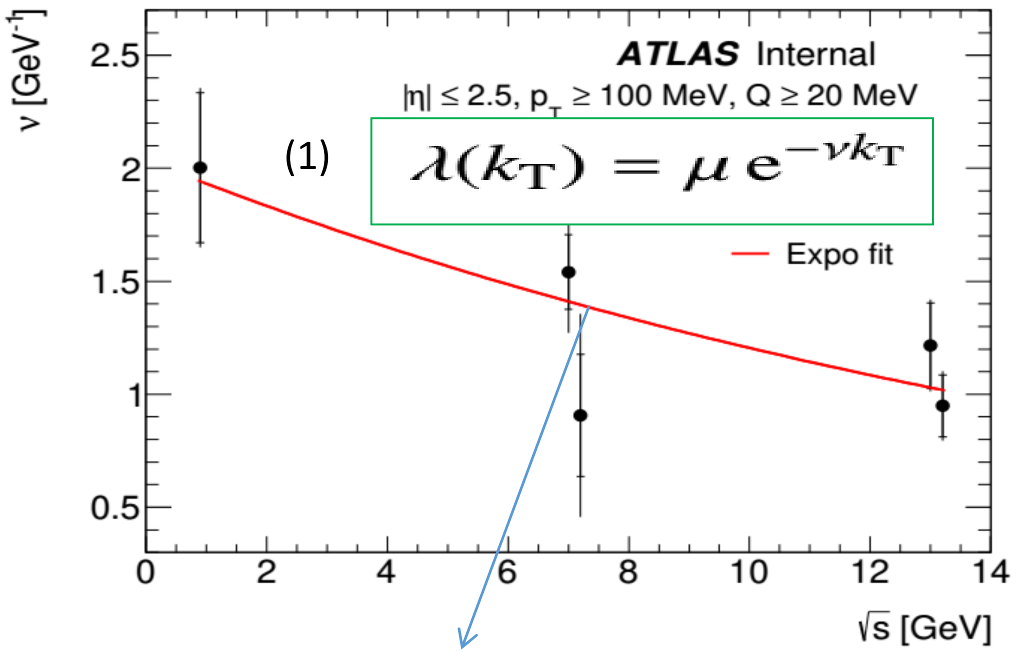

$$\lambda(k_T) = \mu\, e^{-\nu k_T}$$

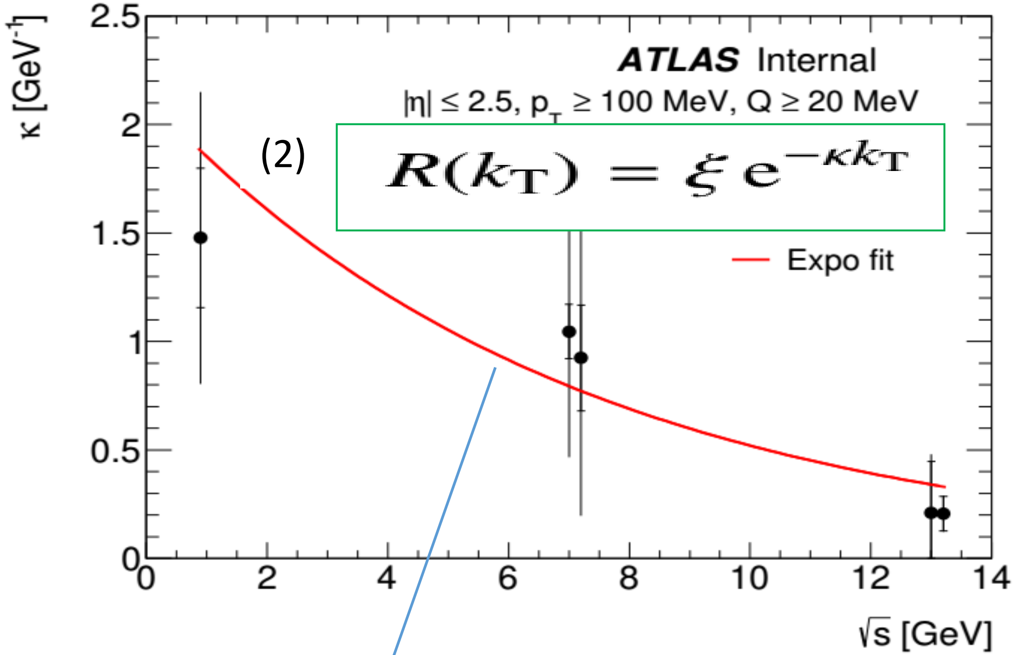

$$R(k_T) = \xi\, e^{-\kappa k_T}$$

$$(2.03 \pm 0.40 \pm 0.30)\,[\mathrm{GeV}^{-1}]\, e^{-(0.053\pm0.021\pm0.003)\,[\mathrm{GeV}^{-1}]\sqrt{s}} \quad (\chi^2/ndf = 5/3)$$

Energy dependence of the parameter ν in Eq. (1) for correlation strength λ from the pair transverse momentum. Energy dependence of the parameter κ in Eq. (2) for source radius R from the pair transverse momentum. The two points at 7 and 13 TeV are MB and HMT results, respectively. The error bars represent the statistical and systematic uncertainties.

$$(2.1 \pm 0.6 \pm 1.1)\,[\mathrm{GeV}^{-1}]\, e^{-(0.141\pm0.034\pm0.005)\,[\mathrm{GeV}^{-1}]\sqrt{s}} \quad (\chi^2/ndf = 9/3)$$

K_T DEPENDENCE OF BEC PARAMETERS AT P_T-CUTS

ATL-COM-PHYS-2016-1621

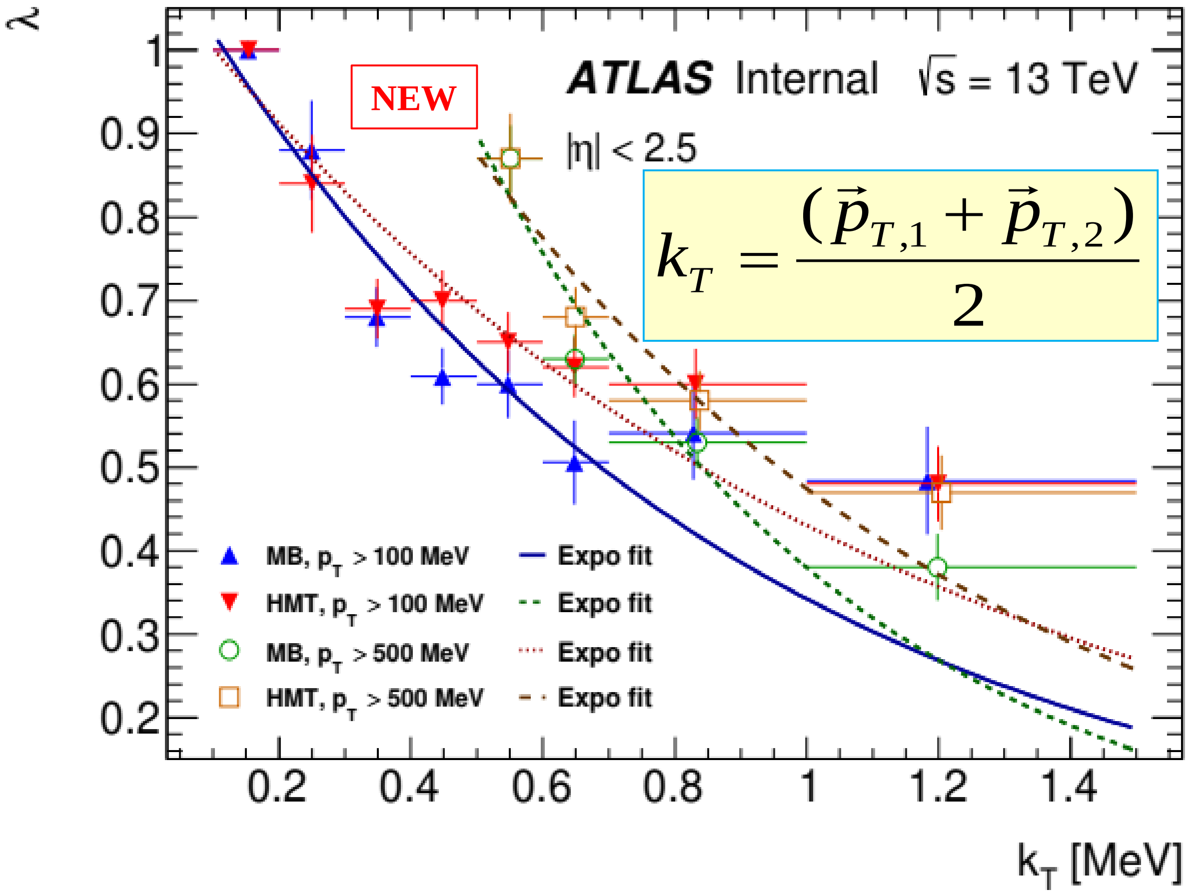

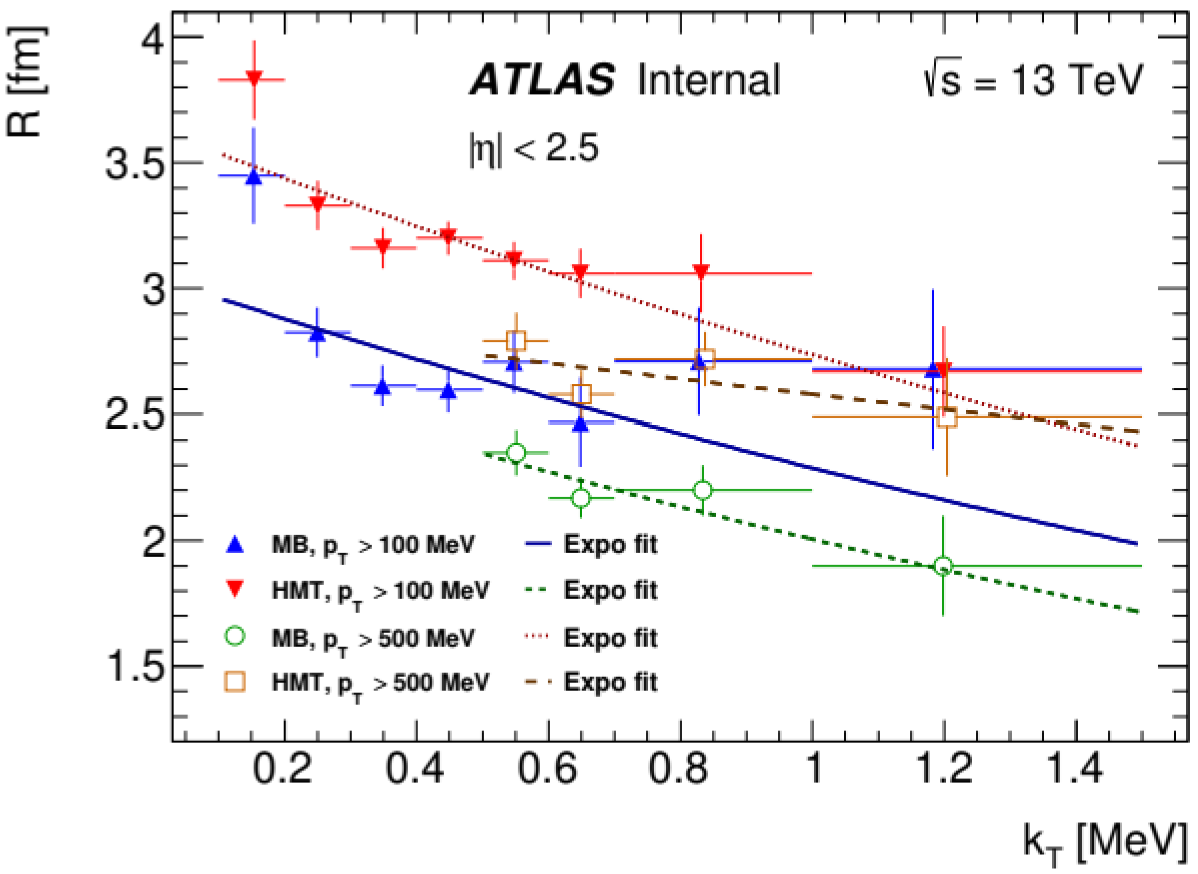

The k_T dependence of the correlation strength, $\lambda(k_T)$, and (b) source radius, $R(k_T)$, obtained from the exponential fit to the $R_2(Q)$ correlation functions for tracks with $p_T > 100$ MeV and $p_T > 500$ MeV at 13 TeV for MB and HMT events. The uncertainties represent the quadratic sum of the statistical and systematic contributions. The curves represent the exponential fit of the $\lambda(k_T)$ and $R(k_T)$.

MULTIPLICITY DEPENDENCE OF BEC PARAMETERS FOR (N_{CH}, K_T) FOR P_T>100 MEV

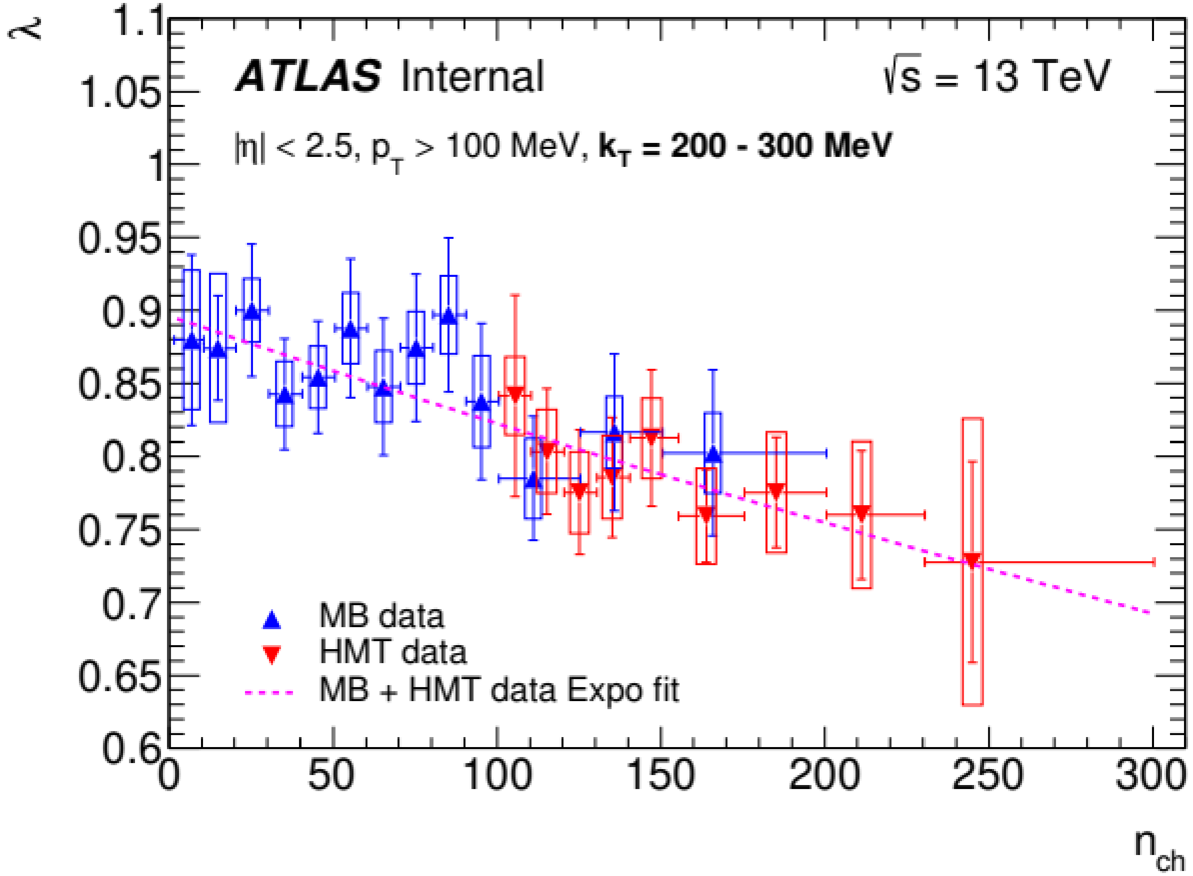

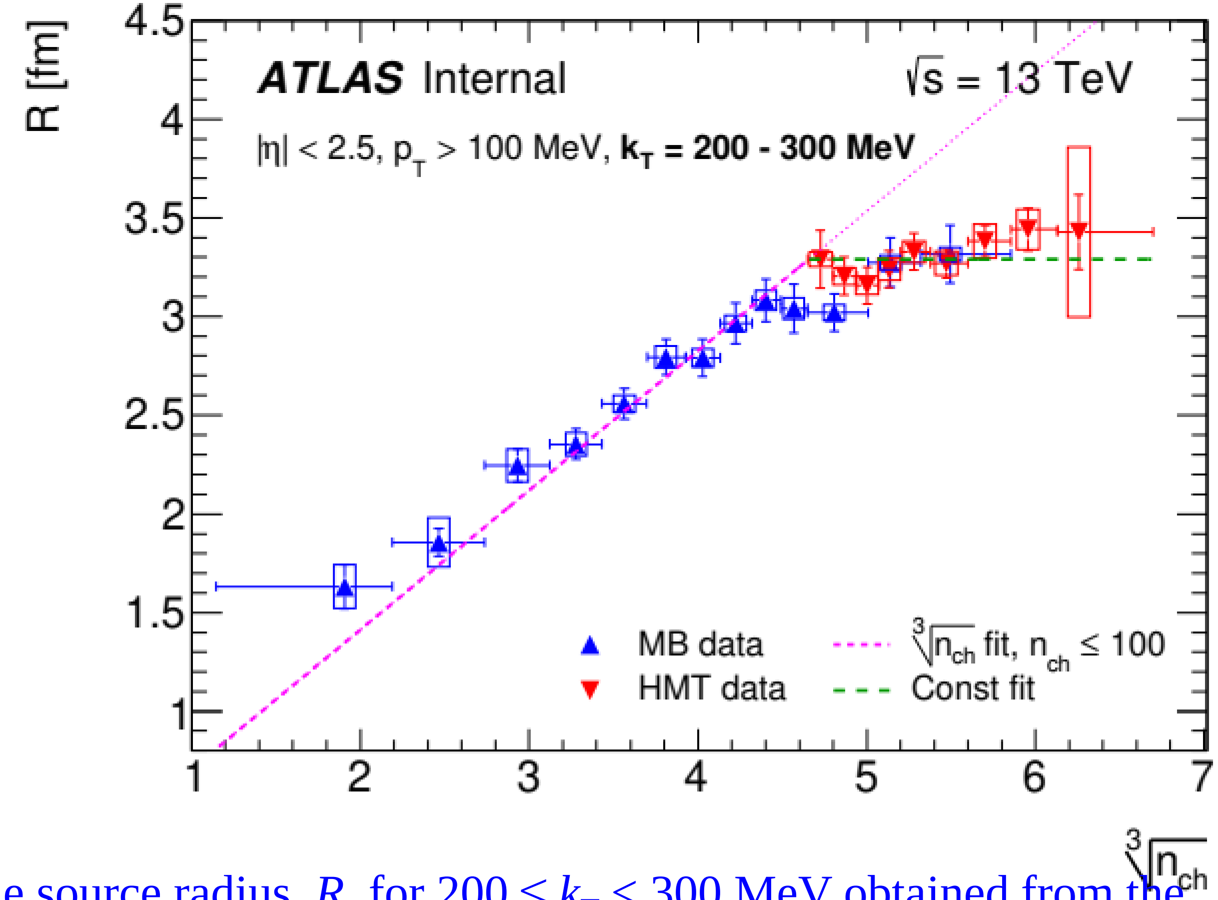

The multiplicity dependence of the correlation strength, λ, and the source radius, R, for $200 \leq k_T < 300$ MeV obtained from the exponential fit to the $R_2(Q)$ correlation functions using the MB and HMT samples.

The error bars shown represent the statistical uncertainties. The boxes represent the systematic uncertainties.

(left) The violet dashed curve represents the exponential fit of the λ multiplicity dependence. (right) The violet dashed curve represents the fitted the $R(n_{ch})$ dependence for $\sqrt[3]{n_{ch}} < 4.7$. The violet dotted curve is a prolongation of the violet dashed curve to stress a disagreement of the fit with data for $\sqrt[3]{n_{ch}} > 4.7$ region. The green dashed curve represents the constant fit of R.

MULTIPLICITY DEPENDENCE OF BEC PARAMETERS FOR (N_{CH}, K_T) FOR P_T>100 MEV

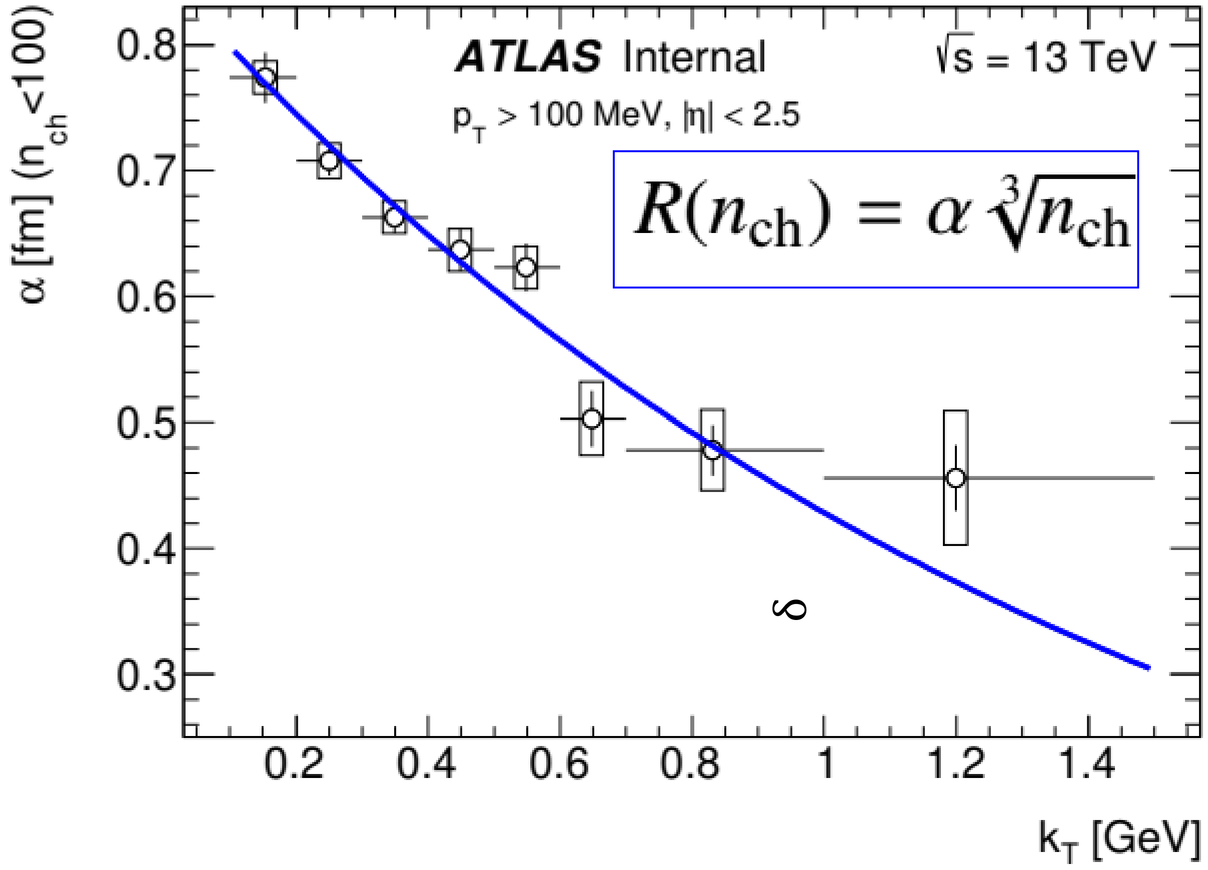

$$R(n_{\rm ch}) = \alpha \sqrt[3]{n_{\rm ch}}$$

δ

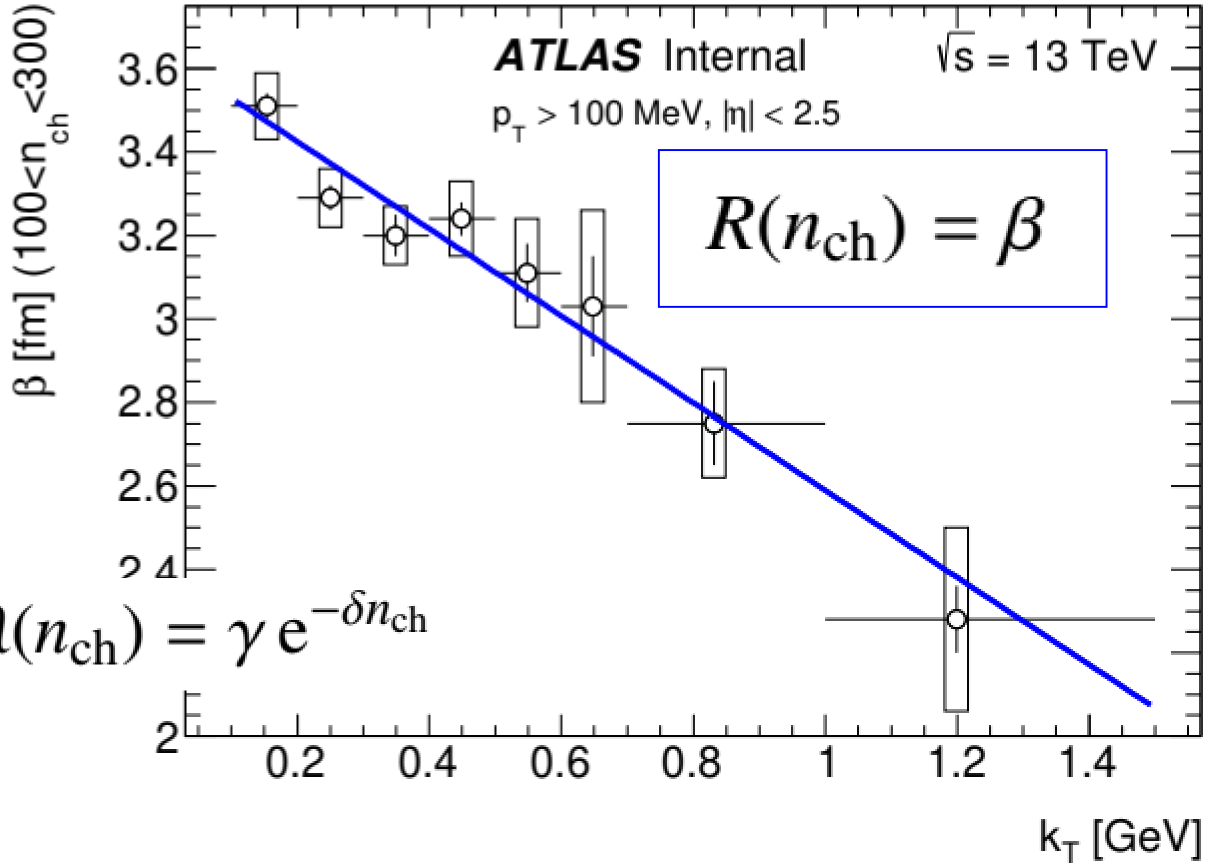

$$R(n_{\rm ch}) = \beta$$

$$\lambda(n_{\rm ch}) = \gamma\, e^{-\delta n_{\rm ch}}$$

$$(0.856 \pm 0.036 \pm 0.003)\ [\mathrm{fm}]\ e^{-(0.0007\pm0.0001\pm0.0001)\ [\mathrm{MeV}^{-1}]\, k_{\rm T}} \quad (\chi^2/ndf = 6/6).$$

$$(3.63 \pm 0.06 \pm 0.05)\ [\mathrm{fm}]\ e^{-(0.0010\pm0.0002\pm0.0001)\ [\mathrm{MeV}^{-1}]\, k_{\rm T}} \quad (\chi^2/ndf = 5/6)$$

The k_T dependence of the parameters α used in the parameterisation of the R dependence on multiplicity in the multiplicity region n_{ch} < 100, and β, the saturation value for R in the multiplicity region n_{ch} > 100. The error bars and boxes represent the statistical and systematic contributions, respectively. (left) The blue curve represents an exponential fit to α(k_T)-dependence; (right) the blue curve represents the linear fit of the parameter β(k_T)

k_T DEPENDENCE OF BEC PARAMETERS FOR (n_{ch}, k_T) FOR p_T>100 MeV

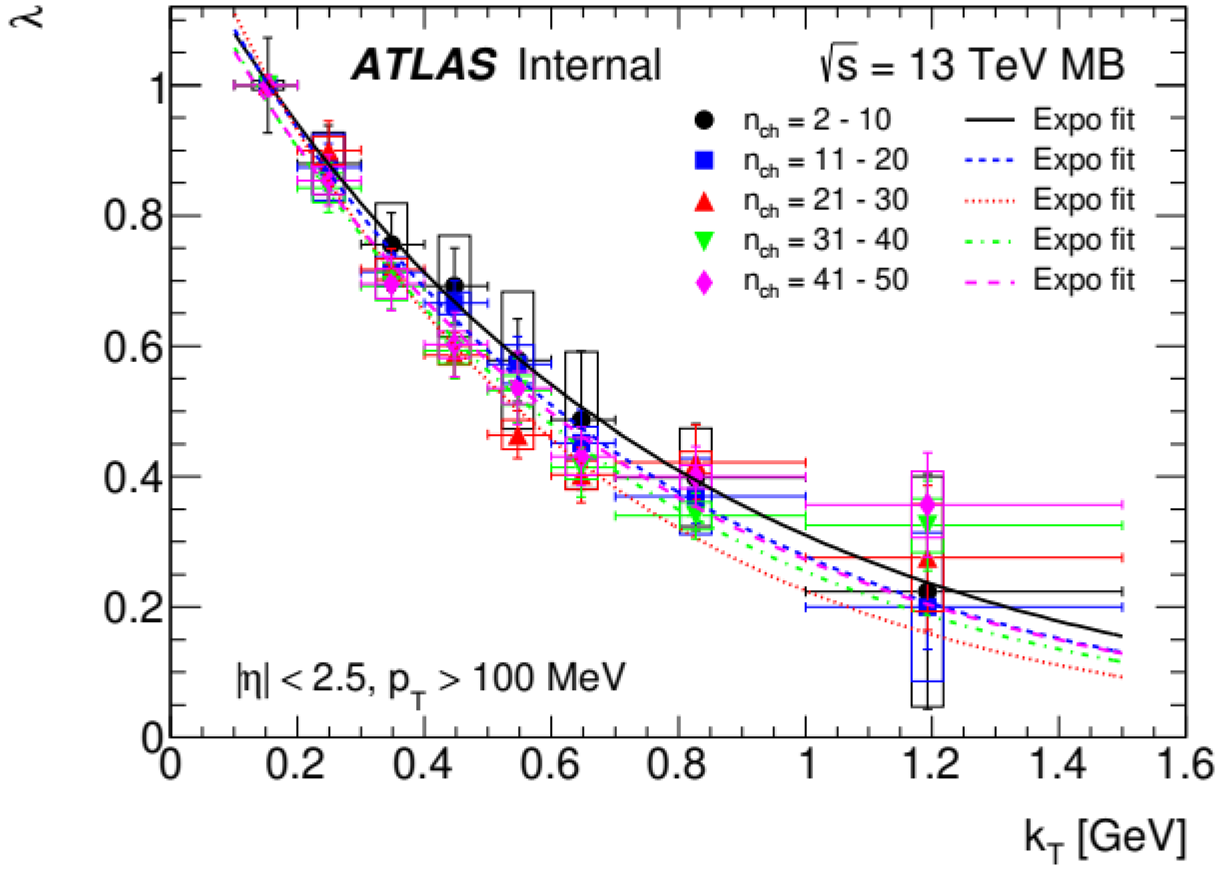

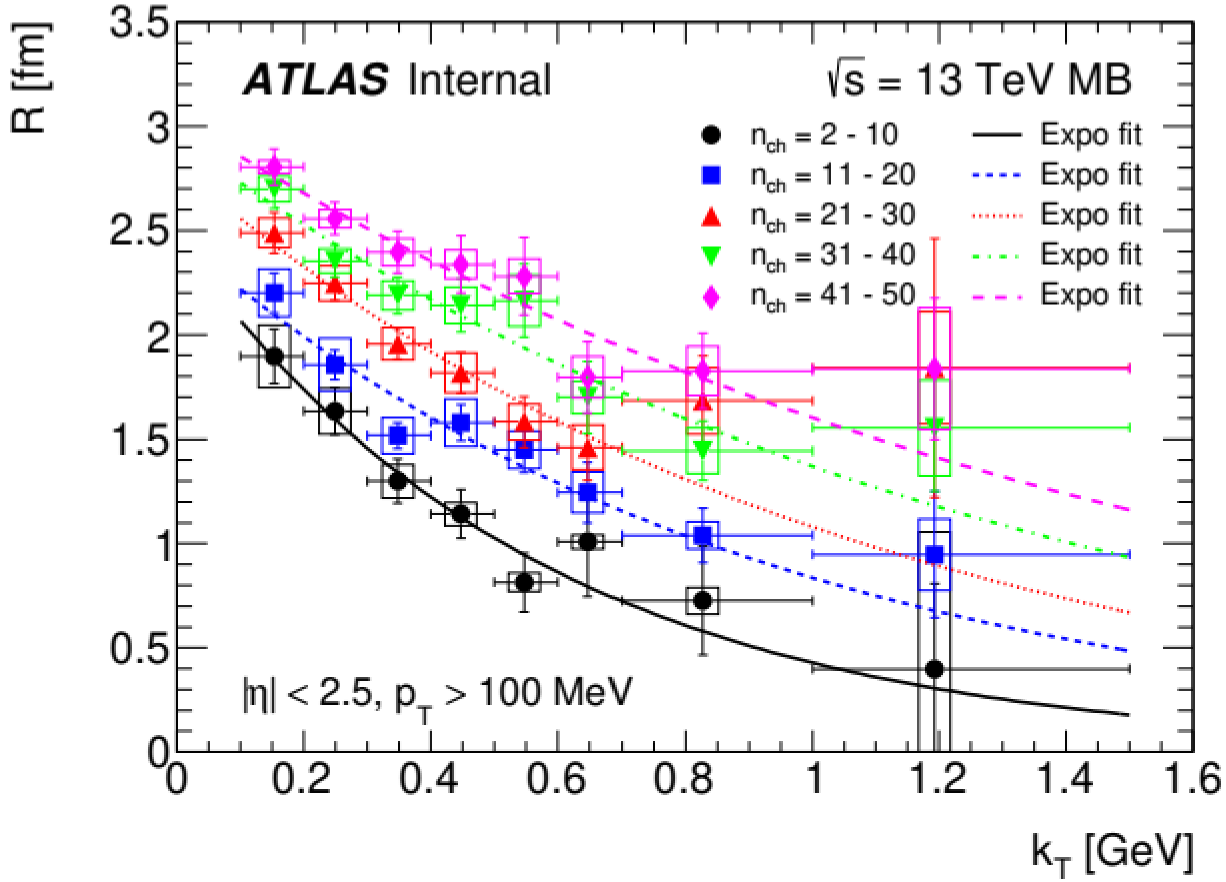

The k_T dependence of the correlation strength, $\lambda(n_{ch}; k_T)$, and (b) source radius, $R(n_{ch}; k_T)$, obtained by fitting to the $R_2(Q)$ correlation functions across five intervals in the multiplicity region $2 \leq n$ch ≤ 50 at 13 TeV in the MB sample. The error bars and boxes indicated represent the statistical and systematic contributions, respectively.

R <N$_{CH}$> dependence for k$_T$-fits for p$_T$>100 & 500 MeV

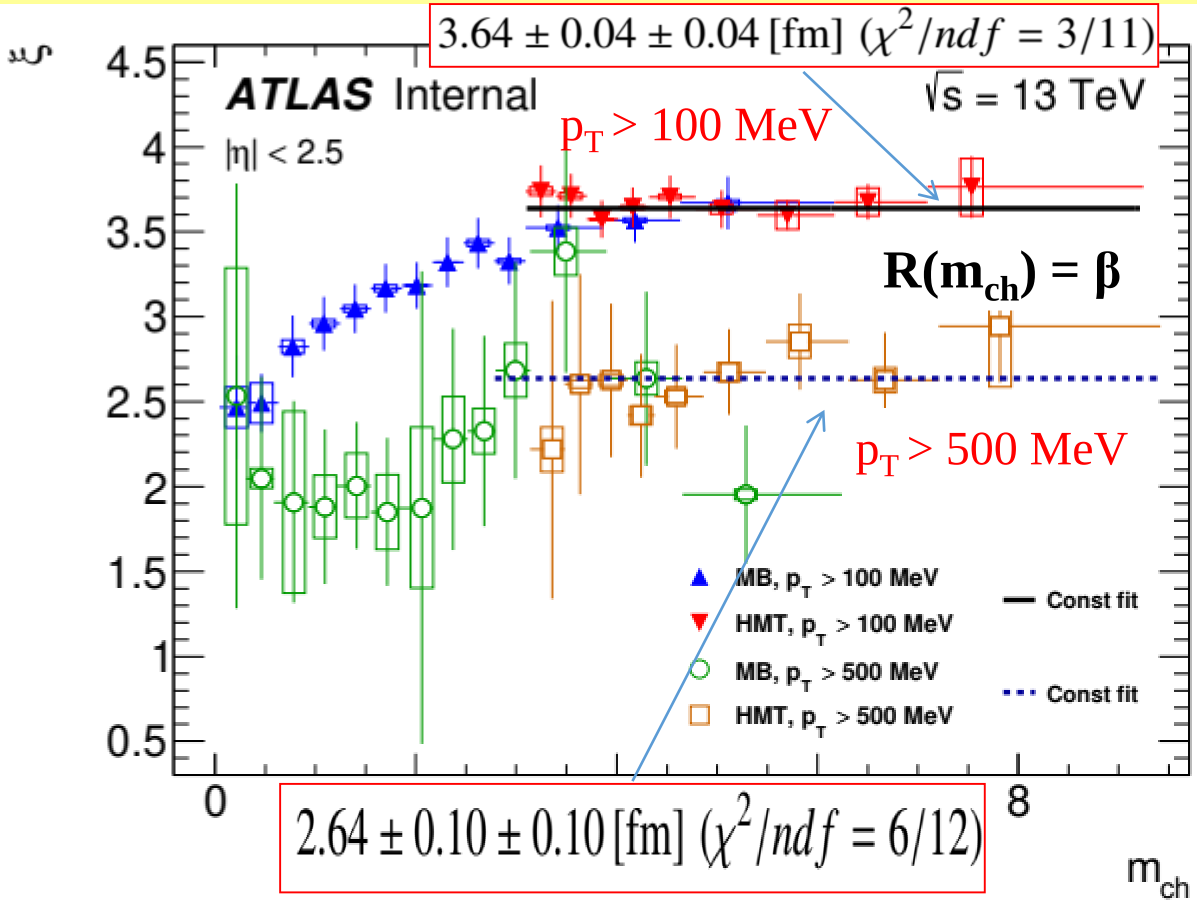

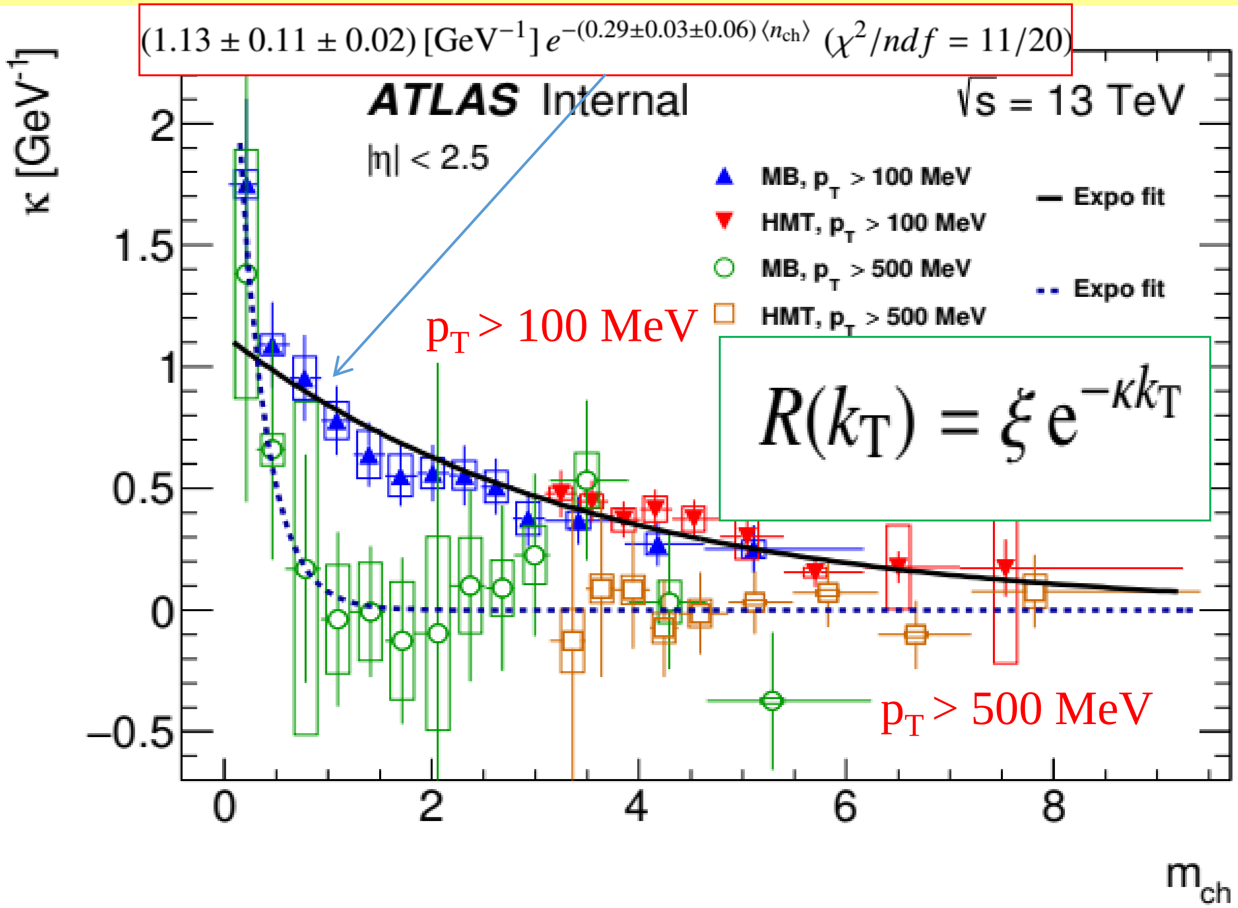

The parameters ξ and κ describing the dependence of the source radius, *R*, on charged particle rescaled multiplicity, m_{ch}, for track p_T>100 MeV and track p_T>500 MeV in MB and HMT samples at 13 TeV. The error bars and boxes shown represent the statistical and systematic contributions, respectively. (left) The black solid and blue dashed curves represent the saturated value of the parameter ξ for m_{ch}>3 for tracks with p_T>100 MeV and for m_{ch}>2.8 for tracks with p_T>500 MeV, respectively. (right) The black solid and blue dashed curves represent the exponential fit to the parameter κ for tracks with p_T>100 MeV and p_T>500 MeV.

LAMBDA $<N_{CH}>$ DEPENDENCE FOR K_T-FITS FOR P_T>100 & 500 MEV

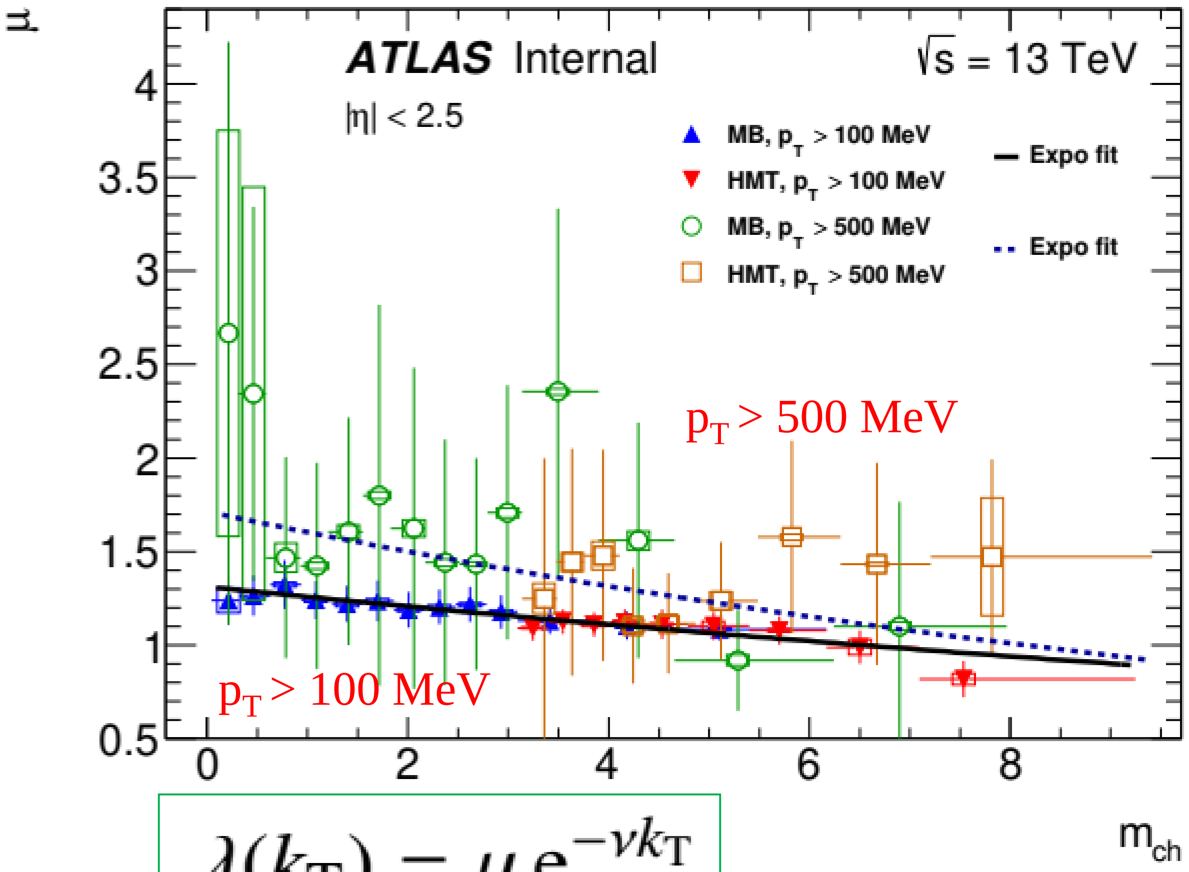

$$\lambda(k_T) = \mu\, e^{-\nu k_T}$$

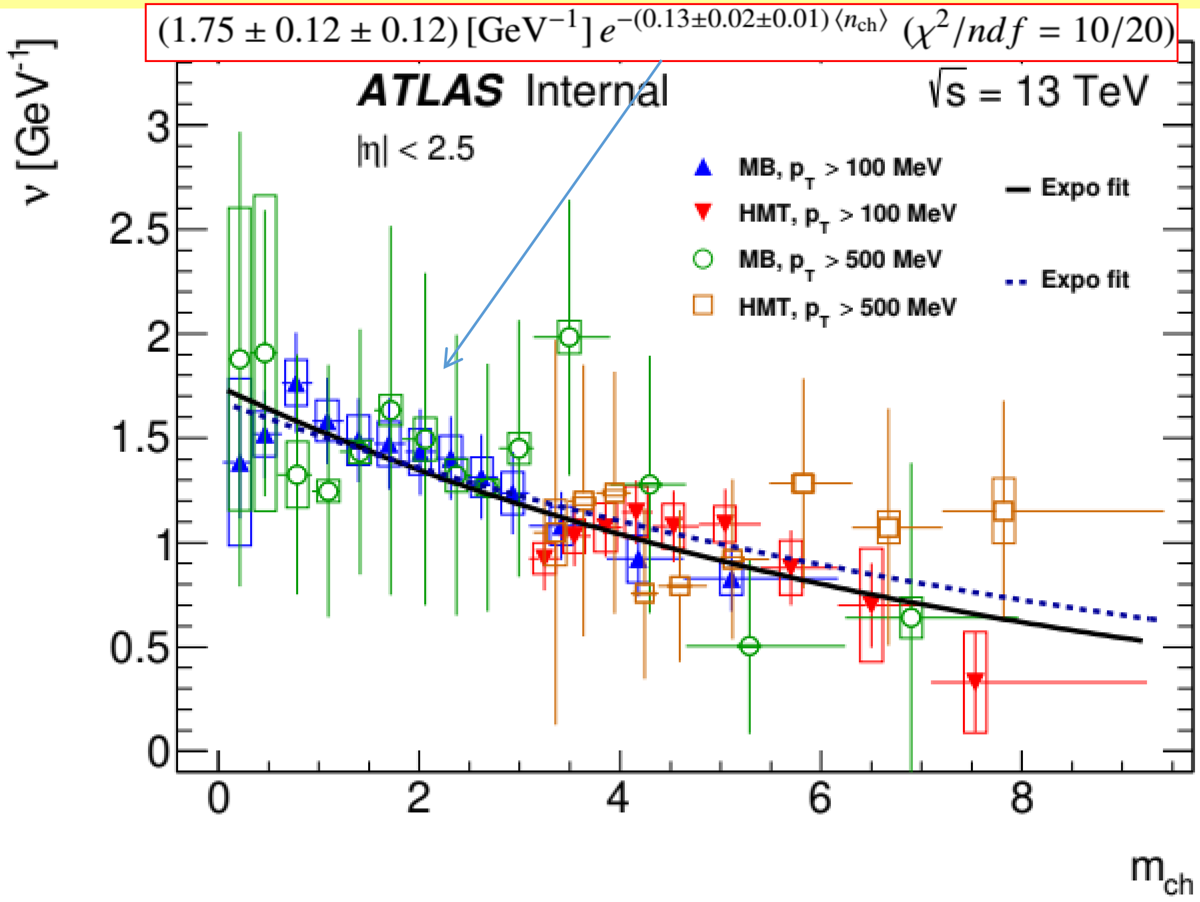

The fit parameters μ and ν describing dependence of the correlation strength, λ, on charged particle rescaled multiplicity, for track p_T>100 MeV and track p_T>500 MeV in MB and HMT samples at 13 TeV. The error bars and boxes shown represent the statistical and systematic contributions, respectively. The black solid (blue dashed) curves represents the exponential fit of the parameter μ (ν) on m_{ch} for tracks with p_T>100 MeV (p_T>500 MeV)

CONCLUSIONS

- The results of the Bose–Einstein Correlations (BEC) studies for like-sign charged particle pairs measured in the kinematic ranges $\boldsymbol{p_T}$**>100 MeV,** $\boldsymbol{p_T}$**> 500 MeV** and **|η|<2.5** in **pp-collisions at √s=13 TeV** with ATLAS at the CERN LHC.
- To properly **compare** the results at **different collision energies and** $\boldsymbol{p_T}$**-cuts**, the **average multiplicity** has been **rescaled from its measured midrapidity values**.
- The BEC parameters characterizing the source radius and particle correlation strength, are investigated as a function of multiplicity **up to three hundred charged-particles** and pair transverse momentum **up to 1.5 GeV**. The double-differential dependencies on multiplicity and average pair transverse momentum are also studied.
- A **saturation effect** in the multiplicity dependence of the BEC source radius is **confirmed for high multiplicity**. **The multiplicity and pair transverse momentum dependencies** of the BEC correlation strength and source radius parameters on the **energy collisions** are observed. The source radius is observed to decrease with $\boldsymbol{p_T}$**-cut** increase.
- The following features of BEC parameters for double-differential intervals are obtained: the source radius decreases exponentially with the pair transverse momentum and increases with multiplicity, and for high multiplicities, it exhibits a saturation effect; the correlation strength decreases exponentially with the pair transverse momentum and independently of multiplicity.

Thank You Very Much for Attention!

BACKUP SLIDES

Example of very-high-multiplicity event

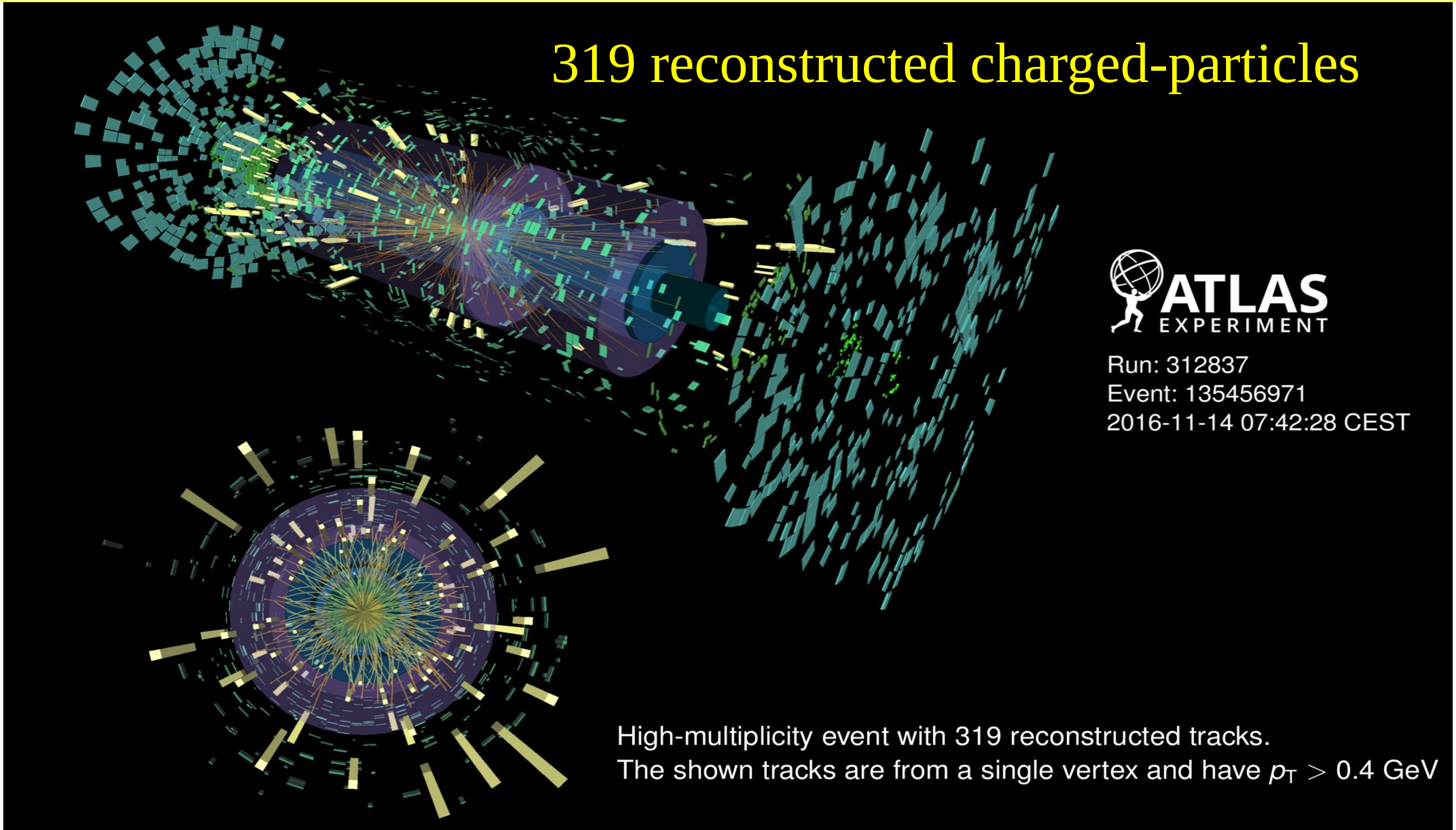

INNER DETECTORS (ID)

ATLAS tracking detectors:
Pixels, SCT & TRT

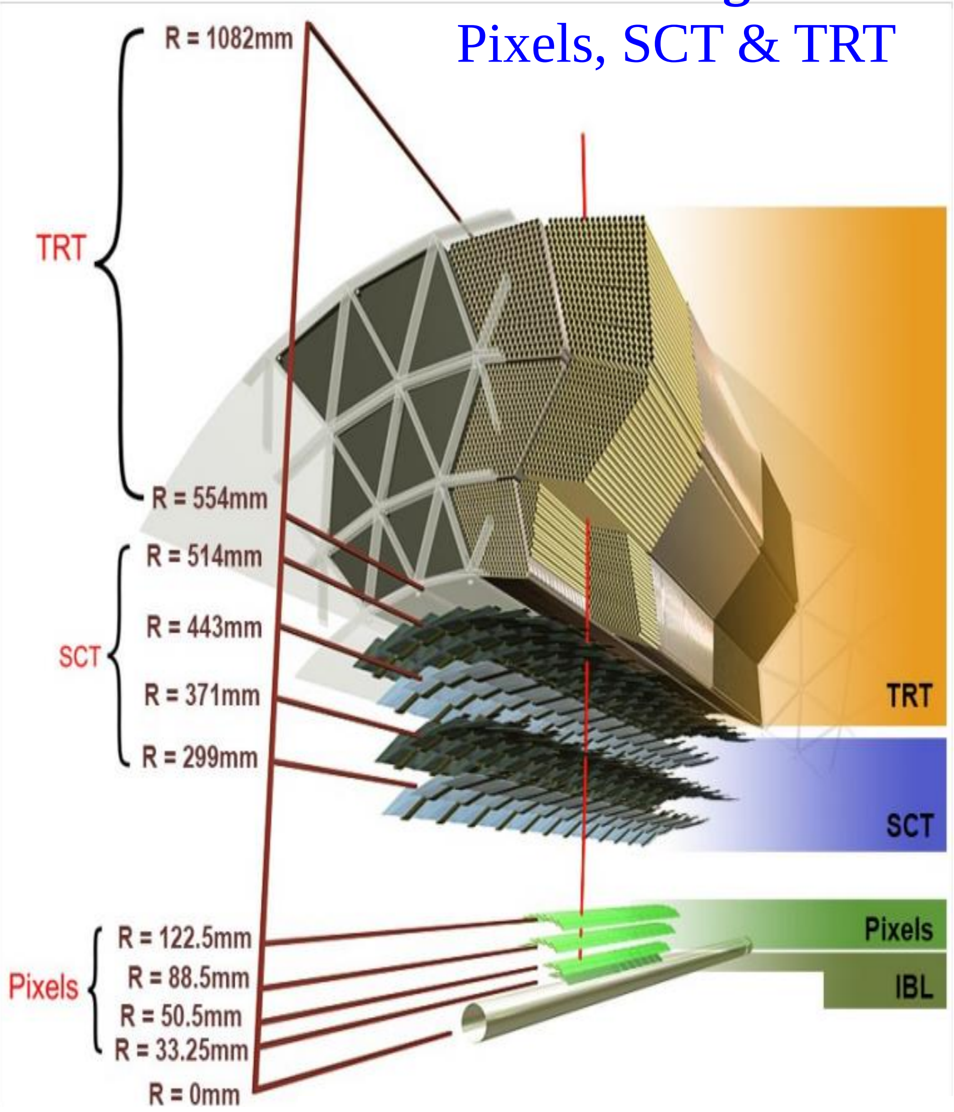

- **New innermost 4-th layer** for the Pixel detector [**IBL** = Insertable B-Layer]
- Required complete removal of the ATLAS Pixel volume
- IBL fully operational

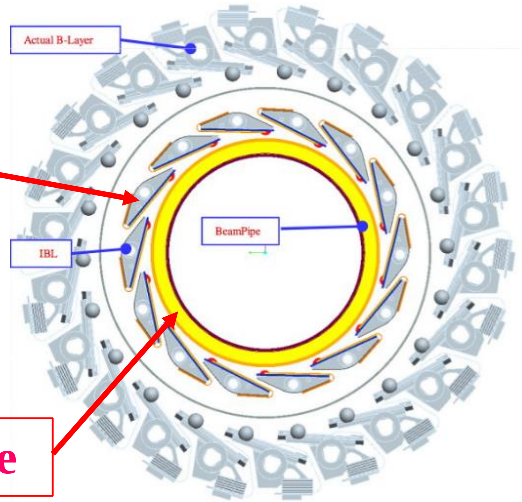

New Be beam pipe

Two times better tracks impact parameters resolution at 13 TeV!

MOTIVATION FOR BOSE-EINSTEIN CORRELATIONS

- Bose-Einstein correlations (BEC) represent a unique probe of the *space-time geometry* of the *hadronization region* and allow the *determination the size and shape of the source* from which particles are *emitted*.

- Studies of the dependence of BEC on *particle multiplicity* and *transverse momentum* are of special interest. They help in the understanding of multiparticle production mechanisms.

- High-multiplicity data in proton interactions can serve as a reference for studies in nucleus-nucleus collisions. The effect is reproduced in hydrodynamical and Pomeron-based approaches for hadronic interactions where high multiplicities play a crucial role.

THE PHASE SPACE CORRECTION

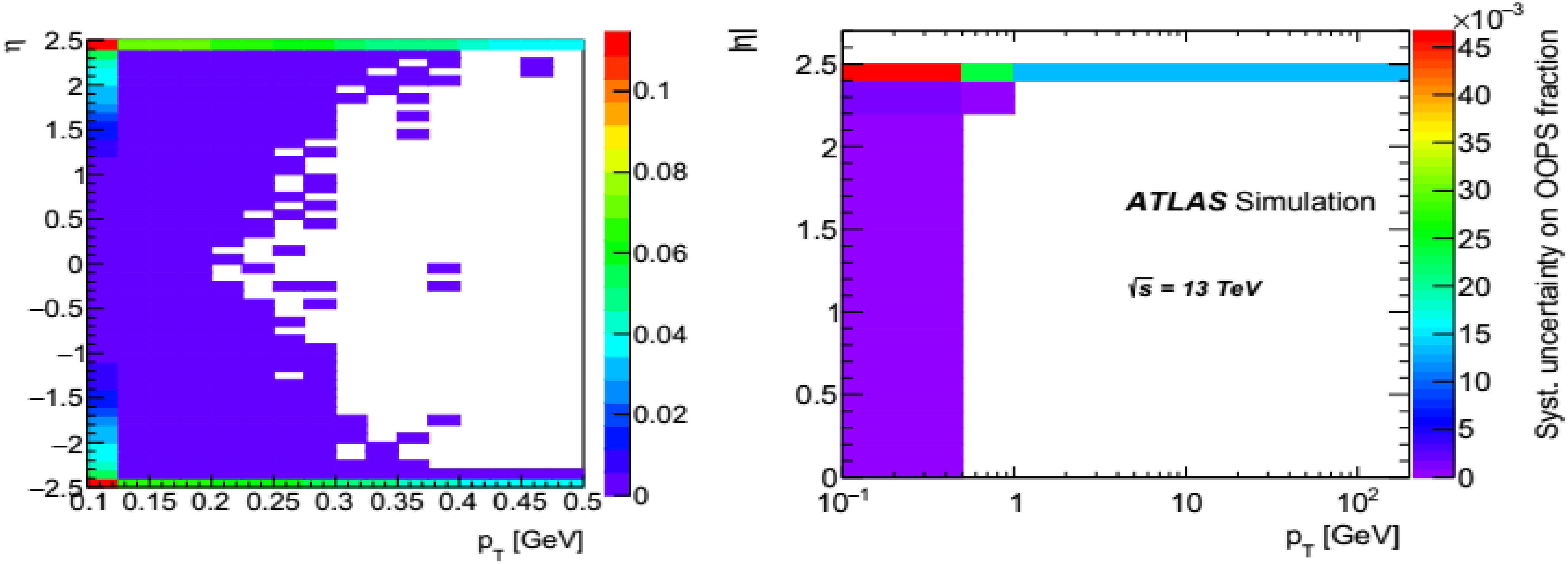

Figure 16: The out of phase space correction (OOPS) in p_T and η bins (left) and the systematic uncertainty on the out of phase space correction fractions (b). The systematic is made up of several contributions added up in quadrature, where each contribution is calculated as the difference in migration fractions between samples (see body text for further explanation).

FAKE TRACK CORRECTION

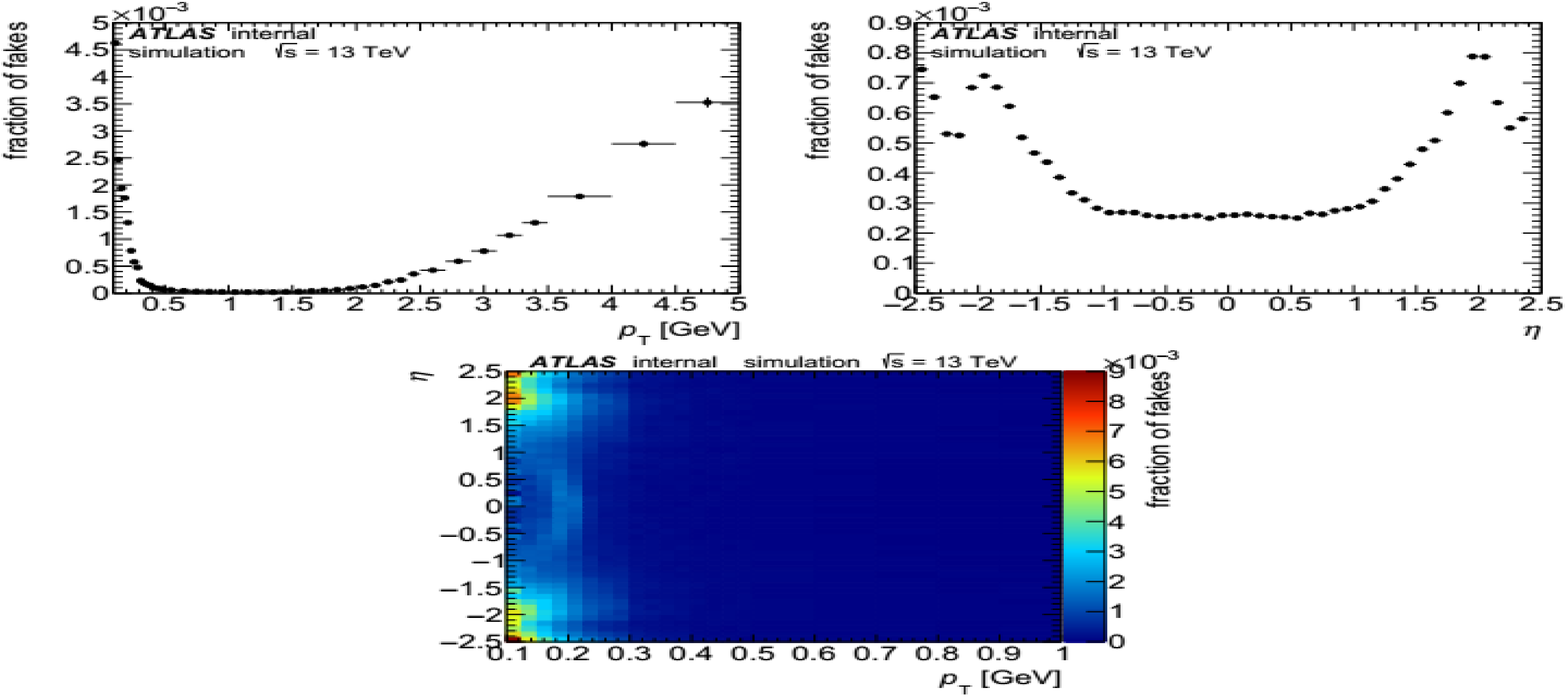

Figure 9: The fraction of fakes after applying the full event selection (see Section 3) as a function of p_T (left top) or η (right top) and the two-dimensional dependency of p_T and η (bottom). The fraction is below 1% and therefore negligible for the analysis.

PILE-UP FOR HMT AND MB EVENTS

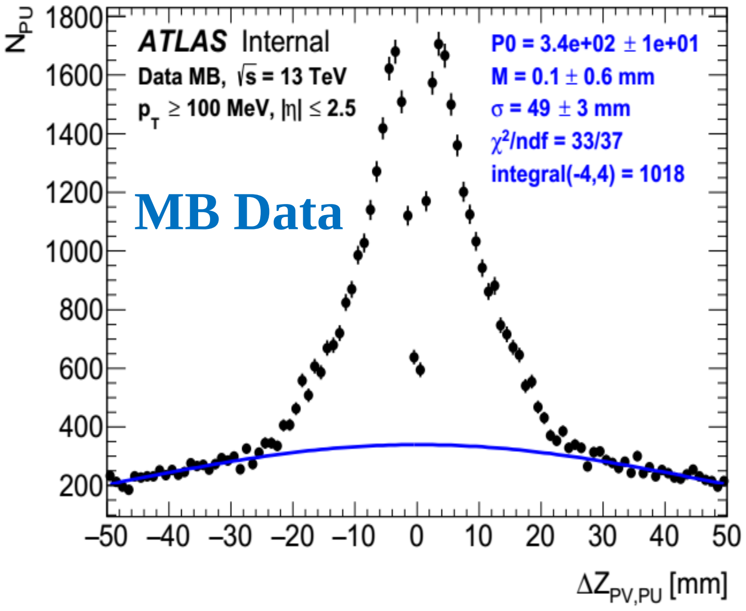

MB trigger

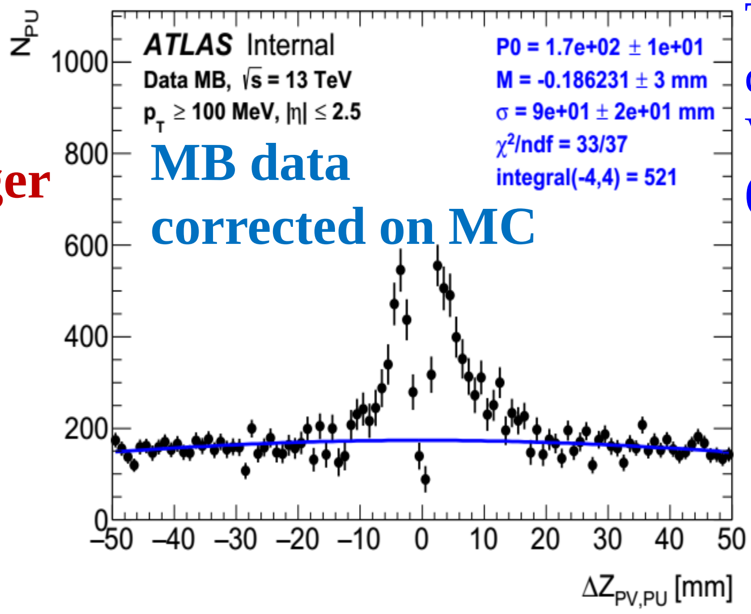

The distribution of the distance between Z coordinates of Primary Vertex and Pile-Up Vertexes for MB and HMT events for Data (left) and Data corrected on MC (right)

For MB events the number of pile-up vertexes in the Primary Vertex (PV) region ±4 mm is ~520 after correction on MC, and the number of tracks in Pile-up vertex is 9.4. Therefore the fraction of pile-up tracks in MB events is **0.002%**

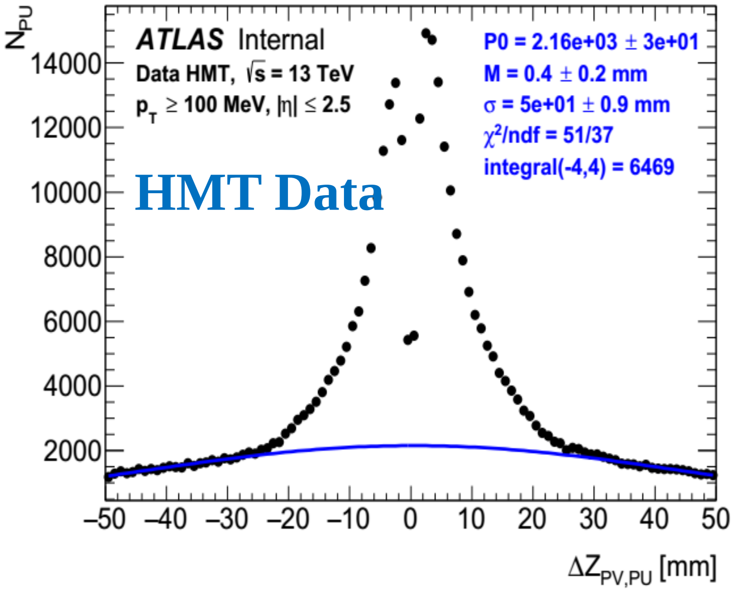

HMT trigger

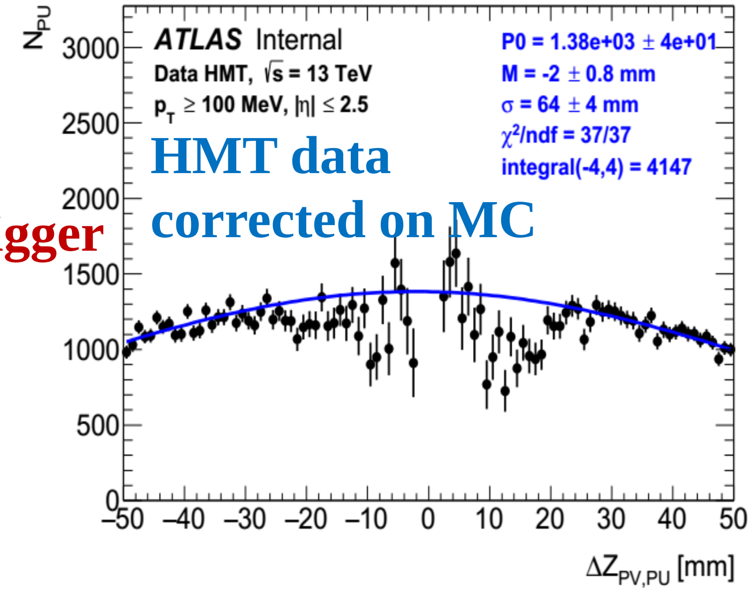

For HMT events the number of pile-up vertexes in the Primary Vertex (PV) region ±4 mm is ~4150, after correction on MC, and the number of tracks in Pile-up vertex is 23. Therefore the fraction of pile-up tracks in MB events is **0.01%**

We can conclude that mean number of pile-up tracks per MB or HMT event is negligible

Mean number of tracks (pile-up tracks) per event: MB – 26 (0.0005) tracks/event; HMT – 108 (0.01) tracks/event

CLOSURE TEST FOR TWO-PARTICLES C_2 CORRELATION FUNCTION

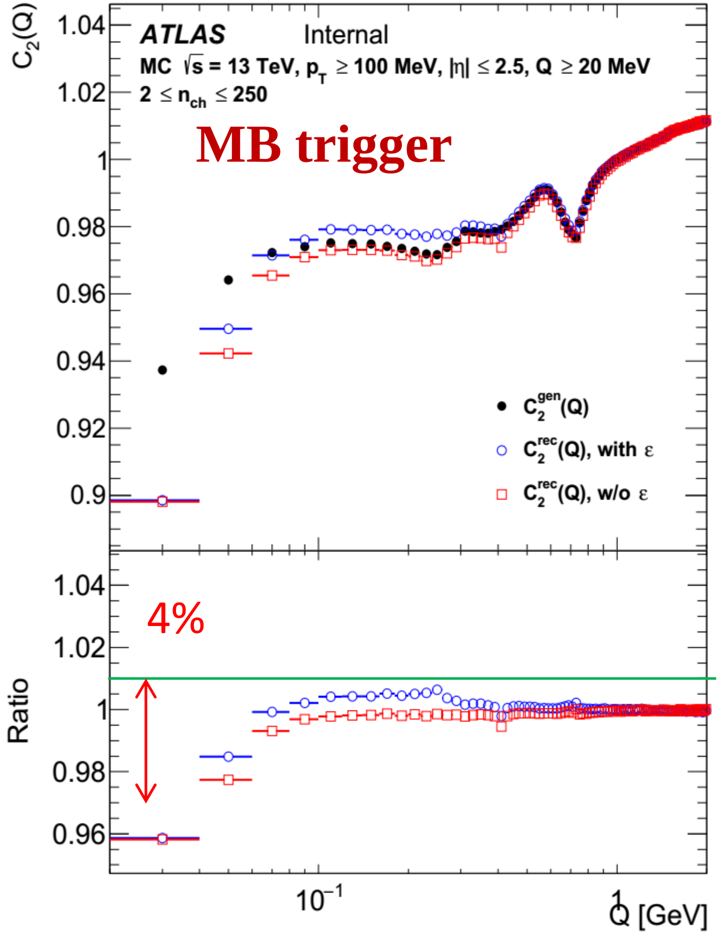

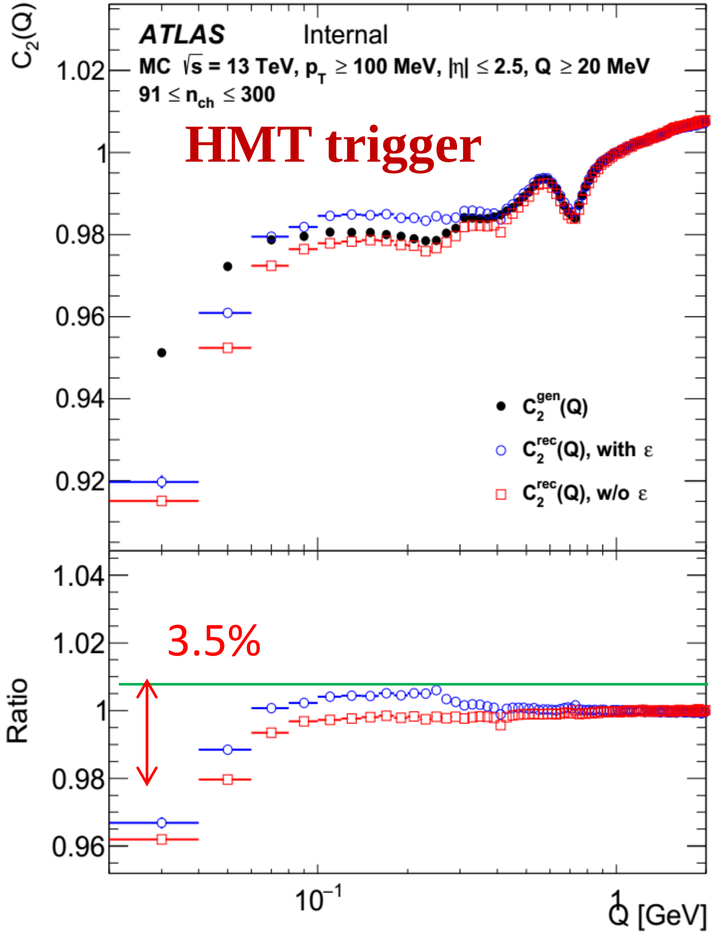

Un-closure between for reconstruction efficiency correction important only for smallest ***k_T* region from 100 to 200 MeV and high multiplicity region *n_{ch}*>60** on the level up to 2%.

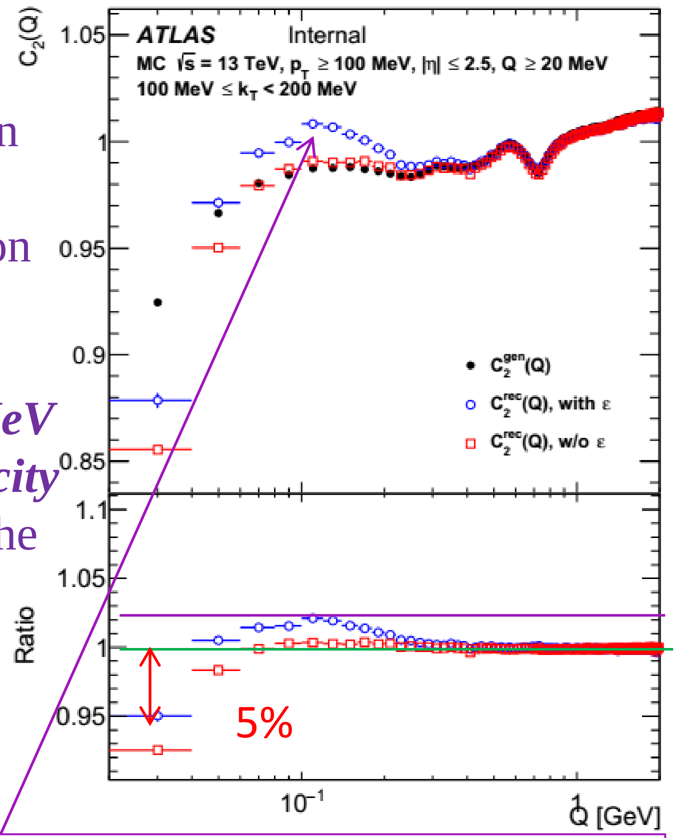

Only for 100<k_T<200 MeV and n_{ch}>60

The closure tests for $C_2(Q)$ correlation function of Pythia8 A2 datasets at 13 TeV MB events for multiplicity $2 \le n_{ch} \le 250$ and HMT events for multiplicity $91 \le n_{ch} \le 300$ built using the unlike-charged particle pair reference sample.

The differences between the particle level distributions and the reconstructed distributions after unfolding are assigned to the full error for bins of $R_2(Q)$ correlation functions and included in the final fitting error of the BEC parameters

CORRECTION OF R_2 CORRELATION FUNCTION

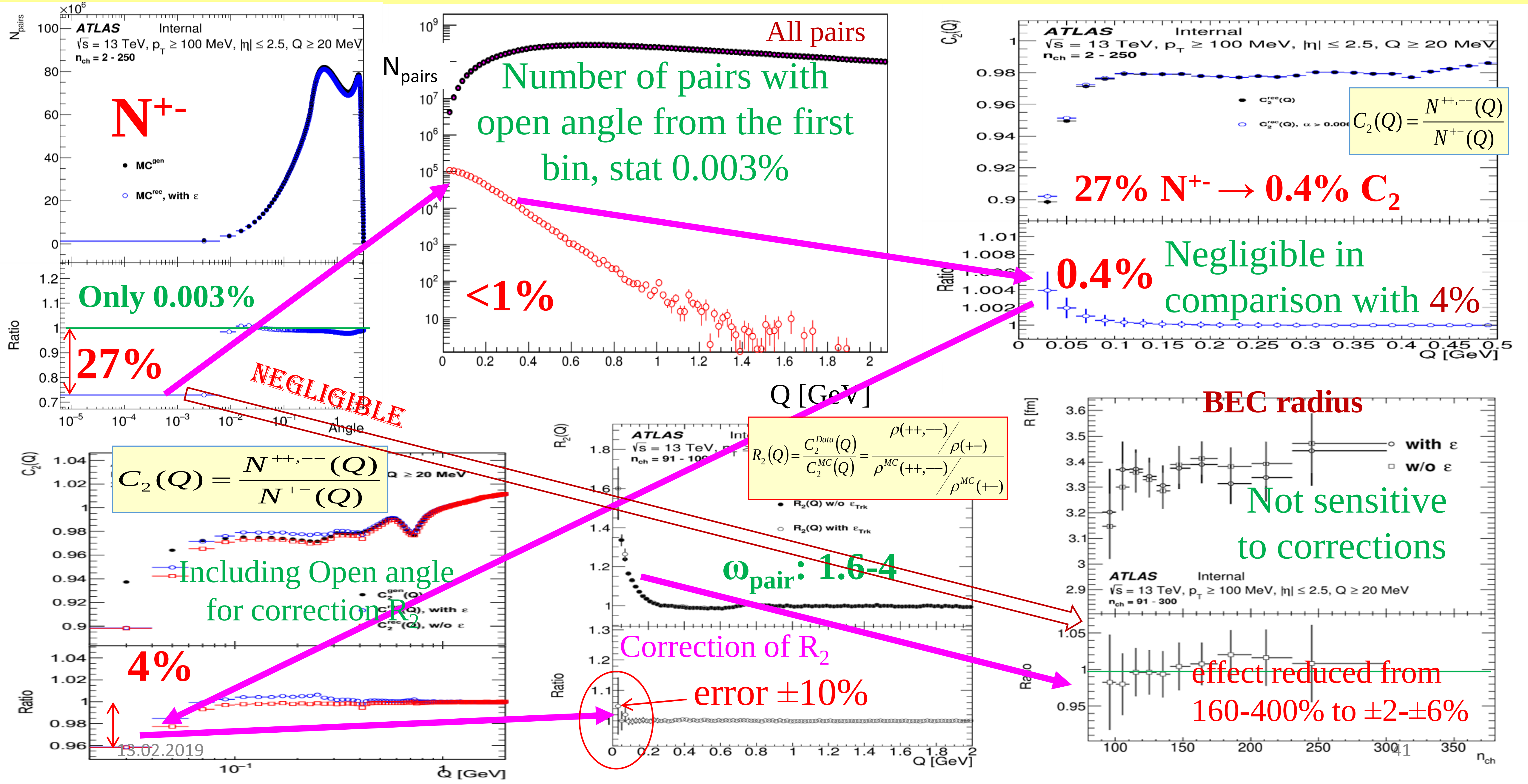

INCLUSIVE R_2 DISTRIBUTIONS

Inclusive MB two particles R_2 correlation function

Lum. ~151 μb^{-1}; Statistic: 9.6×10^6 events with 2.8×10^8 tracks

Inclusive HMT two particles R_2 correlation function

Lum. ~8.4 nb^{-1}; Statistic: 9.1×10^6 events with 9.8×10^8 tracks

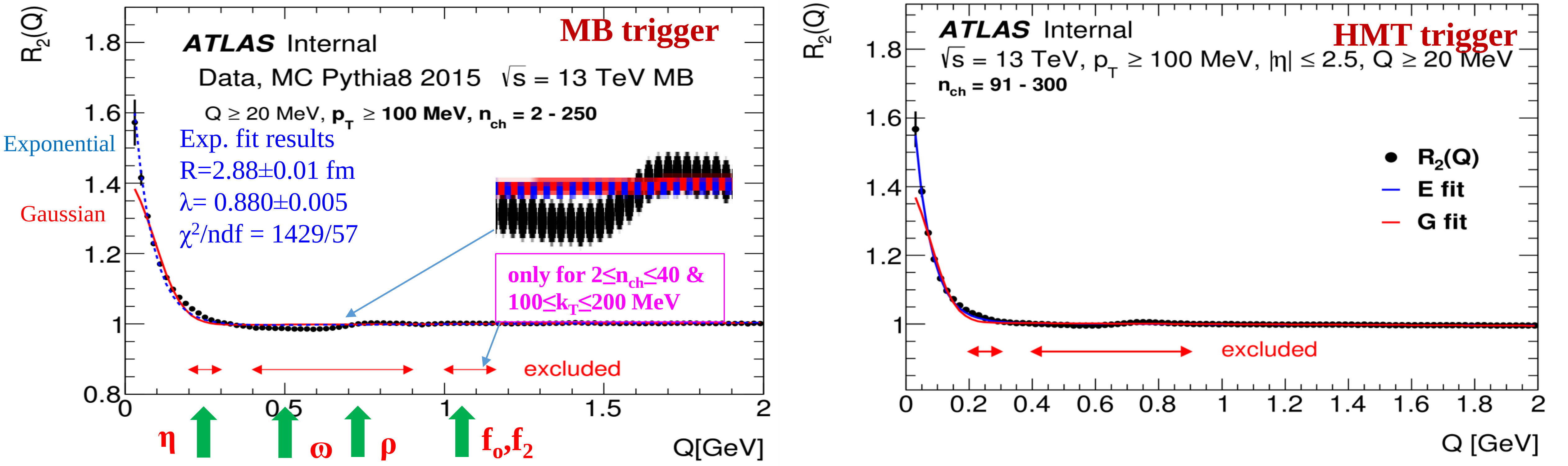

Fit to extract strength and source size. Goldhaber spherical shape with a Gaussian distribution of the source. Exponential, radial Lorentzian distribution of the source -> much better at low Q. Three bumps regions because MC overestimates: 1) $\eta\to\pi^+\pi^-\pi^o$ or $\eta\to\pi^+\pi^-\gamma$; 2) $\omega\to\pi^+\pi^-\pi^o$ and $\rho\to\pi^+\pi^-$, 3) $f_2\to\pi^+\pi^-$; Therefore regions 0.2–0.3 GeV; 0.4–0.9 GeV and 1.0–1.16 GeV (*only for* $2\le n_{ch}\le 40$ *and* $100\le k_T\le 200$ *MeV*) excluded from the fit. Q region is from 0.02 to 2 GeV.

Fit function: $R_2(Q)= C_0[1+\lambda\ \Omega(QR)](1+\varepsilon Q)$, ε-term counts for the *long-range* correlations

Studies of one-dimensional BEC effects in pp collisions for p_T>100 MeV and $|\eta|$ < 2.5 at 13 TeV

MULTIPLICITY DEPENDENCE OF BEC PARAMETERS FOR DIFFERENT MC

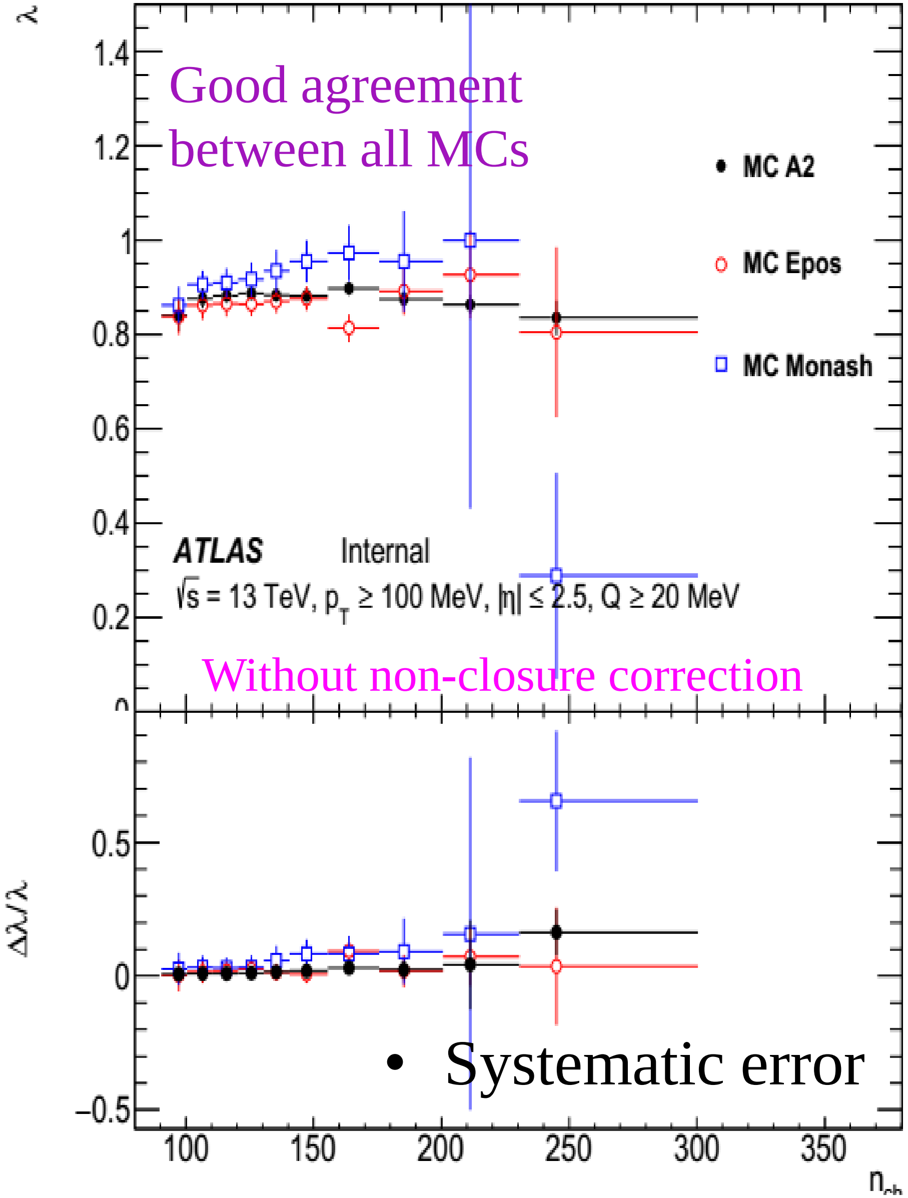

Good agreement between all MCs

Without non-closure correction

- Systematic error

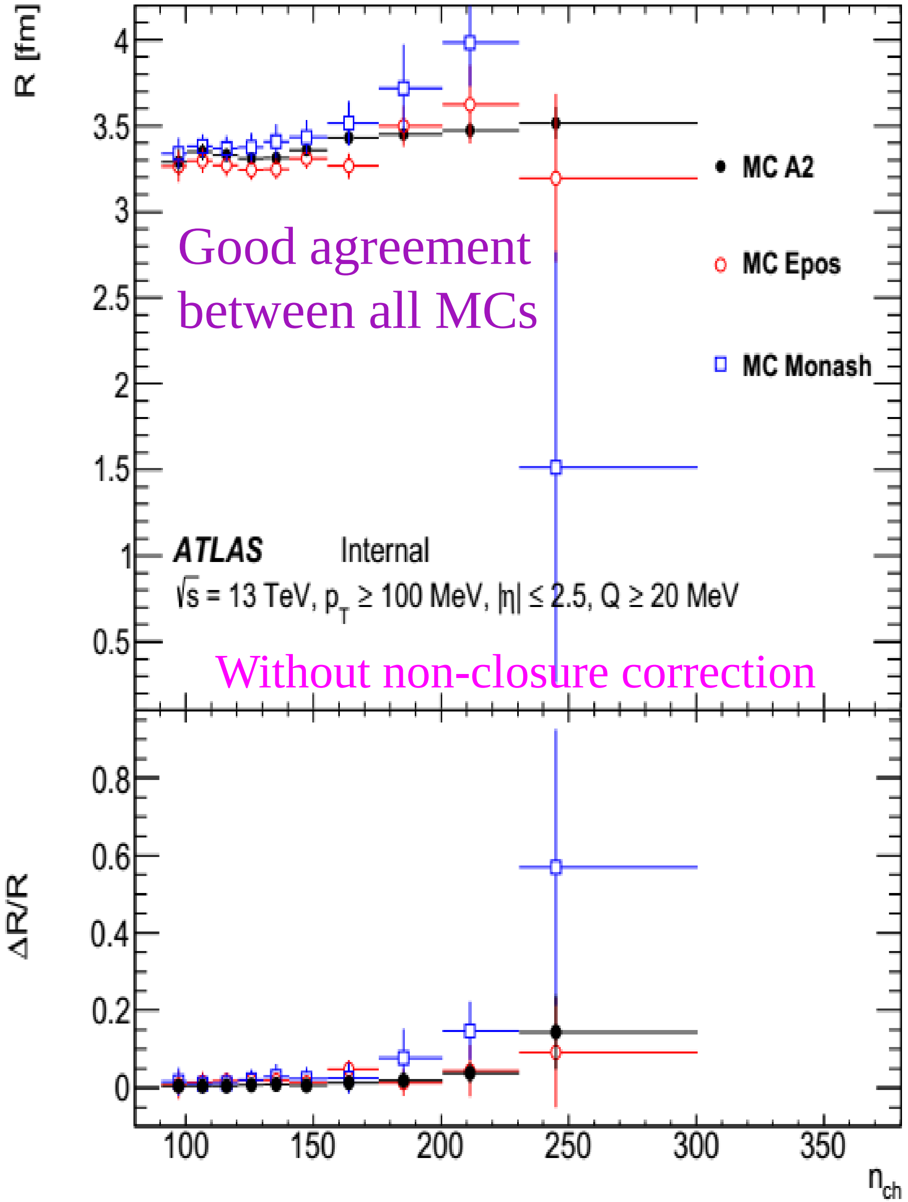

Good agreement between all MCs

Without non-closure correction

HMT trigger

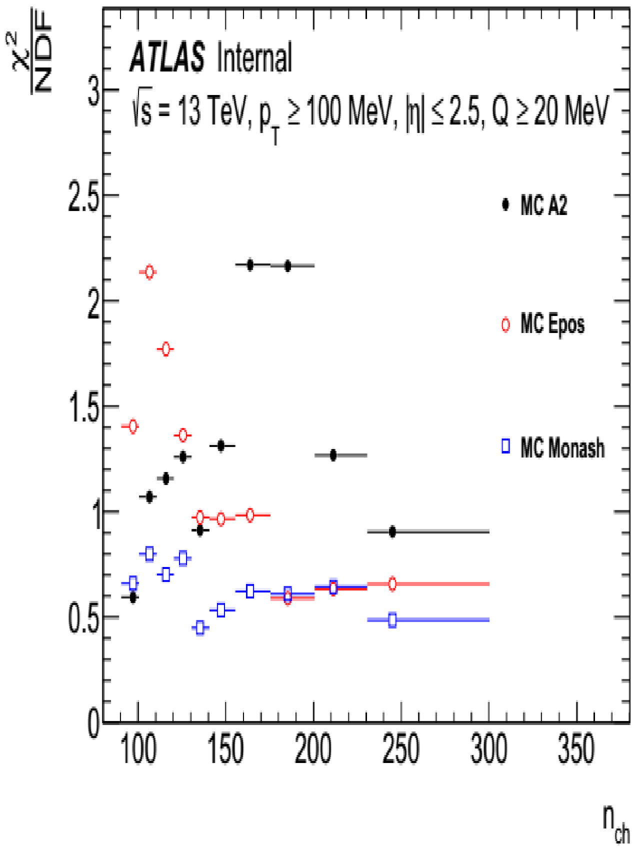

Radius **saturation effect** for all MCs for high multiplicity region

Information about MC samples are given in the Backup slides

COMPARISON WITH OTHER EXPERIMENTS

The results of BEC parameters for

Exponential fits of R_2 used total uncertainties

Statistical uncertainties are below 2–4 %

Energy [GeV]	n_{ch}	λ	$R^{(E)}$ [fm]
0.9	≥2	0.74 ± 0.10	1.83 ± 0.25
7	≥2	0.71 ± 0.07	2.06 ± 0.22
7 (HMT)	≥150	0.74 ± 0.06	2.36 ± 0.30
13	≥2	0.88±0.01	2.83±0.05
13 (HMT)	>100	0.94±0.02	3.58±0.04

Comparison with results of previous experiments

$$R^{(G)} = R^{(E)} / \sqrt{\pi}$$

Energy [GeV]	n_{ch}	$R^{(G)}$ [fm]
0.9	≥2	1.03 ± 0.14
7	≥2	1.16 ± 0.12
7 (HMT)	≥150	1.33 ± 0.17
13	≥2	1.60±0.03
13 (HMT)	>100	2.02±0.02

ATLAS √s = 13 TeV

ATLAS √s = 7 TeV HMT

ATLAS √s = 7 TeV

ATLAS √s = 0.9 TeV

Larger kinematic region

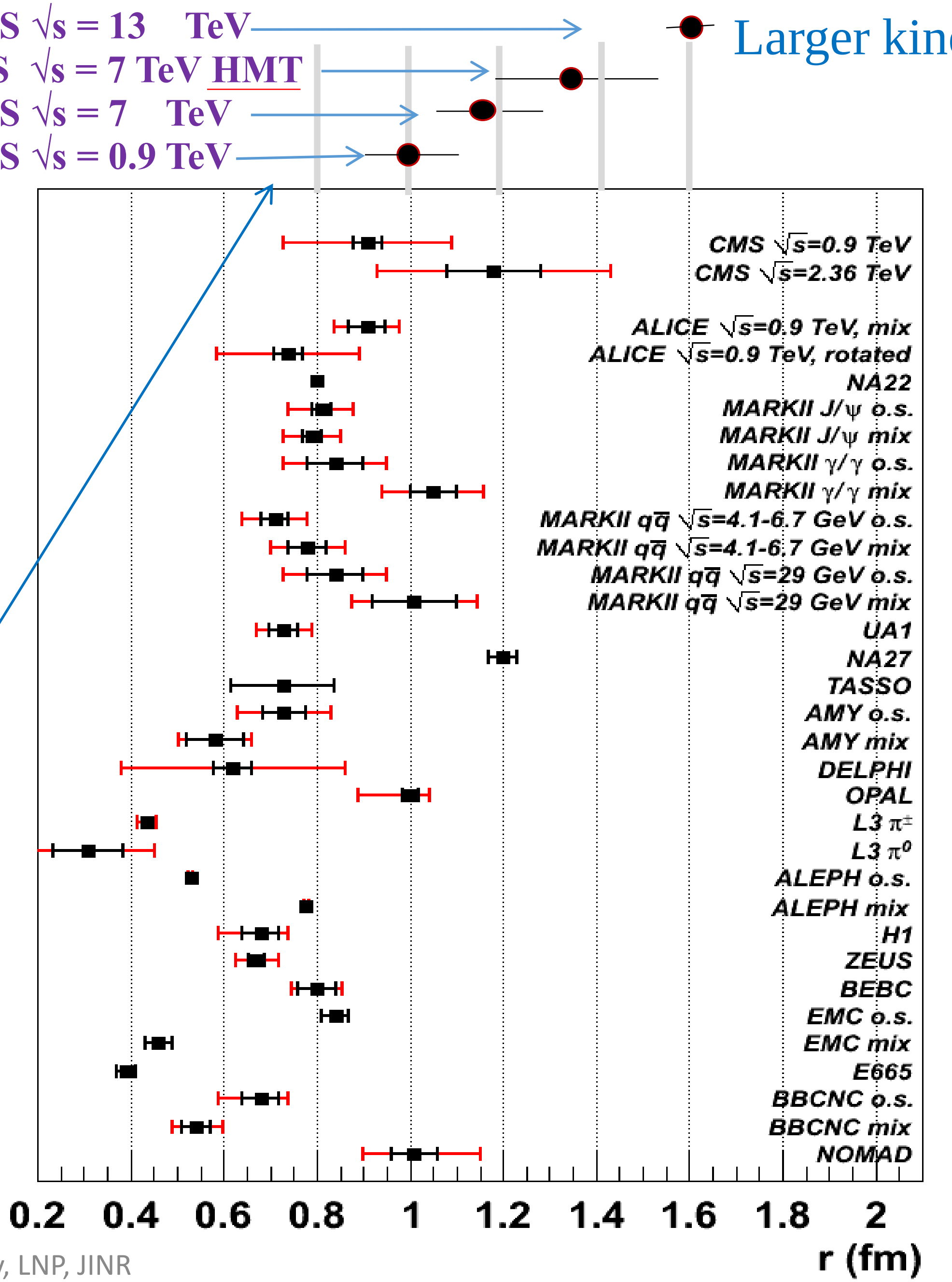

THEORY PREDICTION FOR R PARAMETER OF BEC

V.A.Shegelsky, et al, Pomeron universality from identical pion correlations at the LHC, Phys.Letter B703 (2011) 288.
M.G.Ryskin, V.A.Shegelsky, Nucl.Phys B219 (2011) 10.

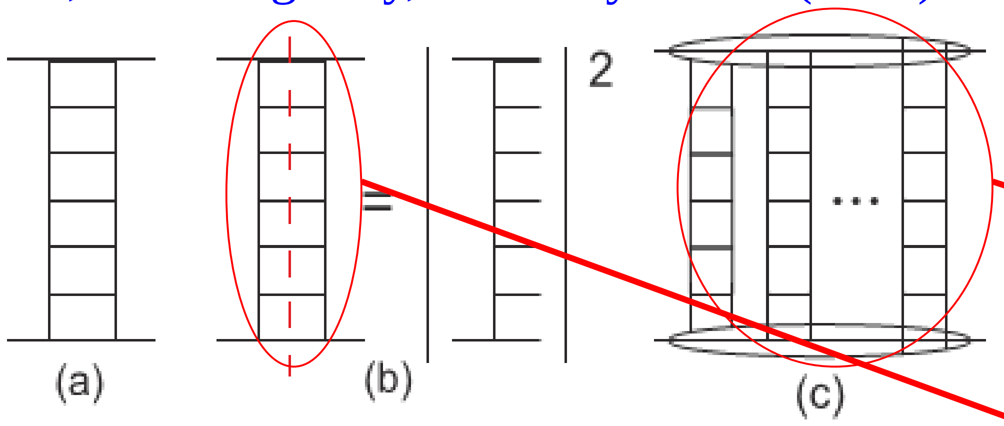

The ladder diagram for one-Pomeron exchange; (b) cutting one-Pomeron exchange leads to the multiperipheral chain of final state particles; (c) a multi-Pomeron exchange diagram.

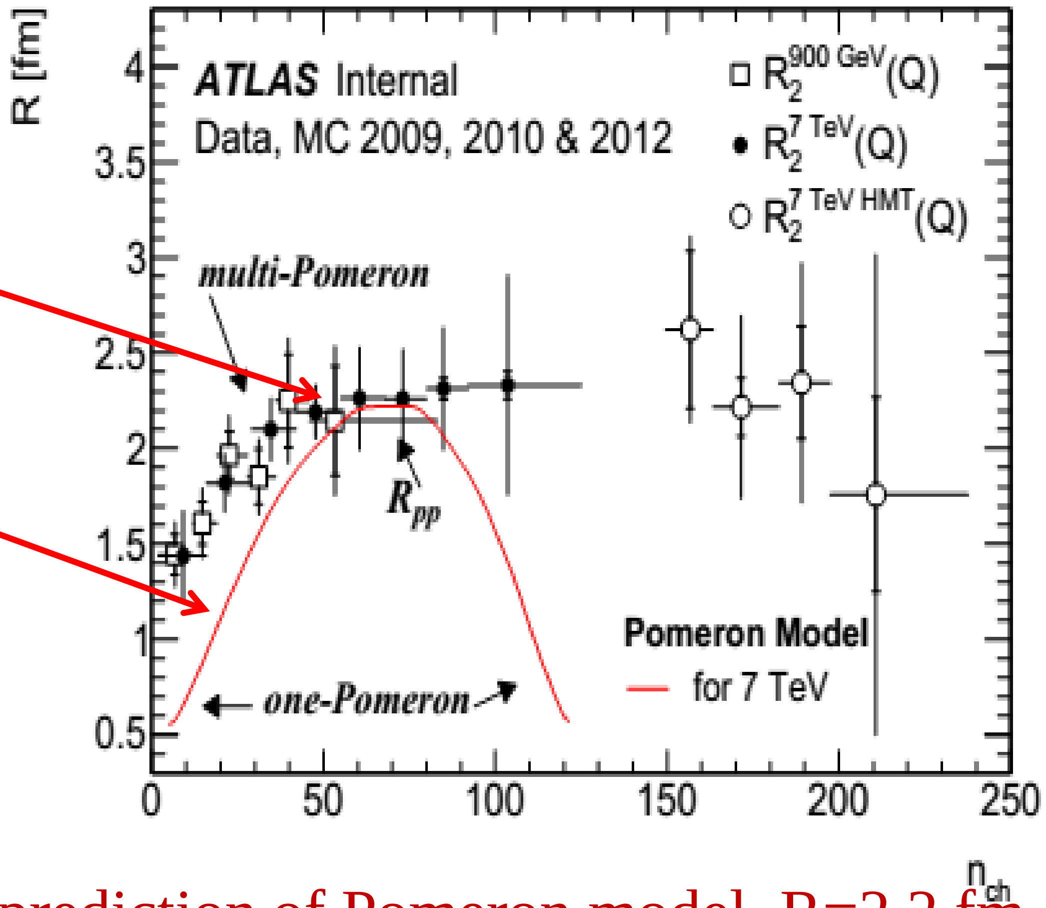

Interpretation: ► The BEC radius for one parton-parton interaction (underline events, cut Pomeron) is ~1 fm, like for smallest multiplicity. ►For high multiplicity events we see BEC signal from some parton-parton interactions. ►The radius for high multiplicity can be interpret as an average distance between separate parton-parton interactions is ~2 fm.

The prediction of Pomeron model R=2.2 fm is in agreement with saturated radius R=2.3 fm at 7 TeV for middle multiplicity region. There is not agreement with data for n_{ch}>80.

k_T dependence of BEC parameters for (n_{ch}, k_T) at p_T>500 MeV

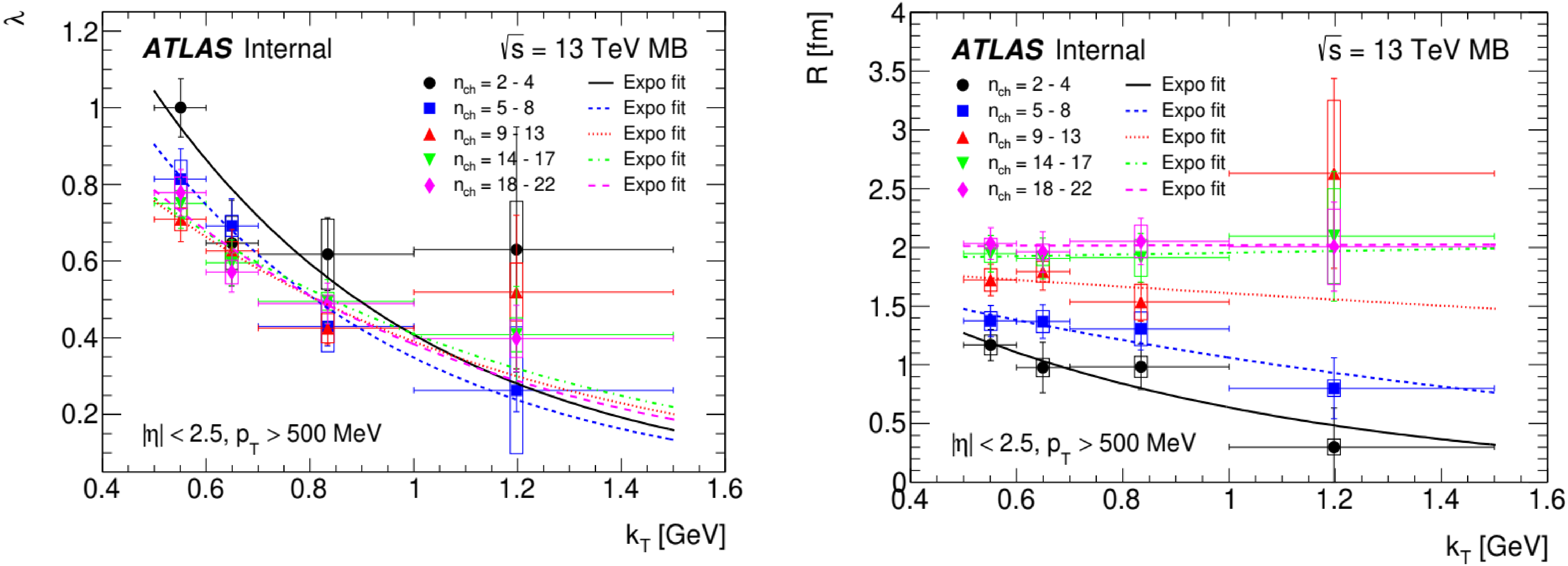

The k_T dependence of the correlation strength, λ, and source radius, *R*, for track p_T > 500 MeV at 13 TeV, obtained by fitting to the *R*2(*Q*) correlation functions, for multiplicity region $2 \le n_{ch} \le 22$ for MB sample and using the unlike-charge particle pair reference sample. The error bars and boxes indicated represent the statistical and systematic contributions, respectively. The curves represent the exponential fit of the λ and *R* k_T-dependences.

CHARGED-PARTICLE MULTIPLICITIES VS η AND ENERGY

PL B758 (2016) 67–88, Eur. Phys. J. C (2016) 76:502

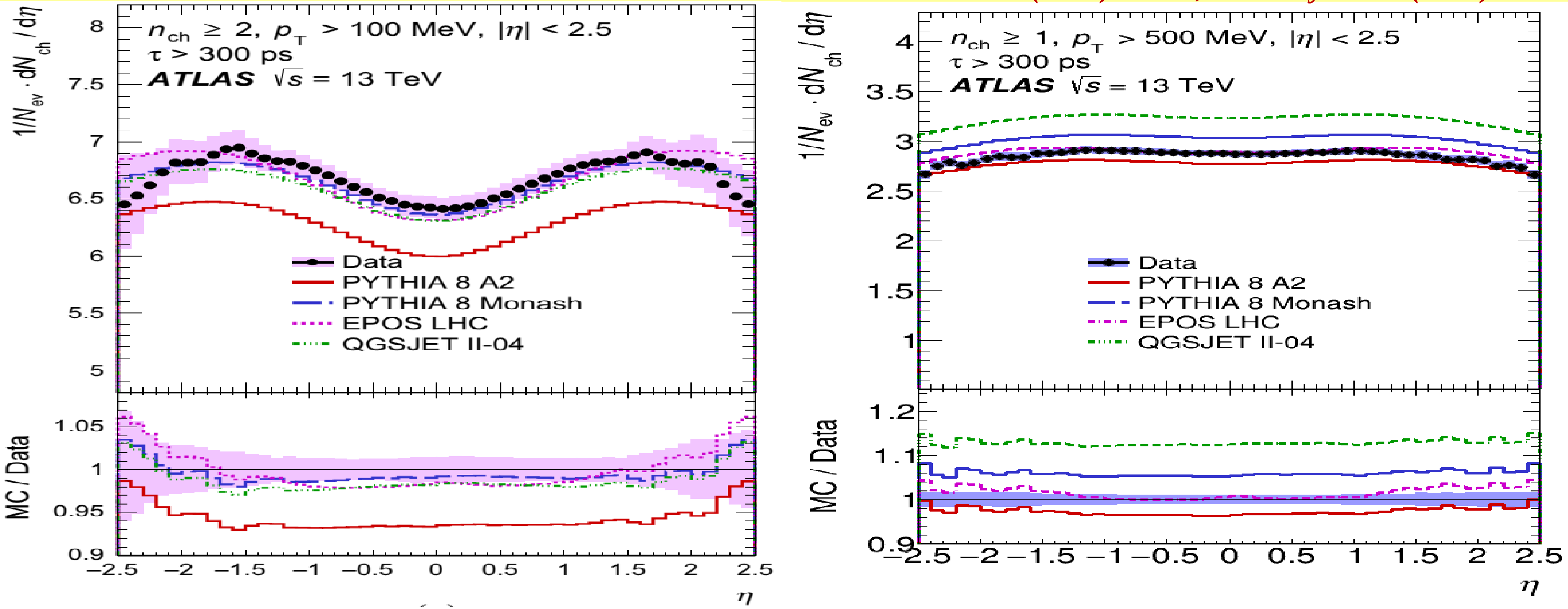

Charged-particle multiplicity as a function of the η distribution for p_T>100 MeV (left) and p_T>500 MeV (right)

The *black dots* represent the data and the *coloured curves* the different MC model predictions. The *vertical bars* represent the statistical uncertainties, while the *shaded areas* show statistical and systematic uncertainties added in quadrature.

The same shape in Models but different normalisation. **EPOS** and **Pythia8 Monash & A2** give remarkably good predictions

CHARGED-PARTICLE MULTIPLICITIES VS MULTIPLICITY

Eur. Phys. J. C 76 (2016) 502; PL B758 (2016) 67–88

This track reconstruction efficiency for MB events was used for n_{ch}<250, similar to HMT

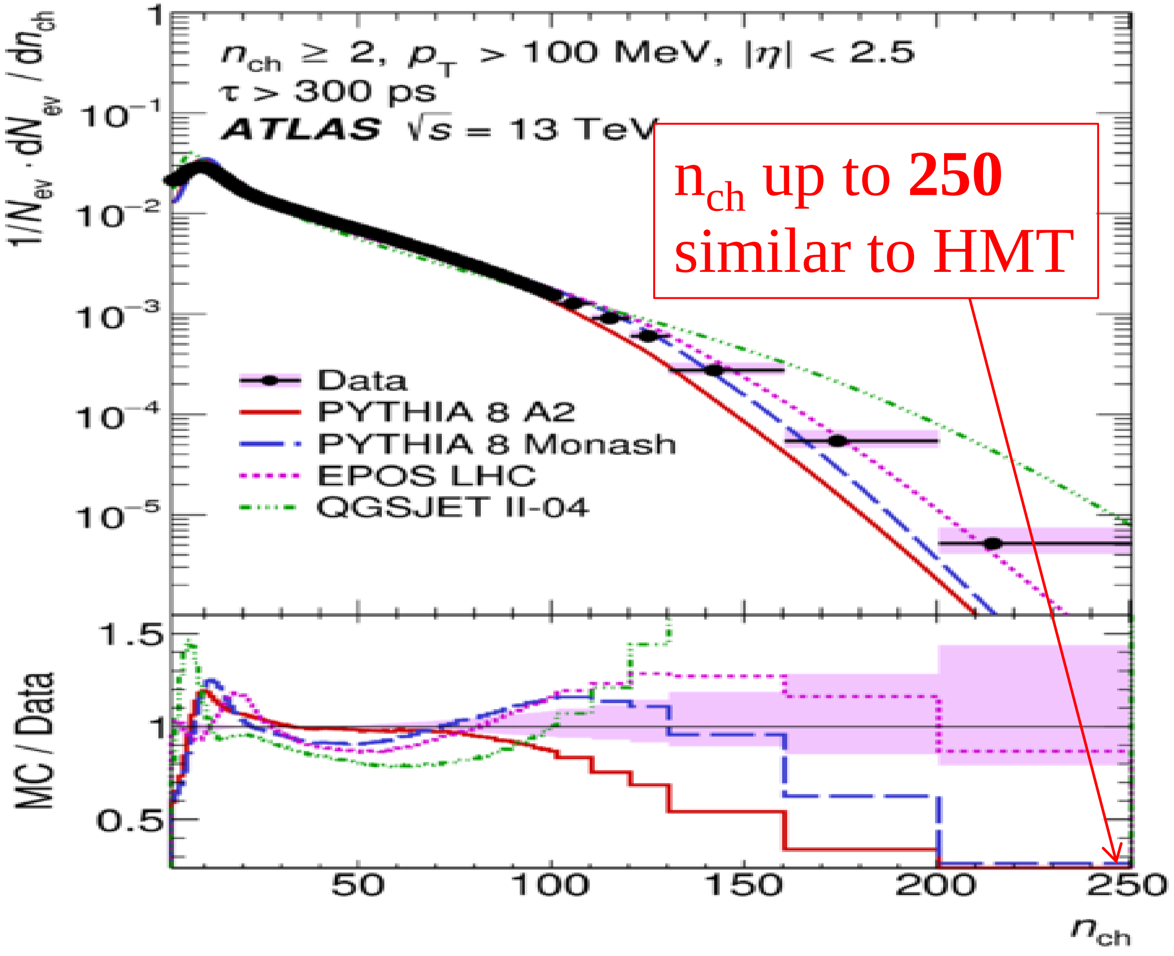

Charged-particle events as a function of the multiplicity distribution for p_T>100 MeV

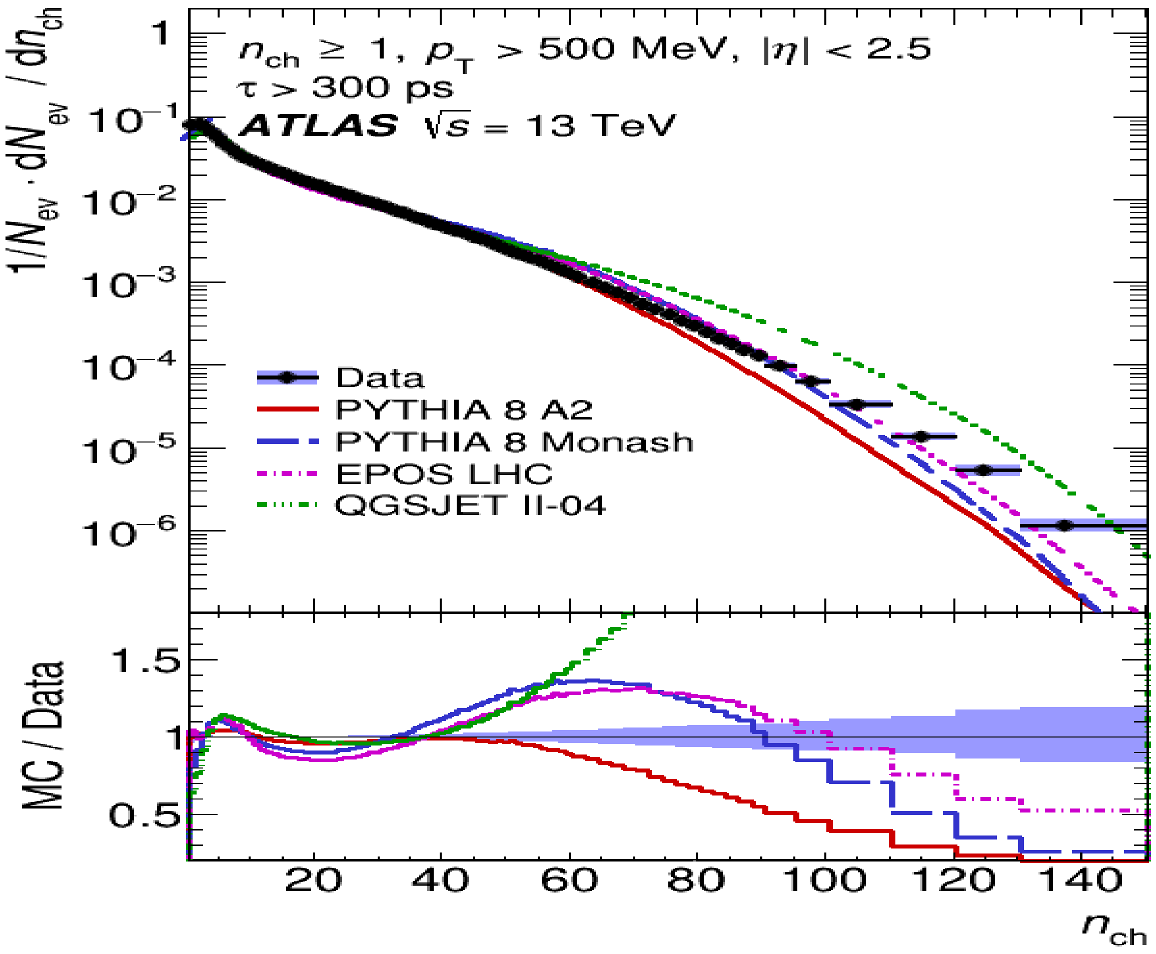

Charged-particle events as a function of the multiplicity distribution for p_T>500 MeV

Low n_{ch} not well modelled by any MC; because of large contribution from diffraction.

MULTIPLICITY DEPENDENCE OF CHARGED PARTICLES <p_T>

Eur. Phys. J. C 76 (2016) 502

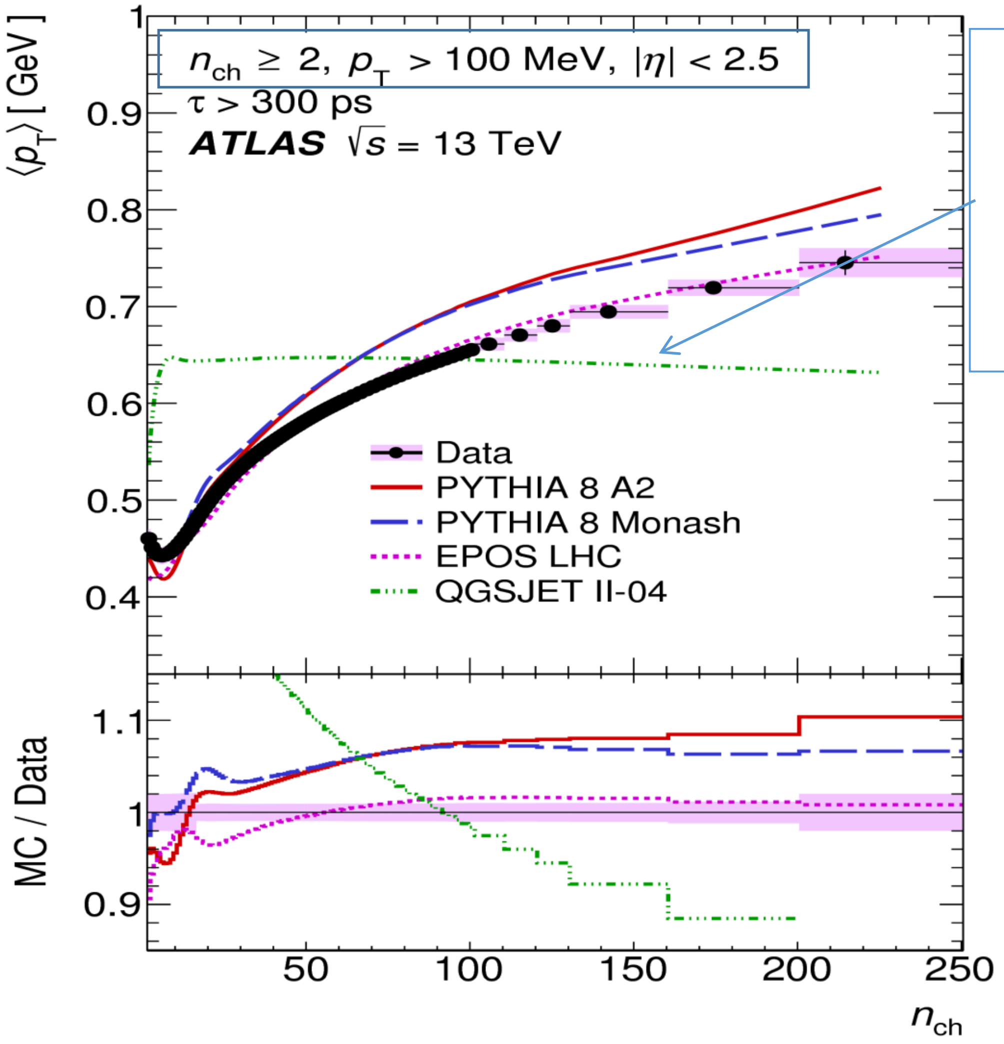

Models without colour reconnection, **QGSJET,** fail to model scaling with n_{ch}

Colour reconnection: strings from independent parton interactions do not independently produce hadrons, but fuse before hadronization

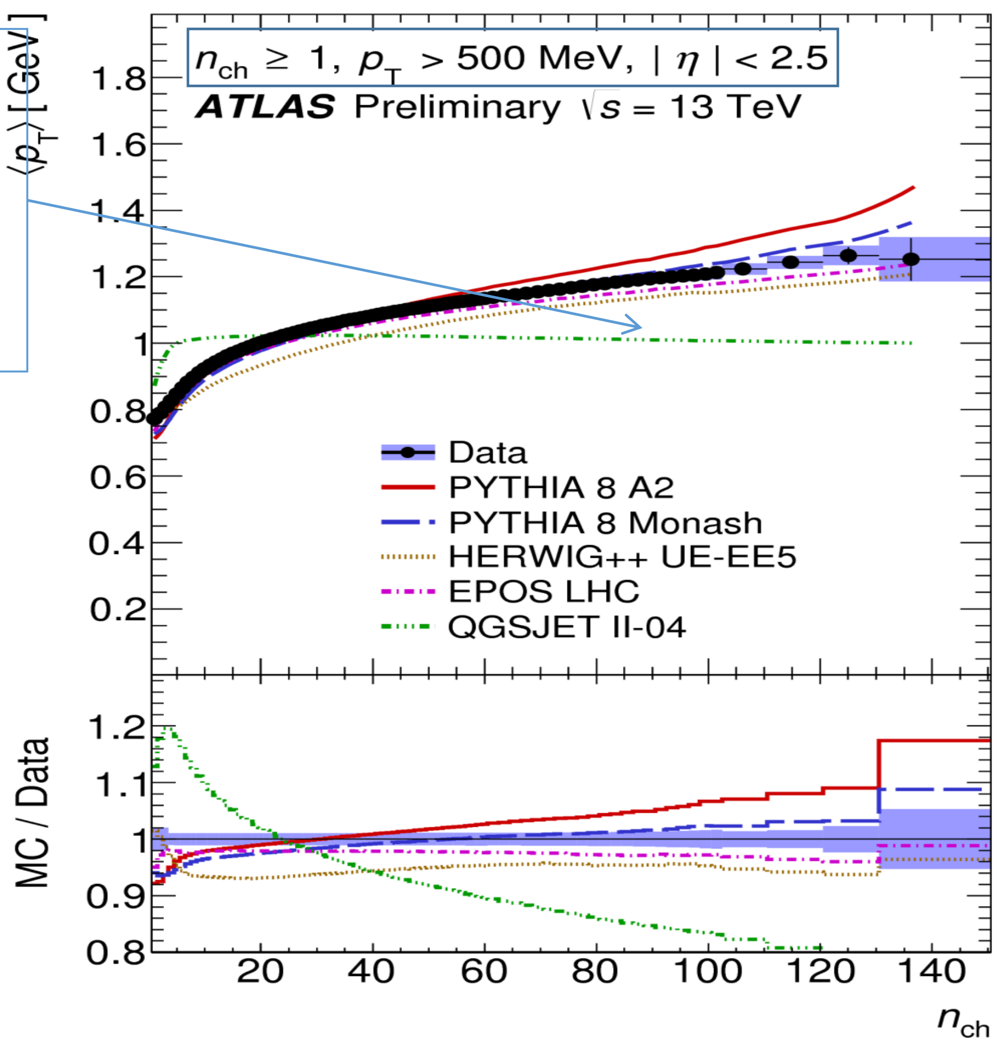

Avarage transverse momentum of charged particles as a functions of multiplicity

The dots represent the data and the curves the predictions from different MC models

The bottom inserts show the ratio of the MC/Data